SEM-4 IS A NOVEL PROTEIN IN THE BRAP-2/SKN-1/ROS DETOXIFICATION PATHWAY

ADILYA RAFIKOVA

A THESIS IS SUBMITTED TO THE FACULTY OF GRADUATE STUDIES IN PARTIAL FULFILLMENT OF THE REQUIREMENTS FOR THE DEGREE OF MASTER OF SCIENCE

GRADUATE PROGRAM IN BIOLOGY
YORK UNIVERSITY
TORONTO, ONTARIO

January 2016

Abstract

Oxidative stress causes damage to cells by creating reactive oxygen species (ROS). The overproduction of ROS is detrimental, having been linked to the onset of premature ageing and age-related diseases. Our lab has previously found that a partial deletion of *brap-2* (BRCA-1 associated protein 2) significantly increased the expression of *gst-4,* a phase II detoxification enzyme in *C.elegans*. An RNAi screen for 940 transcription factors on a *brap-2;gst-4::gfp* strain resulted in more than 20 candidates that are proposed to alter expression of *gst-4* in BRAP-2/SKN-1/ROS detoxification pathway, and one of those genes, *sem-4,* was chosen for the further studies. A significant reduction in *gst-4* mRNA levels was observed in *sem-4;brap-2* double mutants and *sem-4* mutants. We also found that higher levels of ROS were generated in *sem-4* mutants in comparison to N2 worms, indicating that SEM-4 is required to prevent overproduction of ROS *in vivo*. Furthermore, the lifespan of *skn-1* overexpressing worms was dependent on presence of *sem-4*. Next, survival of worms exposed to constant oxidative stress was decreased in *sem-4* mutants. Lastly, we determined that SEM-4 is a transcriptional regulator of *skn-1c.* Together, these results indicate a newly identified role of SEM-4 in regulating expression of phase II detoxification enzymes and preventing the harmful effects caused by overproduction of ROS.

Acknowledgements

I could never have reached the heights or explored the depths without the help, support, guidance and effort of many people while writing this thesis. First, I would like to express my deepest gratitude to Dr. Terrance Kubiseski for providing me with an opportunity to conduct the research under his supervision. The freedom provided by Terry in designing and conducting experiments helped me to grow as a researcher. I believe that the most memorable saying from him is: “After all, it is your research”. It made me feel more confident in my work and helped me to take the initiative when it was needed. Terry is very approachable and attentive person when it comes to his students and his excitement in the research encouraged me to strive in my studies. He was the supervisor who encouraged my critical thinking and initiative.

Next, it is my privilege to thank my advisor, Dr. John McDermott for providing his constructive critique and guidance during the development of my project. He was very inquiring about the course of my research, and I have always received extensive and elaborative comments that helped to move the project forward. I could not have asked for a better advisor.

Further, I would like to acknowledge Lesley MacNeil and Marian Walhout for performing RNAi screen. My project would not exist without their work.

I would also like to share how grateful I am to have my two lab colleagues, Queenie and Dayana. They constantly supported me throughout the time of my study. I am very appreciative for their time and patience teaching me laboratory techniques in the world of *C.elegans*. They were always the first people I could go for an advice or help, and I would never get a “NO” for an answer from them. Both of them continuously pushed me towards my goal and became dear friends to me. Dayana and Queenie always provided moral support and cookies during the rough times and made me feel like I am at home. I feel very blessed to have them as my teammates.

Next, I would like to acknowledge members of Dr. Peng's lab: Heyam, Jelena, Mohamed, Shahin and Stephanie. All of them were very welcoming, shared their knowledge and provided suggestions for my research. And we always found time to share a good laugh at the end of the day.

I would like to sincerely thank my husband, Richard, for his consistent encouragement throughout my candidature period, and his practical and emotional support in my personal development.

Grateful acknowledgement is expressed to my beloved parents for their constant support in my choice of joining the graduate school. My mother, Guzal, encouraged and inspired me throughout my life, and taught me to always achieve my goals. My father, Raif, was always proud for me following his footsteps and provided his valuable opinion in my study. I also would like to thank my sister and brother who tended to add an anecdotic side to my research to make me laugh and be cheerful about the life. I would not be able to finish my research without them in my life.

Table of Contents

List of Abbreviations

Term	Description
4E-BP1	Eukaryotic translation initiation factor 4E-binding protein 1
AGE-1	AGEing alteration 1
AKAP3	A-Kinase anchor protein
AKT1/2	AKT kinase family 1/2
ARE	antioxidant response element
ASI	Amphid Sensila neurons
ASK1/2	Apoptosis-signal-regulating kinase 1/2
BMK1	ERK5/big MAP kinase 1
BRAP-2	BRCA-1 Associated Protein 2
bZIP	basic leucine zipper
c-TAK1	Cdc25C-associated kinase-1
CEH-6	C.elegans Homeobox 6
CMV UL44	Cytomegalovirus UL44 Protein
CNC	Cap and Collar
DAF-15	abnormal DAuer Formation 15
DAF-16	abnormal DAuer Formation 16
DAF-18	abnormal DAuer Formation 18
DAF-2	abnormal DAuer Formation 2
DLK1	Protein Delta homolog 1
DNMT1	DNA methyl transferase 1
EGF	epidermal growth factor
EGFR	epidermal growth factor receptor
EGL-27	Egg-laying defective 27
EGL-5	Egg-laying defective 5
ELT-2	Erythroid-Like Transcription factor family
ER	Endoplasmic Reticulum
ERK1/ERK2	extracellular-signal regulated kinase 1/2
FDA	Federal Drug Administration
FOXO	Forkhead Box Protein O
FOXO1	Forkhead Box Protein O1
FOXO3a	Forkhead Box Protein O3a
FTT-2	fortheen-three-three family
GSK3β	glycogen synthase kinase β
GST-4	Glutathionine S-Transferase
HMG20A	High Mobility Group 20A
HSF-1	heat Shock Factor 1

IGF-1	Insulin like growth factor 1
IMP	impedes mitogenic signal propagation
JNK	c-Jun N-terminal kinase
Keap 1	Kelch-Like ECH-Associated Protein 1
KSR	kinase suppressor of Ras
LCR	low-complexity region
LIN-39	abnormal cell LINeage
LIN-45	abnormal cell LINeage
MAPK	mitogen-activated protein kinase
MAPKAPK2	Mitogen-Activated Protein Kinase-Activated Protein Kinase 2
MAPKK	mitogen-activated protein kinase kinase
MAPKKK	mitogen-activated protein kinase kinase kinase
MEC-4	sodium channel
MEK-2	MAP kinase kinase
MEKK1	MAP kinase kinase kinase 1
MEKK3	MAP kinase kinase kinase 3
MEKK4	MAP kinase kinase kinase 4
MKK3	Dual specificity mitogen-activated protein kinase kinase 3
MKK6	Dual specificity mitogen-activated protein kinase kinase 6
MKP	MAPK phosphatase
MKP-4	MAPK phosphatase 4
MLK3	MAP kinase kinase kinase 11
MPK-1	MAP kinase
mTOR	mechanistic Target of Rapamycin
mTORC1/2	mTOR Complex 1/2
NF-κB	nuclear factor kappa-light-chain-enhancer of activated B cells
Nrf2	NF-E2-related factor 2
NSY-1	Neuronal SYmmetry 1
NuMA1	Nuclear mitotic apparatus protein 1
PAR-5	abnormal embryonic PARtioning of cytoplasm
PDGF	platelet-derived growth factor
PDGFR	platelet-derived growth factor receptor
PDK-1	Phosphoinositide-dependent kinase1
PHLPP1	PH domain and leucine rich repeat protein phosphatase 1
PI3K	Phosphoinositide 3-kinase
PKB	Protein kinase B
PKC	Protein kinase C
PMK-1/2/3	P38 Map Kinase family 1/2/3
PTEN	phosphatase and tensin homolog
Raf	serine/threonine specific protein kinase

RAPTOR	Regulatory-associated protein of mTOR
Ras	small GTPase discovered in RAt Sarcoma
ROS	Reactive Oxygen Species
RTK	receptor tyrosine kinase
S6K	ribosomal S6 kinase
SALL1/2/3/4	Spalt-Like Transcription Factor 1/2/3/4
SCF complex	SKP, Cullin, F-box containing complex
SEK-1	SAPK/ERK kinase 1
SEM-4	SEx Muscle abnormal
SGK	Serum- and Glucocorticoid- inducible Kinase homolog
SKN-1	SKiNhead 1
SNP	single nucleotide polymorphism
SOX-2	SRY(sex-determining region Y)-box 2
SV40 T-ag	Sivian virus 40 large T antigen
SYNE2	Spectrin Repeat Containing, Nuclear Envelope 2
TBC	Tre2-Bub2-Cdc16
Trx	Thioredoxin
TSC1/2	tubeorous sclerosis complex 1/2
UNC-55	UNCoordinatted family member
UPR	unfolded protein response
WDR-23	WD Repeat protein 23
XBP-1	X-box binding protein 1
ZnF	zinc finger
β-TrCP	beta-transducin repeat containing

List of Tables

List of Figures

1. Introduction

1.1 Ageing

Ageing is a physiological process common to all living organisms. Ageing is negatively correlated with lifespan and every known organism has a specified life expectancy. It (life expectancy) has been associated with overall size, *i.e.* the smaller the animal, the less its life expectancy (Kenyon 2005). Even though ageing is a natural process, the fight against the causes of ageing and identifying ways to extend lifespan has become a major focus for modern research. With age comes an increase in disease, and there are many well-known age-related diseases, such as Alzheimer's, Parkinson's, as well as the onset of cancer. Environmental factors also contribute to premature ageing and the development of age-related diseases. One of these external factors is oxidative stress (Martindale and Holbrook 2002; Weinberg and Chandel 2009), the result of an overproduction of reactive oxygen species (ROS) and hypothetically the main cause of ageing. ROS are formed in cells endogenously as byproducts of the electron transport chain found in mitochondria, as well as exogenously by the environment as a result of exposure to UV light, toxins and ionizing radiation (Finkel and Holbrook 2000). Under this constant threat that contributes to the acceleration of ageing, extending healthy life expectancy in human beings is now currently a vigorous area of study.

The discovery of pathways affecting lifespan began in 1988, with the IGF-1/Insulin-like signaling (IIS) pathway first identified in *Caenorhabditis elegans*. A mutation in the *age-1* gene (AGEing alteration 1) (the worm PI3K (Phosphoinositide 3-kinase) homolog) resulted in long-lived worm (Friedman and Johnson 1988). Further research demonstrated the requirement of *daf-16* (abnormal DAuer Formation) (FOXO (Forkhead Box Protein O) ortholog, Table 1) (Morris et al. 1996) *hsf-1* (HSF1 (Heat Shock Factor 1 ortholog) (Hsu et al. 2003), and *skn-1* (SKiNhead 1) (Nrf2 (NF-E2-related factor 2) ortholog) expression (Tullet et al. 2008) for the prolonged

lifespan of *age-1* mutants. The importance of IGF-1/Insulin-like pathway was confirmed in other model organisms, such as *Drosophila* (Clancy et al. 2001), Yeast (Fabrizio et al. 2001), and mice (Holzenberger et al. 2003). It is also suggested that in humans, some SNPs (single-nucleotide polymorphisms) in insulin/IGF-1, AKT1, FOXO1, and FOXO3a (components of IGF-1/Insulin pathway) are correlated with prolonged lifespan (Suh et al. 2008; Willcox et al. 2008; Flachsbart et al. 2009; Pawlikowska et al. 2009). Therefore, IGF-1/Insulin signaling pathway is an important player in the regulation of lifespan.

The mTOR (Target Of Rapamycin) pathway was also found to affect lifespan in *C. elegans*, where low levels of mTOR resulted in a longer lifespan (Vellai et al. 2003). This same decrease in mTOR also prolonged lifespan in mice (Harrison et al. 2009), Yeast (Kaeberlein et al. 2005) and the fruit fly (Kapahi et al. 2004). Both pathways, insulin signaling and mTOR, affect lifespan, and there is experimentally proven interconnection between them. For instance, mTORC1 (mTOR Complex 1) and mTORC2 (mTOR Complex 2) both regulate nuclear localization of SKN-1, while only mTORC1 regulates nuclear localization of DAF-16 (Robida-Stubbs et al. 2012). In addition, DAF-16 regulates expression of *daf-15* (RAPTOR (Regulatory-associated protein of mTOR) ortholog, Table 1) (Jia et al. 2004). This demonstrates that pathways affecting lifespan regulate expression and localization of the same genes.

One condition regarding lifespan extension is the tradeoff between longevity and reproduction. Several experiments on worms have shown that gonad removal results in a longer lifespan (Friedman and Johnson 1988; Arantes-Oliveira et al. 2003; Mukhopadhyay and Tissenbaum 2007) and resistance to pathogens (Alper et al. 2010). Besides worms, experiments conducted on mice that transplanted an ovary from a younger mouse to an older one, resulted in a 60% increase in lifespan (Cargill et al. 2003). Similarly, in *Drosophila* lifespan is also

dependent on reproduction (Sgro and Partridge, 1999). In short, there is a definite link between lifespan and reproduction.

Our lab is interested in using *C.elegans* to study the mechanism of the ROS detoxification response. *C.elegans* was proposed as a model organism in 1974 by Sydney Brenner (Brenner 1974); it has a short lifespan (21 days), is transparent and contains 41% human gene orthologs (Lai et al. 2000; Shaye and Greenwald 2011). Worms reach adulthood in 3 days, from egg hatching to progressing through four larval stages (L1, L2, L3 and L4). In addition, genes involved in important biological processes, such as protecting against ROS, are present in *C.elegans.* Also, expression of different genes can be monitored throughout each different stage, which makes *C. elegans* an excellent model for genetic and developmental studies.

Table 1. List of *C.elegans* and mammalian orthologs

***C.elegans* protein**	**Mammalian ortholog**
AGE-1	PI3K
BRAP-2	BRAP2
CEH-6	POU2F2
DAF-15	RAPTOR
DAF-16	FOXO
DAF-18	PTEN
DAF-2	IGF-1R
ELT-2	GATA4
FTT-2	14-3-3
GST-4	Hematopoietic prostaglandin D synthase
LET-60	Ras
LET-363	mTOR
LIN-39	Homeobox protein Hox-A5
LIN-45	RAF1
MPK-1/2	ERK1/2
NSY-1	ASK1
PAR-5	14-3-3
PMK-1/2/3	p38
SEK-1	MAP2K3
SEM-4	SALL1/2/3/4
SKN-1	Nrf2
SOX-2	SRY
UNC-55	COUP transcription factor 2
WDR-23	DCAF11
XBP-1	XBP1

1.2. Oxidative Stress and Ageing

Normal growth and development of the cell is dependent on homeostasis between ROS and antioxidant defenses. ROS are formed in cells endogenously (as a byproduct of the electron transport chain in mitochondria) and exogenously (environmental input, such as UV light, toxins, and ionizing radiation) (Finkel and Holbrook 2000). Oxidative stress is the consequence of ROS overproduction and is proposed to be one of the main causes of premature ageing and age-related diseases (Martindale and Holbrook 2002; Weinberg and Chandel 2009). Cell damage by ROS is manifested as oxidative damage of DNA, proteins and lipids (Van Raamsdonk and Hekimi 2010) (Figure 1). The cellular defense response against ROS is comprised of three phases: solubilization of lipophilic endobiotics by Cytochrome P450, reduction of ROS by phase II enzymes, and removal of toxins by ATP-binding cassette (ABC) type transport proteins (Oliveira et al. 2009).

Harman's research was the first to propose a relationship between ageing and oxidative stress (Harman 1956). According to his proposed theory, cells are constantly under attack by free radicals formed endogenously, and this is the cause of ageing. Harman updated his theory in 1972, where he proposed that damage to mitochondria is the main cause for the accumulation of ROS, which leads to ageing and death (Harman 1972). Later on, his theory was both vigorously supported (Honda et al. 1993; Van Raamsdonk and Hekimi 2010; Rodriguez et al. 2013) and challenged (Lapointe and Hekimi 2010; Yang and Hekimi 2010; Fu et al. 2015; Schaar et al. 2015) by many researchers. The main concern with respect to the reliability of the theory arose when long-lived *C.elegans* mutants were found to contain high levels of ROS. In addition, it was found that use of antioxidants decreases lifespan of these long-lived mutants (15-38%), while low levels of pro-oxidant increases lifespan in all worms (3-58%). Therefore, researchers

proposed a model where high levels of ROS act as a protective mechanism during ageing in long-lived mutants (Yang and Hekimi 2010).

Another theory suggests that ROS formed in mitochondria induces the opposite effect to ROS formed in cytoplasm. According to Schaar and colleagues, high levels of ROS in mitochondria positively affect lifespan, while increased levels of ROS in cytoplasm decrease lifespan in long-lived mutant nematodes. In support of the research conducted by Yang and Hekimi, Shaar and colleagues discovered a negative relationship between antioxidants and lifespan in long-lived mutant (Schaar et al. 2015). A more recent theory that opposes the free radical theory of ageing proposes the oxidative fluctuation hypothesis of ageing. Fu and colleagues experimented on *C.elegans* by knocking down multiple genes and using different concentrations of hydrogen peroxide. The results showed significant correlation between lifespan and levels of fluctuation of oxidative stress, where low fluctuations in ROS positively affect lifespan, while high fluctuations decrease the lifespan of these animals (Fu et al. 2015). Briefly, even though the free radical theory of ageing is constantly challenged, it is still reasonable to say that ROS, especially accumulated exogenously, does cause breaks in DNA, protein carbonylation and lipid peroxidation, which all contribute to cell damage and ageing. There are multiple pathways activated by oxidative stress that are conserved and studied, from simple unicellular to complex multicellular organisms. I will review Insulin/IGF-1 signaling, MAPK (mitogen-activated protein kinase) signaling pathways and the mTOR pathway in more detail below.

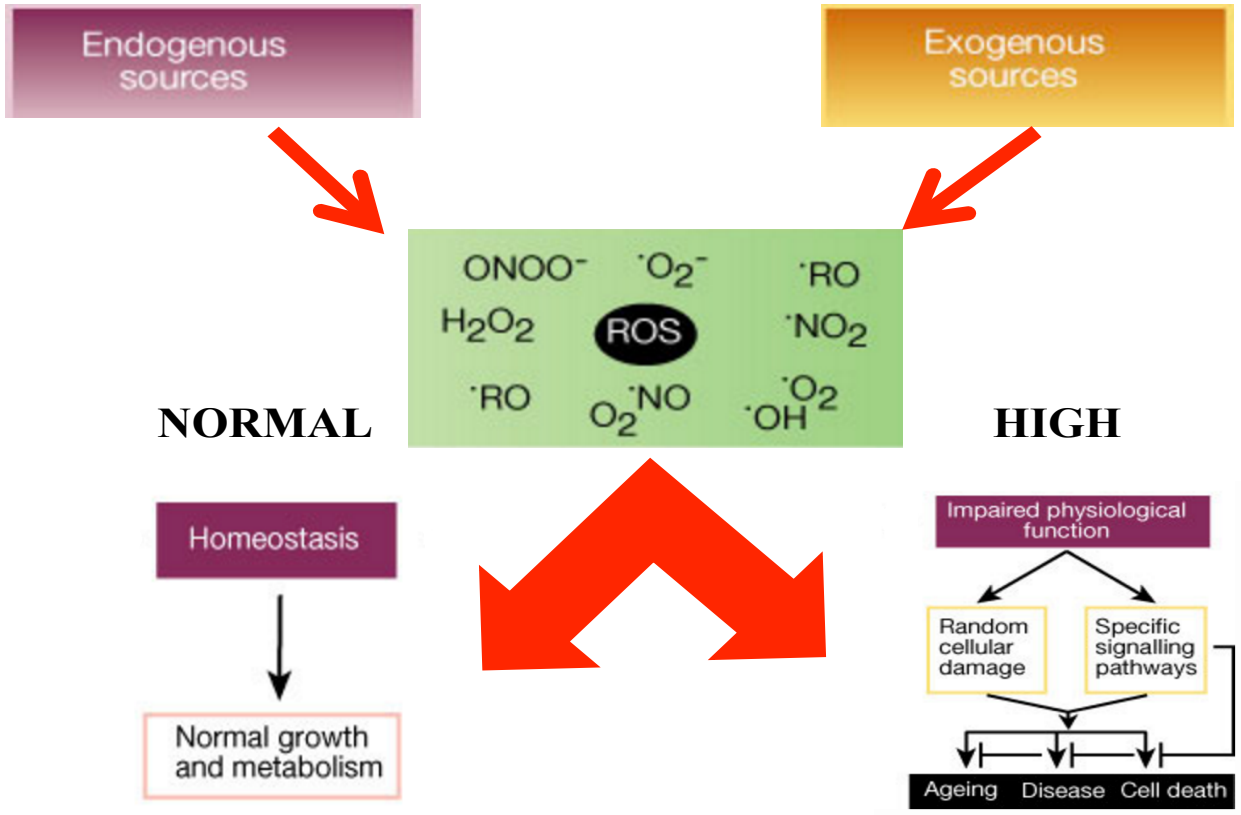

Figure 1. The sources of ROS and possible outcomes. Overproduction of ROS from endogenous and exogenous sources leads to ageing and age-related diseases. At the same time, homeostasis allows normal growth and metabolism. Figure was adapted from Finkel and Holbrook, 2000.

1.2.1 Insulin/IGF-1 signaling pathway

Insulin/IGF-1 signaling (IIS) pathways are evolutionary conserved and are well studied in all model organisms, with most studies conducted in *C.elegans* (O'Neill et al. 2012). Insulin/IGF-1 pathway has been negatively associated with lifespan and age-related diseases, such as Alzheimer's, Parkinson and multiple types of cancer (King and Wong 2012; O'Neill et al. 2012). The pathway itself consists of ligand – insulin or insulin-like hormones, receptor – insulin or insulin-like growth factor receptor, insulin receptor substrate proteins, PI3K (PI3-kinase), phosphoinositide-dependent kinase-1 (PDK-1) and the main serine/threonine protein kinase B (PKB/AKT) (Figure 2). The downstream cascade of this pathway is further divided into multiple pathways regulated by AKT. One of them is mTOR, where the inhibitor of mTOR known as the TSC complex, is phosphorylated by AKT. Another pathway that is activated is ERK1/ERK2 (extracellular signal-regulated kinase 1/ 2) MAPK pathway. AKT kinase also phosphorylates the FOXO (Forkhead box O) transcription factor, and phosphorylated FOXO is unable to enter nucleus (King and Wong 2012; O'Neill et al. 2012). In addition, AKT negatively phosphorylates GSK3β (glycogen synthase kinase β), which is part of the Wnt pathway. Negative regulation of IIS pathway is achieved by de-phosphorylation of PI3K by PTEN (phosphatase and tensin homolog) (O'Neill et al. 2012).

Studies that began in *C.elegans* in 1988 demonstrate that inhibition of IIS pathway extends the lifespan of worms by more than two fold (Friedman and Johnson 1988) and this was conserved in fruit flies (Clancy et al. 2001) and mice (Holzenberger et al. 2003). In addition to pathway activated by ligand binding, it can also be activated by overproduction of ROS, where ROS can lead to autophosphorylation of the receptor, as well as inactivation of PTEN (Papaconstantinou 2009). The end effect is over-activation of mTOR, ERK1/ERK2, as well as

inhibition of nuclear localization of FOXO and the overall effect is reduction of organismal lifespan.

In *C.elegans,* IIS pathways are combined into one. There is a single receptor, DAF-2, instead of Insulin receptor and IGF-1R (Insulin-like growth factor 1 receptor) (Table 1). The downstream of the receptor contains all orthologs that are present in mammals (Table 1): AGE-1 (PI3K), DAF-18 (PTEN), PDK-1 (PDK1), AKT-1/2 and SGK-1 (AKT), and DAF-16 (FOXO) (Figure 2). In addition to DAF-16 (FOXO), in worms, AKT-1/2 and SGK-1 also phosphorylate another important transcription factor for antioxidant enzyme production, SKN-1 (Nrf-2) (Blackwell et al. 2015). The first evidence of the IIS pathway to regulate lifespan came from experiments conducted with *C.elegans,* where a mutation in *age-1* increased survival of worms by 40-60% (Friedman and Johnson 1988). The next mutation altered the receptor of the pathway, *daf-2*, and also increased the lifespan of animals (Kenyon et al. 1993). Furthermore it was discovered that a mutation in *daf-16* significantly decreases lifespan in long-lived worms (Hsu et al. 2003).

Oxidative stress in *C.elegans* affects multiple pathways and the *age-1* pathway is one of them. During overproduction of ROS, the IIS pathway is over activated, which leads to a shorter lifespan in worms due to a higher level of activation of mTOR and ERK1/ERK2 pathways, and inhibition of the transcription factors responsible up-regulation of detoxification enzymes. Indeed, it was shown that *age-1* and *daf-2* mutants survive longer during oxidative stress (Haigis and Yankner 2010). Thus, IIS pathway in *C.elegans* is well studied and can be used as model for studies in other organisms.

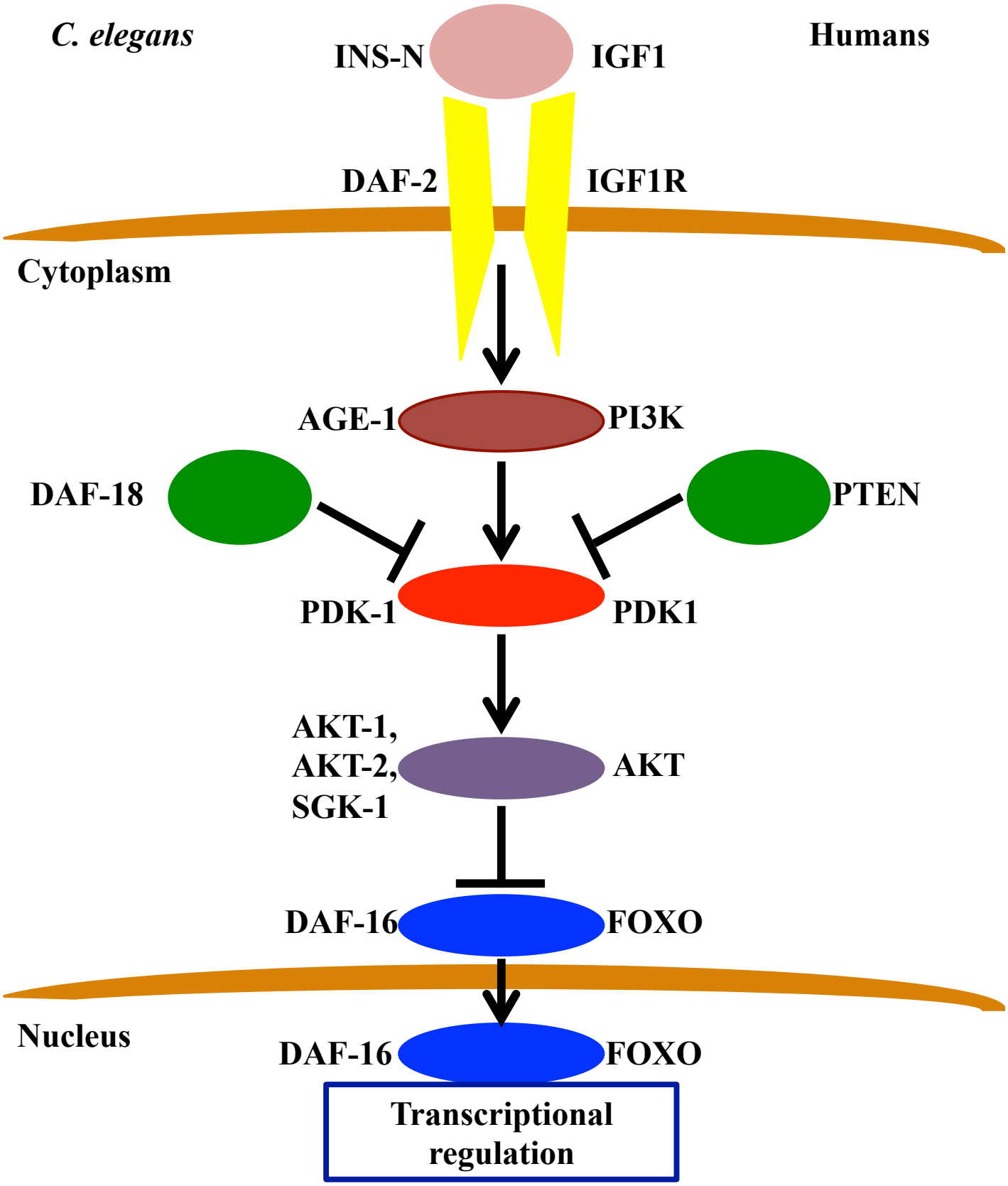

Figure 2. Insulin/IGF-1 signaling pathway. The homology of cascade of IIS pathway is shown in *C.elegans* and Humans. The figure is adapted from Christensen et al. 2006.

1.2.2 MAPK signaling pathways

MAPK (mitogen-activated protein kinase) intracellular signaling pathways consist of multiple players. The general principle of MAPK pathways is a chain reaction of phosphorylation, where MAPKKK phosphorylates MAPKK, and then MAPKK phosphorylates MAPK (Runchel et al. 2011). Phosphorylation is the only way to activate inactive players of the MAPK pathway, and the way to control over activation is achieved by MAPK phosphatases (MKPs), such as MKP-4 that inactivates ERKs and p38 MAPKs (Son et al. 2013). There are four known typical MAPK families in mammals, where each can be activated by ROS in addition to their conventional way of activation. They are: ERK 1/2 (extracellular signal-regulated kinase 1 and 2), BMK1 (ERK5/big MAP kinase 1), JNK (c-Jun N-terminal kinase), and p38 (Runchel et al. 2011). For the purpose of my thesis, I will review two MAPK pathways, ERK 1/2 and p38, in more detail below.

1.2.2.1 ERK 1/2 signaling pathway

ERK 1/2 is the most complicated pathway of all known MAPK signaling pathways. ERK 1/2 can be activated in multiple ways, but the most conventional and studied way is through the ligand (EGF (epidermal growth factor) or PDGF (platelet-derived growth factor)) binding to the receptor (EGFR (epidermal growth factor receptor) or PDGFR (platelet-derived growth factor receptor)), and activating the cascade (Kolch 2005; Runchel et al. 2011) (Figure 3). Binding of the ligand leads to phosphorylation of receptor tyrosine kinase (RTK) and activation of small G protein Ras, and Ras activates Raf (MAPKKK). The cascade then continues with activation of MEK 1/2 (MAPKK) and then ERK 1/2 (MAPK). Active ERK 1/2 has at least 160 known targets, where some of them are located in the nucleus (transcription factors, such as c-Myc and c-Fos),

and some are in cytoplasm (*i.e.* ribosomal S6 kinase). ERK 1/2 signaling is considered a pro-survival pathway, but it was found to play a pro-apoptotic role in opposium kidney and human glioma cells in response to treatment with hydrogen peroxide (Runchel et al. 2011).

Besides activation of the pathway through ligand binding, it was discovered that oxidative stress is also able to activate the pathway through multiple mechanisms (Yoon et al. 2002; Torres and Forman 2003; McCubrey et al. 2007; Runchel et al. 2011; Son et al. 2013). One mechanism is ligand-independent receptor activation, where H_2O_2 leads to phosphorylation and dimerization of EFGR and PDGR. Another way is to directly activate Ras or Src, both of which directly activate Raf. Furthermore, ERK 1/2 can be activated through an increase of Calcium in the cytoplasm, where activation of PKC (Protein Kinase C) leads to activation of Raf. One important target of ERK 1/2 during oxidative stress related activation is Nrf2 (NF-E2-related factor 2), where Nrf2 is a transcription factor for many antioxidant enzymes (Runchel et al. 2011).

In addition to the known mechanism of pathway regulation, the presence of scaffolding protein KSR (kinase suppressor of Ras) was discovered in *C.elegans* and *Drosophila* (Morrison 2001). The role of this scaffolding protein was first unknown and was considered to be a kinase, due to its homology to the Raf protein (Kolch 2005), but it was then discovered that KSR binds to Raf, MEK 1/2, and ERK 1/2 (Morrison 2001; Kolch 2005) (Figure 3). Besides three kinases, KSR also binds c-TAK1 (Cdc25C-associated kinase-1), 14-3-3, IMP (impedes mitogenic signal propagation) and PP2A (protein phosphatase 2A), where the first three players keep KSR inactive, while PP2A activates it by de-phosphorylating S392 on KSR. Activation of KSR is achieved in multiple steps. At first, activated Ras recruits IMP, where IMP autoubiquitinates and degrades. Second, PP2A becomes active and de-phosphorylates S392 on KSR, which leads to a

conformational change in KSR and the ability to bind Raf and MEK. Lastly, KSR becomes phosphorylated at T274 and binds Raf and MEK, and cascade becomes active (Kolch 2005).

ERK 1/2 signaling is conserved in all animal species, including *C.elegans*, where players of the pathway are: LIN-45 (MAPKKK), MEK-2 (MAPKK) and MPK-1 (MAPK) (Table 1) (Sakaguchi et al. 2004). In addition, *C.elegans* contains KSR orthologs, KSR-1 and KSR-2 (Ohmachi et al. 2002), IMP ortholog, BRAP-2 (BRCA1 Associated Protein 2) (Koon and Kubiseski 2010), and 14-3-3 orthologs, PAR-5 and FTT-2 (Berdichevsky et al. 2006) (Table 1). Besides orthologs of MAPK pathway, *C.elegans* contains an ortholog for Nrf2, known as SKN-1, and the role of SKN-1 is to activate main phase II detoxification enzymes in response to stress (Blackwell et al. 2015). The fact of that the pathway is highly conserved makes *C.elegans* a suitable model to study the role of oxidative stress.

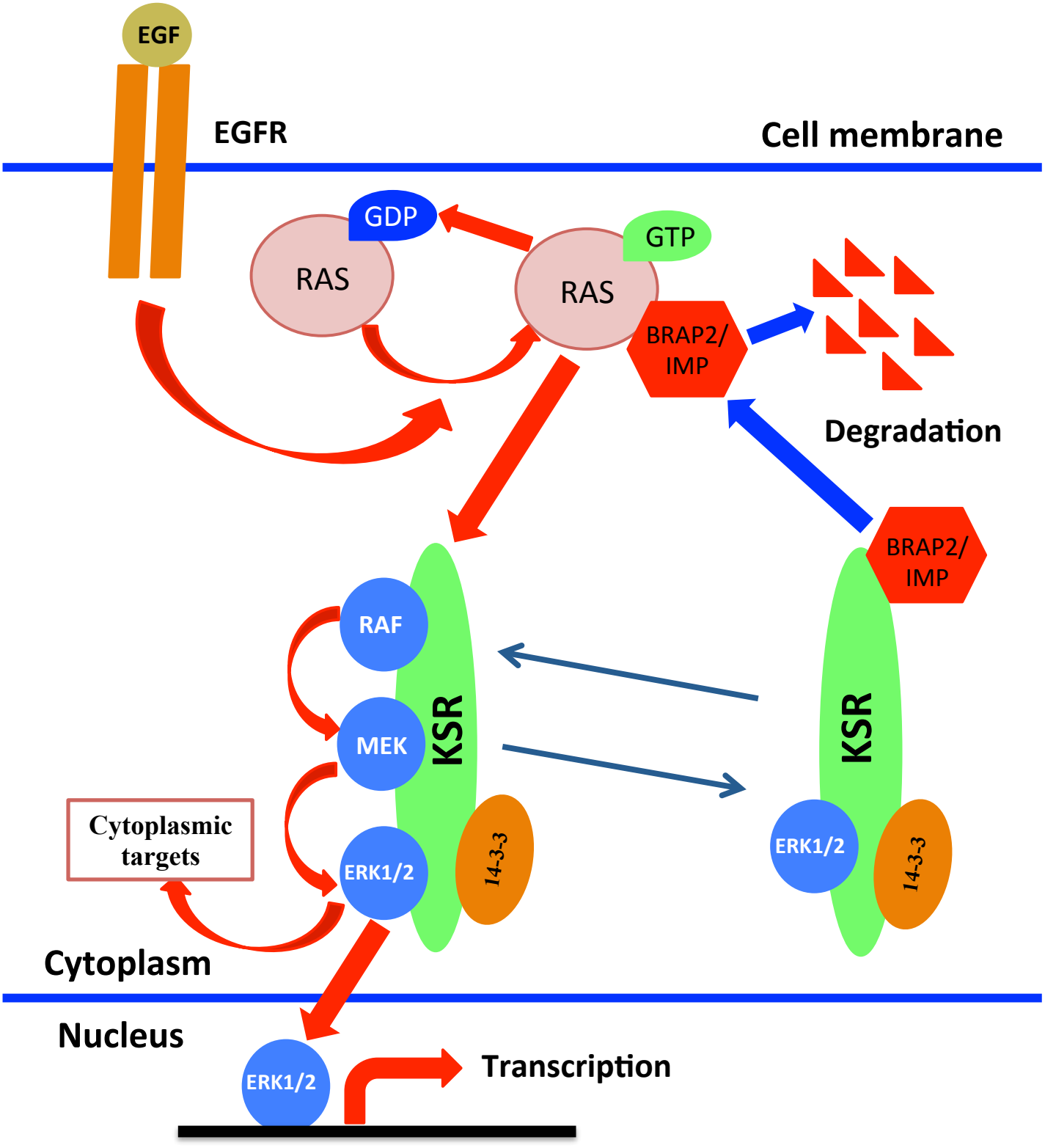

Figure 3. Schematic representation of MAPK pathway. Brap2/IMP interacts with KSR in quicient cells and inhibits formation of KSR/RAF/MEK complex. Upon stimulation, Brap2/IMP translocates and binds to RAS-GTP, and that results into autoubiquitination and degradation of Brap2/IMP. KSR allows RAF-MEK-ERK1/2 cascade activation. Adapted from Kolch 2005.

1.2.2.2 p38 signaling pathway

The p38 pathway is also conserved among species as a MAPK signaling pathway, but opposes ERK 1/2, as a pro-apoptotic pathway. The pathway consists of multiple MAPKKKs (ASK1/2, MEKK1, MLK3, TAK1, DLK1, TAO1/2, ZAK1, MEKK3, and MEKK4), MAPPKs (MKK3/MKK6), and four p38 kinases (p38α, p38β, p38γ and p38δ) (Runchel et al. 2011; Son et al. 2013). Activation of the pathway is dependent on a broad spectrum of stressors, such as oxidative stress, cytokines, and osmotic shock (Tormos et al. 2013). The most studied pathway involves three major kinases, ASK1, MKK3/MKK6 and p38α (Runchel et al. 2011). During non-stress conditions ASK1 (apoptosis signal-regulating kinase 1) is bound to antioxidant protein Thioredoxin (Trx), keeping ASK1 in an inactive state. The complex ASK1-Trx dissociates by sensing a stress condition in the cell, which leads to oxidation of Trx, release of ASK1 and activation of the cascade. Besides Trx, binding of 14-3-3 to phosphorylated Ser966 on ASK1also inhibits ASK1, and the ASK1-14-3-3 interaction also dissociates during stressful conditions (Runchel et al. 2011). Among targets of p38 are transcription factors (MEF2C, Elk-1, ATF2, CHOP, and CREB), and kinases, *i.e.* MAPKAPK2 (Runchel et al. 2011; Tormos et al. 2013). Importantly, p38 is able to regulate Nfr2 (as mentioned in ERK 1/2 pathway), but the exact mechanism of this in mammals is still unknown. It is only known that the presence of p38 is required for proper activity of Nrf2, and to stabilize the Nrf2-Keap1 complex, where Keap1 (Kelch-like ECH-associated protein 1) is inhibitor of Nrf2. Therefore, p38 has dual version of activation/inhibition of Nrf2 (Runchel et al. 2011).

As with ERK 1/2, the p38 signaling pathway is conserved in *C.elegans.* The orthologs of the pathway are: NSY-1 (MAPKKK), SEK-1 (MAPKK) and PMK-1/2/3 (MAPK) (Table 1), and the pathway is also activated in response to stressful conditions in the worm, *i.e.* oxidative stress or pathogens (Sakaguchi et al. 2004). Even though the mechanism of regulation of Nrf2 by p38

is unknown in mammals, it was found that PMK-1 phosphorylates SKN-1 on Ser164 and Ser430 in response to oxidative stress. Phosphorylation of SKN-1 by PMK-1 leads to nuclear localization of SKN-1, and thus an increase in activation of transcription of detoxifying enzymes (Inoue et al. 2005).

Overall, the p38 pathway was once considered as pro-apoptotic, but recent research now argues its role as "pro-survival" in some cell types (Tormos et al. 2013), and definitely pro-survival in *C.elegans* (Mertenskotter et al. 2013).

1.2.3 mTOR pathway

mTOR was first identified in yeast during studies on rapamycin, an antifungal macrolide from soil bacteria (Johnson et al. 2013). Later on, mTOR was classified into two separate complexes, mTORC1 and mTORC2, where each complex has a specific function. There are many proteins in both complexes, with six proteins in mTORC1 and seven in mTORC2 (Laplante and Sabatini 2012). The main player of both complexes is mTOR, a serine/threonine protein kinase, considered as an important part in regulation of cellular survival in response to stress and nutrients. There are multiple known functions of mTORC1, and the main one is mRNA translation by activating S6K (ribosomal protein S6 kinase) and inhibiting 4E-BP1 (eukaryotic translation initiation factor 4E-binding protein 1). Other functions include lipid biosynthesis, autophagy, glucose metabolism, and mitochondrial respiration (Johnson et al. 2013). Activation of mTORC1 is dependent on the availability of nutrients and stress, where both play the opposite roles on the complex. During normal conditions, where nutrients are available, mTORC1 becomes activated when its inhibitor complex, containing three proteins, TSC1 (tuberous sclerosis complex 1), TSC2 (tuberous sclerosis complex 2), and TBC (Tre2-Bub2-Cdc16), is phosphorylated by Ras-ERK or PI3K-AKT pathways (Dibble and Manning 2013). On the other hand, stress related conditions block the mTORC1 pathway by activating the TSC complex (Laplante and Sabatini 2012). In addition, inhibition of mTORC1 has been linked to extended lifespan in many model organisms, and rapamycin is FDA approved for treatment of multiple cancers. Moreover, mTORC1 is associated with many age-related diseases, such as Alzheimer's, cognitive decline, type 2 diabetes, and heart disease (Johnson et al. 2013). Different from mTORC1, less is known about mTORC2, especially the mechanisms of regulation of other pathways by the complex. As of today, mTORC2 has been shown to regulate metabolism, apoptosis, cell survival, cellular growth and proliferation. The known targets of mTORC2 are

SGK (serum- and glucocorticoid-regulated kinase), PKC (protein kinase C), and AKT (Laplante and Sabatini 2012).

Both complexes, mTORC1 and mTORC2, are conserved among species, and *C.elegans* is not an exception. There has been a lot of interest in the mTOR complexes since the discovery of their involvement in extension of the lifespan (Johnson et al. 2013). It was discovered that stress resistance of animals is increased in the absence of any of the mTORC1 players, and nuclear localization of two main transcription factors, DAF-16 and SKN-1, for antioxidant enzymes is increased (Robida-Stubbs et al. 2012). In earlier years, it was discovered that DAF-16 inhibits transcription of *daf-15* (ortholog of RAPTOR, Table 1), suggesting interconnection between mTORC1 and IIS (Insulin/IGF-1 signaling) pathways (Jia et al. 2004). Also, in *C.elegans* mTORC1 was shown to activate ELT-2 (GATA transcription factor) in response to hypoxia and extend lifespan (Schieber and Chandel 2014).

1.2.4 Transcription factors involved in the *C.elegans* oxidative stress response

1.2.4.1 SKN-1/Nrf2

SKN-1 is a transcription factor in *C. elegans* known for the activation of genes involved in the phase II detoxification pathway, metabolism, and mesodermal development (An and Blackwell 2003). There are four predicted and three *in vivo* confirmed isoforms of SKN-1, and all isoforms are believed to be expressed in different tissues of the worm. For instance, SKN-1a contains N-terminal transmembrane domain, which, as Blackwell speculates in his review, should be cleaved from the endoplasmic reticulum (ER) membrane in order to be activated (Blackwell et al. 2015). Both, SKN-1a and SKN-1c, are found to be expressed in intestinal nuclei and cytoplasm, as well as in the hypodermis (An and Blackwell 2003; Bishop and Guarente 2007). In contrast, expression of SKN-1b is found in ASI neurons, and is required in dietary restricted long-lived mutant animals (Bishop and Guarente 2007). At first, SKN-1 was identified as a gene required for tissue specification during embryogenesis (Bowerman et al. 1992). Later on it was determined that SKN-1 responds to oxidative stress by activating phase II detoxification genes (An and Blackwell 2003), and one of the genes activated by SKN-1 is Glutathione S- Transferase 4 (*gst-4*) (Oliveira et al. 2009). In addition, SKN-1 also induces genes from phase I and III detoxification pathways (Blackwell et al. 2015). Recently, a novel function of SKN-1 was discovered, where SKN-1 plays a role in unfolded protein response (UPR) and protects animals from ER stress (Glover-Cutter et al. 2013). It was shown that SKN-1 regulates ER stress genes and SKN-1 is activated by ER stress. In addition, overexpression of SKN-1 significantly increased *C. elegans* lifespan (Tullet et al. 2008).

Multiple pathways and kinases control nuclear localization of SKN-1 (Figure 4). So far, there are five known Serines on SKN-1 that can be phosphorylated. For instance, PMK-1 activates SKN-1 in response to pathogens and ROS by phosphorylating SKN-1 on Ser164 and

Ser430. In addition, phosphorylation of SKN-1 by MPK-1 also increases nuclear localization of SKN-1 (Okuyama et al. 2010). In contrast, phosphorylation of SKN-1 on Ser12 by AKT-1/2 and SGK-1 inhibits nuclear localization of SKN-1. Additionally, SKN-1 is inhibited by mTORC1 and mTORC2, as well as by GSK-3; and activated by ER stress response protein, XBP-1 (X-box binding protein 1) (An et al. 2005; Tullet et al. 2008; Blackwell et al. 2015).

The human ortholog of SKN-1, Nrf2 (NF-E2-related factor 2, Table 1) was first isolated in 1994 and was speculated to be a transcription factor for β-globin genes. In addition, Nrf2 was classified as a basic leucine zipper transcription factor (bZIP), as well as cap and collar protein (CNC) (Moi et al. 1994). Later on, dimerization of Nrf2 with Maf proteins in order to bind ARE (antioxidant response element) and activation of antioxidant proteins was discovered (Itoh et al. 1997). Continued research examined the regulation of Nrf2, and it was discovered that during physiological conditions in the cell, Nrf2 is bound to Keap1 and degraded by Cullin3 E3 ubiquitin ligase (Itoh et al. 1999; Kobayashi et al. 2004). During oxidative stress, Cystine 151 on Keap1 becomes oxidized and the interaction between Nrf2 and Keap1 (Kelch-like ECH-Associated Protein 1) is lost, and that leads to nuclear localization of Nrf2 and activation of detoxification enzymes. In addition to Keap1, it was recently discovered that another protein, β-TrCP (beta-transducing repeat containing protein), binds to phosphorylated by GSK-3 sites on Nrf2 and serves as an adaptor protein for Cullin1 E3 ubiquitin ligase. Besides the adaptor proteins, multiple signaling pathways regulate stability of Nrf2. For instance, mTORC1 activates Nrf2 by phosphorylating p62, which serves as inhibitor of Keap1. Another pathway that positively regulates Nrf2 is Insulin/IGF-1 signaling pathway, where Akt inhibits activity of GSK-3 and TSC1/2 (Inhibitors of mTORC1) (Tebay et al. 2015). Even though Nrf2 is mostly known for transcriptional activation of antioxidant proteins, the importance of this transcription factor has been identified in multiple cancers, neurodegenerative diseases and cell proliferation

(Calkins et al. 2009; Huang et al. 2015; Murakami and Motohashi 2015).

Comparing Nrf2 and SKN-1, there are many similarities and differences. For instance, there is no known adaptor protein for SKN-1, except for WDR-23 (WD Repeat protein 23), which was shown to interact with SKN-1c, but the mechanism of action is still unknown (Leung et al. 2015) (Figure 4). Another difference lies in regulation of these transcription factors, where AKT1/2 and SGK-1 inhibit SKN-1, while Akt activates Nrf2. In addition, SKN-1 is missing a bZIP domain for dimerization (Blackwell et al. 2015). Despite these differences, both SKN-1 and Nrf2 are conserved in their function in transcriptional activation of phase II detoxification genes.

1.2.4.2 DAF-16/FOXO

DAF-16 is another transcription factor that is vital for the oxidative stress response and longevity in *C.elegans*. The first discovery of DAF-16 took place in 1981 during a search for dauer mutants (developmental arrest at L2 due to lack of nutrients or crowding) (Riddle et al. 1981). DAF-16 is a downstream target of AGE-1 (PI3K ortholog, Table 1), where mutation in *age-1* resulted in the first long-lived *C.elegans* mutant (Friedman and Johnson 1988). Further studies demonstrated necessity of DAF-16 in *age-1* long-lived mutants (Hsu et al. 2003), and sequencing in 1997 confirmed the orthology between DAF-16 and FOXO (Lin et al. 1997). One of the first discovered targets of DAF-16 was superoxide dismutase 3 (*sod-3*) (Honda and Honda 1999), and until today it is still used as a reporter gene for the activity of DAF-16. In 2006, a chromatin immunoprecipitation (ChIP) assay identified 103 genes regulated by DAF-16, with most of them involved in longevity, metabolism and diapause (Oh et al. 2006). The ability of DAF-16 to regulate expression of its downstream targets is dependent on pathways upstream of DAF-16 (Figure 4). The main negative regulator of DAF-16 is AGE-1 (PI3K), and phosphorylation by AGE-1 does not allow nuclear localization of DAF-16. In addition to AGE-1, nuclear localization of DAF-16 is blocked by binding of 14-3-3 protein orthologs, PAR-5 and FTT-2 on phosphorylated DAF-16 (Figure 4, Table 1) (Berdichevsky et al. 2006). Besides IIS pathway, mTORC1 also plays a role in the inhibition of DAF-16 transcriptional activity (Robida-Stubbs et al. 2012). At the same time, DAF-16 was shown to inhibit member of mTORC1 complex, DAF-15 (Table 1) (Jia et al. 2004), which demonstrated an example of the interconnection among these pathways. In short, DAF-16 is an essential transcription factor with numerous targets required for lifespan regulation, metabolism and oxidative stress response.

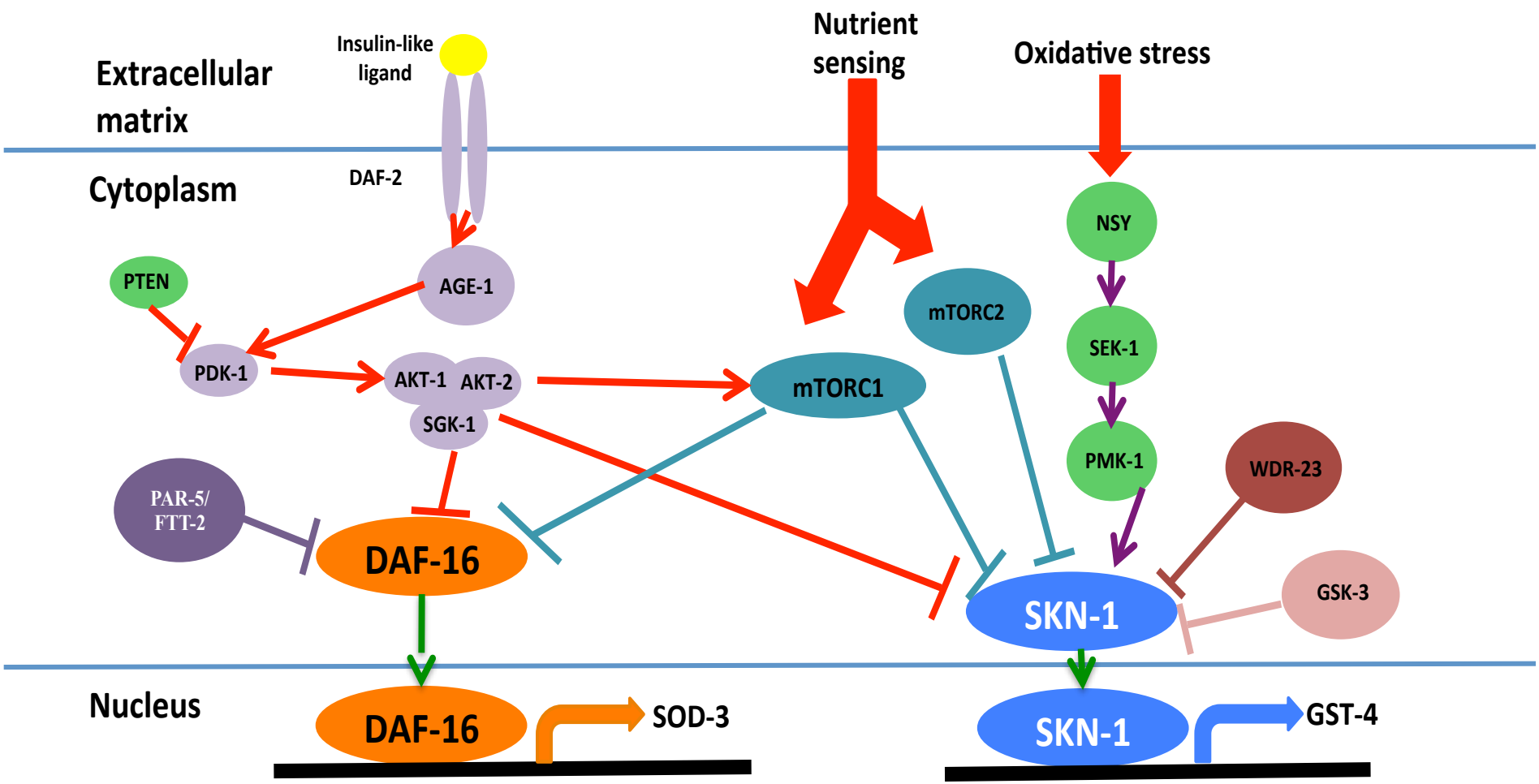

Figure 4. **Regulation of two transcription factors, DAF-16 and SKN-1, by multiple pathways.** Nuclear localization of two transcription factors is inhibited by Insulin/IGF-1 signaling pathway (DAF-2) and mTORC1. SKN-1 is additionally inhibited by mTORC2 and GSK-3. Nuclear localization of SKN-1 is activated by PMK-1/p38 during oxidative stress. Another inhibitor of nuclear localization of SKN-1 is WDR-23 (binds to SKN-1 and inhibits nuclear localization). Upon entrance to the nucleus, DAF-16 mainly activates transcription of Phase I detoxification enzymes, such as SOD-3, while SKN-1 activates transcription of Phase II detoxification enzymes, such as GST-4. Figure adapted from An *et al.* 2005, Tullet *et al.* 2008, Blackwell *et al.* 2015.

1.3 BRAP-2

BRAP2 (BRCA-1 Associated Protein 2) was first identified as protein binding to a nuclear localization motifs of BRCA1 in human B lymphocytes in 1998 (Li et al. 1998). The protein consists of 592 amino acids, and there are three known domains: Coiled-coil (residue 429-537), Ring-type zinc finger (residues 264 to 304) and UBP-type zinc finger (residue 315 to 336). The same study showed conservation of the protein in yeast with 23.7% of overall similarity and 62% similarity in zinc finger domain. Later work has shown that BRAP2 plays a role in many different pathways. Firstly, it was described as IMP (Impedes Mitogenic signal Propagation), where it binds to KSR1 and blocks the formation of a complex between RAF and MEK in quiescent cells, and serves as negative regulator of the RAS/MAPK pathway. The mechanism involves E3 ligase activity of BRAP2, where BRAP2 is auto-ubiquitinated and auto-degradated during the RAS/MAPK pathway activation, and that results in KSR1 release (Matheny et al. 2004; Kolch 2005). Secondly, it has been shown to play a role in the cytoplasmic retention of cell cycle inhibitor, p21 (Asada et al. 2004), specific testicular proteins, HMG20A, NuMA1 and SYNE2 (Davies et al. 2013), and viral proteins SV40 T-ag and CMV UL44 (Fulcher et al. 2010). It was also shown that BRAP2 plays a role in NF-κB pathway by binding to SCF complex (SKP, Cullin, F-box containing complex) and postponing the translocation of NF-κB (nuclear factor kappa-light-chain-enhancer of activated B cells) into the nucleus (Takashima et al. 2013). In addition, BRAP2 is responsible for ubiquitination of the human protein phosphatase, HsCdc14A (Chen et al. 2009). A recent paper showed the role of BRAP2 in germ cells in testis, where binding of BRAP2 to three important proteins in mouse testis, PHLPP1 (PH domain and leucine rich repeat protein phosphatase 1), AKAP3 (A-Kinase anchor protein) and DNMT1 (DNA methyl transferase 1), was demonstrated by co-

immunoprecipitation assay (Fatima et al. 2015). Overall, the main role of mammalian BRAP2 was demonstrated as cytoplasmic retention protein.

The ortholog of BRAP2 in *C.elegans,* BRAP-2, is highly homologous and also consists of 592 amino acids, but with five distinct domains (Figure 5). The *C. elegans* BRAP-2 contains a BRAP-2 domain (residue 144 to 253) in the N-terminal region, which permits binding to the nuclear localization signal motif. The leucine heptad repeats sequence located in the C-terminus (residue 439 to 550), is a coiled coil structural motif, necessary for homodimerization and involved in gene expression. A low complexity region (residue 576 to 590) is predicted to be involved in translation and stress response (Coletta et al. 2010; Koon and Kubiseski 2010). BRAP-2 has been implicated in regulation of the oxidative stress pathway in *C. elegans,* where mutation in BRAP-2 (partial deletion in the C-terminal portion (residue 319 to 578) (Figure 5) leads to lethality and developmental arrest of worms in early stages after exposure to hydrogen peroxide and paraquat (Koon and Kubiseski 2010). In addition, BRAP-2 was also confirmed to bind to KSR-2, which suggests it is a part of ERK-1/2 Ras pathway in worms as well (Hu *et al.* Manuscript in preparation). Furthermore, nuclear localization of SKN-1 (activated by MPK-1 (ortholog of ERK1)) (Okuyama et al. 2010) is increased in *brap-2(ok1492)* mutant worms (Hu *et al.* Manuscript in preparations). In short, the ongoing research on BRAP-2 in nematodes demonstrates the same functional roles as is observed in mammals.

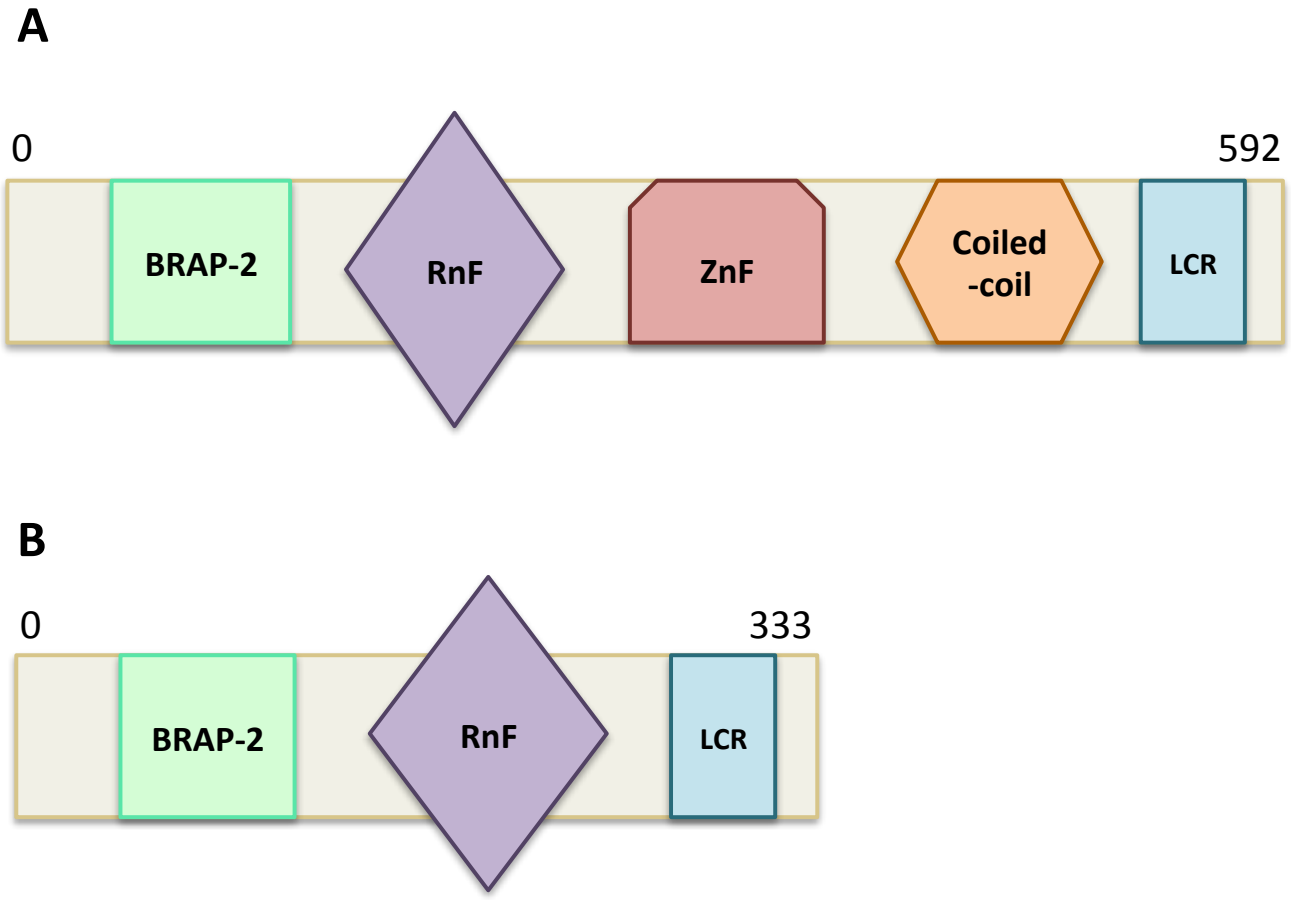

Figure 5. Representation of *C.elegans's* BRAP-2 protein. A. Full length BRAP-2 protein. BRAP2 domain is required for dimerization, Ring Finger domain is required for autodegradation. **B**. C-terminal deletion in BRAP-2, *brap-2(ok1492).* Deletion of UBP ZnF and Leucine heptad Repeats results in nuclear localization of *skn-1* and overexpression of detoxification enzyme, *gst-4.* Figure adapted from Koon and Kubiseski (2010).

1.4 SEM-4

SEM-4 (Sex Muscle abnormal 4) is a zinc finger (ZnF) containing transcription factor in *C.elegans* with eight classical, Cystine-Histidine (Cys_2His_2), zinc fingers in its structure. The size of the protein is 744 amino acids, where zinc fingers are allocated throughout the sequence, with three double zinc fingers and two single ones (Figure 6). In addition to zinc fingers, SEM-4 contains low-complexity regions (LCRs) (SMART structural prediction), which is similar to the structure within BRAP-2 (discussed in Section 1.3). While BRAP-2 contains only one terminal LCR, SEM-4 contains four central and three terminal LCRs. According to Coletta *et.al.* (2010), the location of LCRs plays a role in the function of the protein, where proteins with terminal LCRs are usually important in stress response, translation and transport of proteins, while proteins containing central LCRs are associated with transcription and its regulation. Since SEM-4 contains LCRs in both central and terminal regions, it can easily be associated with stress response, transcription, transcriptional regulation and possibly transport of proteins. It is doubtful that SEM-4 plays a role in translation of protein due to the reported nuclear localization of SEM-4 (Kagias et al. 2012). On the other hand, interaction between SEM-4 and FTT-2 (ortholog of 14-3-3) has been shown with a high throughput Yeast-two-Hybrid system (Simonis et al. 2009). Since FTT-2 is a cytoplasmic protein, it can be speculated that SEM-4 is mostly present in the nucleus, but can also exist in the cytoplasm. The expression of this protein is found throughout the worm, and SEM-4 has been reported to be expressed in motor neurons, body muscle cells, coelomocytes, vulval precursor cells, hypodermis, head, and tail blast cells (Basson and Horvitz 1996; Grant et al. 2000). In addition, SEM-4 has been predicted to have a genetic interaction with many proteins, such as MEC-4 *(*sodium channel), LIN-39 (homeobox protein), UNC-55 (UNCoordinated family member) (Syntichaki and Tavernarakis 2004; Ezziane 2012). Physical

interactions with SEM-4 have been identified with only two proteins, EGL-27 (Egg-laying defective 27) and CEH-6 (*C.elegans* Homeobox 6) (Kagias et al. 2012).

The first *sem-4* mutant worm has been identified through a distinctive phenotype – an egg laying defective, and the mutation was a missense mutation in the C-terminal part of the gene, where last three zinc fingers were not transcribed (*sem-4(n1378)*). In later studies, *sem-4(n1378)* has been considered as a weaker mutant allele, while *sem-4(n1971)* (null allele, where no zinc fingers are transcribed) is the strongest allele for studying effects of SEM-4 expression on the worm (Figure 6). Analysis of M-lineage (post-embryonic lineage that arise from mesodermal blast (MS)) has shown that sex myoblast of wild-type worms are transformed into body muscle cells in the absence of functional SEM-4 (Figure 7) (Basson and Horvitz 1996). Further mutant analysis studies have shown a wide range of expression and functions for SEM-4 in *C.elegans.* In addition to the development of a proper vulva, expression of SEM-4 has been shown to be important for the proper development and function of motor neurons and touch receptor neurons in the animal (Basson and Horvitz 1996; Toker et al. 2003; Kagias et al. 2012). Besides that, recent study found that SEM-4 is part of the NODE complex (CEH-6, EGL-27, SOX-2 (SRY (sex determining region Y)-box 2), SEM-4) that activates EGL-5 (Egg-laying defective 5), and allows transformation of Y cell (rectal epithelial cell) into PDA cell (motor neuron) (Figure 7) (Kagias et al. 2012). Overall, SEM-4 is a multifunctional protein involved in neuronal, vulval and body wall muscle cell fate.

SEM-4 has human orthologs –*SALL1, SALL2, SALL3* and *SALL4,* as well as the *Drosophila* ortholog, known as the SPALT gene (Kuhnlein et al. 1997), but the exact mechanisms of gene regulations by SEM-4, SALL or SPALT are still unknown. There are known diseases associated with mutations in different *SALL* genes in humans. For instance, a mutation in *SALL1* is linked to the autosomal disease, called Townes-Brocks syndrome (Netzer

et al. 2006). Next, mutant forms of *SALL2* are present in human ovarian carcinoma (Toker et al. 2003) and mutation in *SALL4* leads to Okihiro syndrome (Duane-radial ray syndrome) (Kohlhase et al. 2005). The function of *SALL3* was recently discovered as an inhibitor of DNA methylation (Shikauchi et al. 2009). As for the *spalt* gene in *Drosophila*, it is required during embryogenesis and organogenesis in the fly (Kuhnlein et al. 1997). The structures of proteins between species are all well conserved, where zinc fingers and linkers reach up to 90% in conservation (Figure 8).

Mutation alleles of SEM-4 range from weak to null, and are readily available. In addition, SEM-4 transgenic worms are also available. Since, *sem-4* mutant and *sem-4* overexpressing strains are easily obtainable for use, it is possible to test the effects of SEM-4 on different pathways.

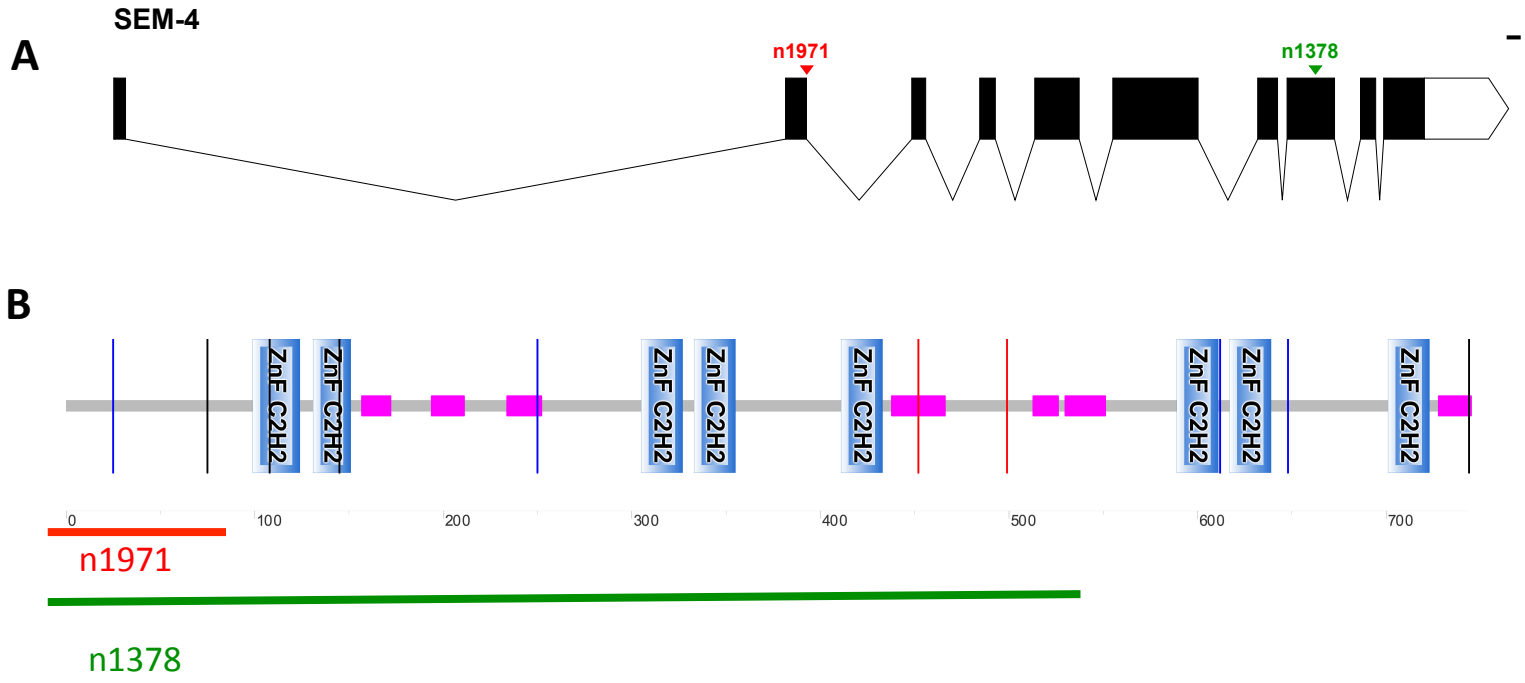

Figure 6. Structure of SEM-4 and mutant allele location. **(A)** Graphical representation of *sem-4* transcript including sites of mutation for two mutant allele, *n1378* and *n1971*. The graph was generated using Exon-Intron Graphical Maker (http://www.wormweb.org/exonintron). **(B)** Structure of SEM-4 with 8 zinc fingers (blue) and 7 LCR regions (pink). Underlined portions show deleted portions of protein in two mutant alleles. *sem-4(n1971)* is expressing first 75 amino acids, and *sem-4(n1378)* is expressing 569 amino acids or first five zinc fingers. The protein structure was predicted by SMART database (http://smart.embl.de/).

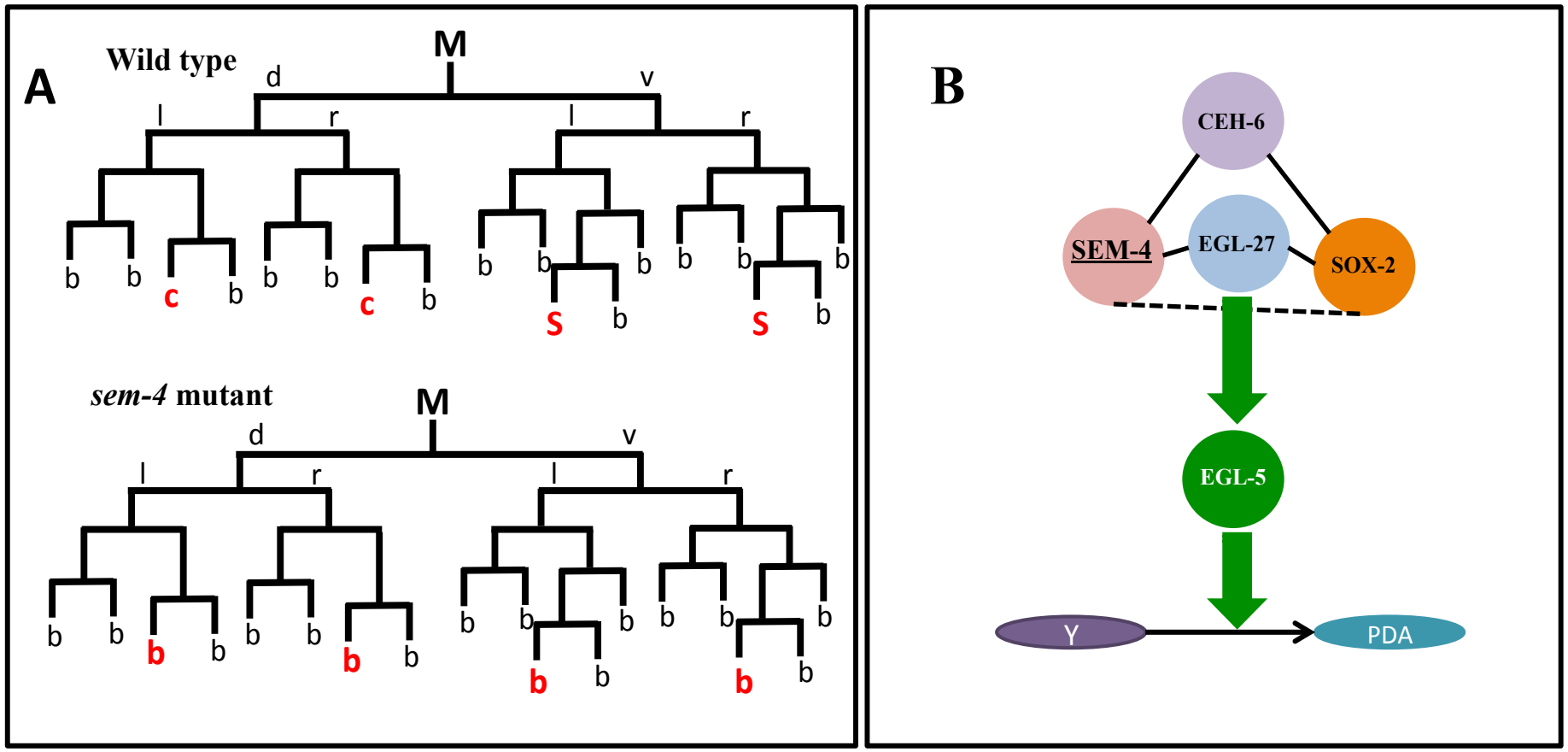

Figure 7. Importance of SEM-4 during development of *C.elegans*. SEM-4's expression is necessary in many tissues for proper development. **A**. Mutation in *sem-4* causes loss of coelomocytes (**c**) and Sex Muscles (**S**) in the worm, which develop into body muscle cells (**b**). Figure adapted from Basson and Horvitz, 1996. **B**. SEM-4 is required for Y to PDA reprogramming. Figure adapted from Kagias *et al.* 2012.

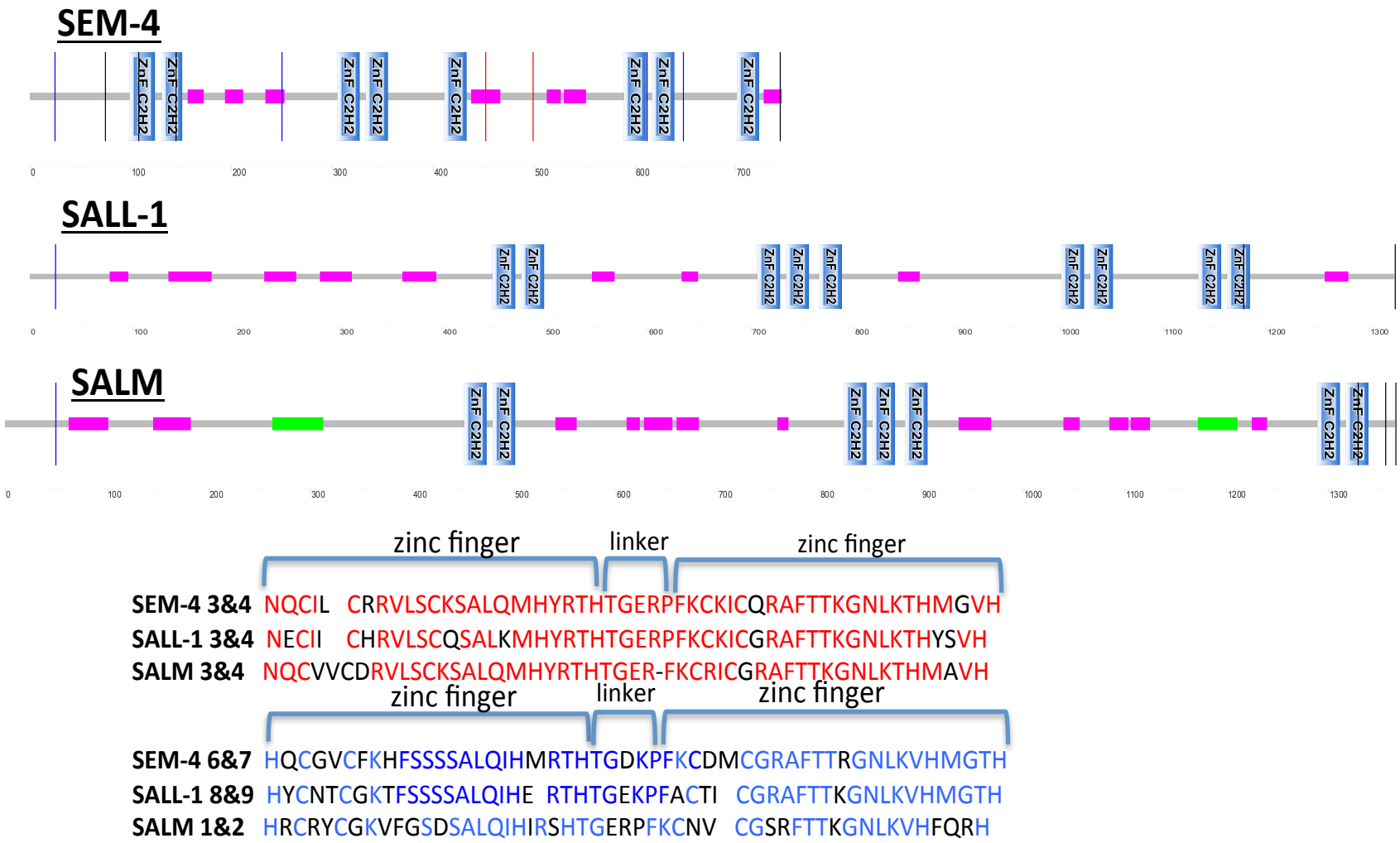

Figure 8. Similarities in protein sequence in SEM-4, SALL-1 and SALM. (A) Structures of SEM-4 (*C.elegans*), SALL-1 (*H.sapiens*) and SALM (*Drosophila melanogaster*) with zinc fingers (blue) and LCR regions (pink) and coiled-coil region in SALM (green). **(B)** Comparison of sequence similarities among zinc fingers in SEM-4, SALL-1 and SALM.

1.5 Research rationale and objective

In this study, SEM-4 was identified as a candidate from an RNAi screen of *C.elegans* transcription factors (TF) (The RNAi screen was performed by Lesley MacNeil and Marian Walhout) (Figure 9, Table 2). The screen analyzed the possible involvement of 940 transcription factors in the BRAP-2/SKN-1 detoxification response in *C.elegans.* SEM-4 was identified as an activator of *gst-4* in a *brap-2* mutant background. The rationale of the screen is described below.

The previous work of our lab reported that C-terminal deletion of BRAP-2 (UBP-ZnF and leucine heptad repeats domains) leads to significant increase in *gst-4* mRNA levels, as well as intestinal nuclear localization of SKN-1 (Hu Q et al. Manuscript in preparation). In order to identify additional players in regulation of *gst-4* expression, our lab performed an RNAi screen of 940 transcription factors (Figure 9). For that purpose, *brap-2(ok1492);Pgst-4::gfp* worms were fed bacteria expressing double stranded RNA (dsRNA) of transcription factors. As a control, worms were fed an empty vector, pL4440. Another control was the use of wild-type strain expressing GFP under *gst-4* promoter (*Pgst4::gfp*). GFP expression for the two strains was quantified, and transcription factors that demonstrated significant decrease of GFP in *brap-2;Pgst-4::gfp* worms, and not *Pgst-4::gfp* worms, were scored as positive candidates for BRAP-2/SKN-1 detoxification pathway. Overall, the screen resulted in more than 20 transcription factors (Table 2). SEM-4 was chosen due to its high expression in various cells and tissues in the worm. In addition, the availability of worms with different mutations in *sem-4* allowed for studying the effects of the gene on the BRAP-2/SKN-1/ROS detoxification pathway.

Here I have identified SEM-4 as a novel protein in the SKN-1/BRAP-2/ROS detoxification pathway, where SEM-4 activates expression of *gst-4* through regulation expression of *skn-1c.* Next, I have determined importance of SEM-4 for the expression other detoxification enzymes besides GST-4, and the requirement of SEM-4 for SKN-1 induced

longevity in worms was experimentally proven. In addition, I have demonstrated that SEM-4 is necessary to cope with overproduction of reactive oxygen species (ROS), and is necessary for survival of worms during constant oxidative stress. Overall, the previously well-studied and developmentally important gene, *sem-4,* was shown to be indispensable for the oxidative stress response pathway.

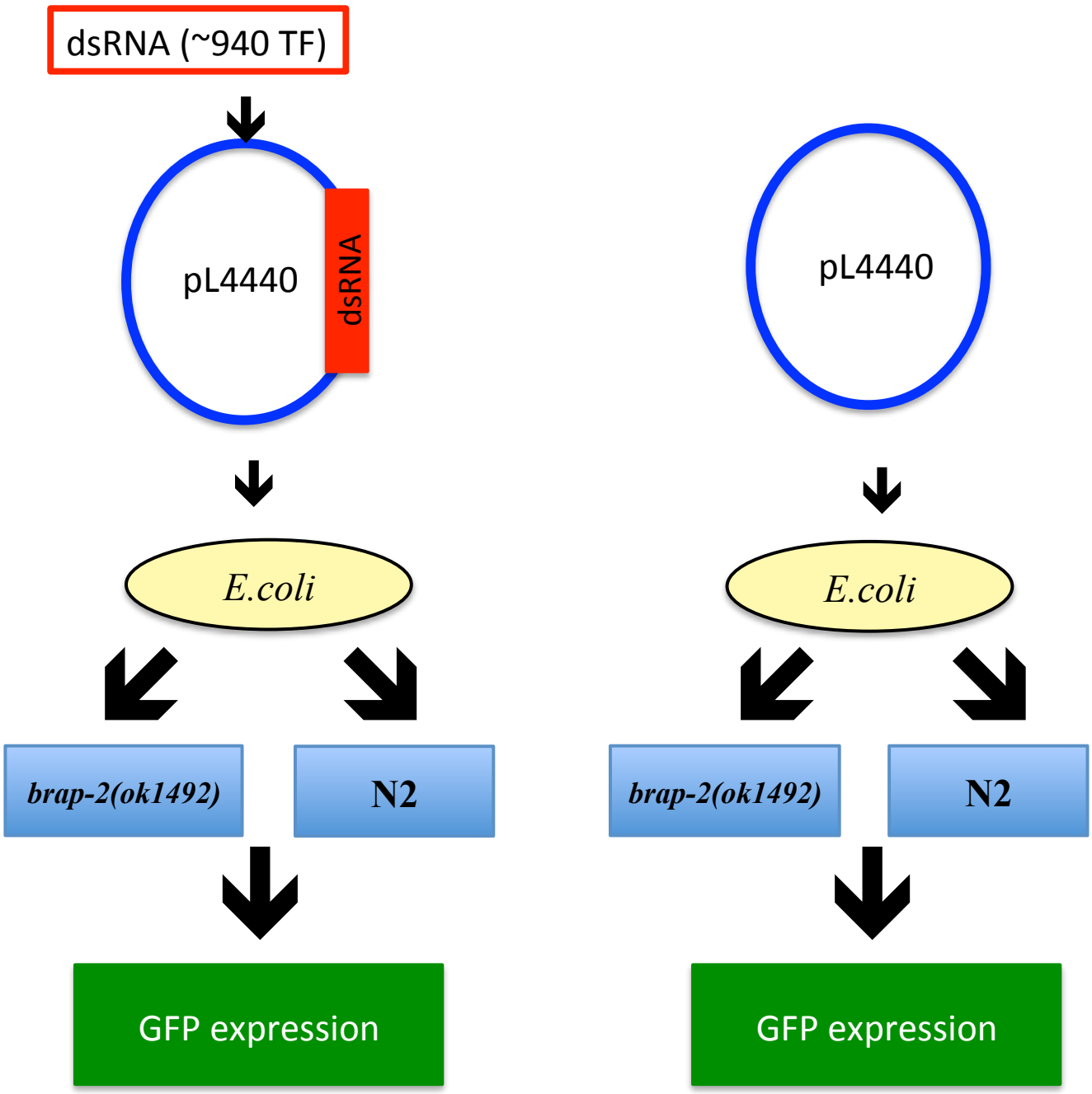

Figure 9. Initial RNAi screen of the project. The screen tested 940 transcription factors and determined that about 20 transcription factors lower *gst-4* expression in *brap-2* worms. For the screen, dsRNA of each transcription factor was fed to wild type and *brap-2* worms in order to determine changes in *gst-4* expression; empty vector was fed as a control. Expression of *gst-4* was based on GFP expression in *Pgst-4::gfp* worms.

Table 2. List of candidate genes for activation of *gst-4* in *brap-2(ok1492)* worms

***C. elegans* gene**	**Vertebrate homolog protein**
elt-2	GATA Family
elt-3	GATA Family
fkh-9	Forkhead/HNF3 family
gei-3	BED finger domain
hlh-11	bHLH/AP4
lin-48	C2H2-type Zinc Finger Protein
nhr-14	Estrogen receptor
nhr-37	Hormone receptor
nhr-49	Hepatocyte nuclear factor 4
pqn-47	C11orf9
sbp-1	Sterol regulatory element
sem-4	**Sal-like protein**
skn-1	Nrf2
tbx-2	T-box transcription factor
vab-3	Pax-6 paired domain
zip-6	bZIP transcription factor

2. Materials and Methods

2.1 *C. elegans* strains, growth and maintenance

Worm strains were grown and maintained at room temperature as described by Brenner (Brenner 1974) for all listed experiments. Strains were obtained from the CGC (*Caenorhabditis* Genetics Center) and NBRP (The National Bioresource Project of Japan). The following strains were used: N2 Bristol, YF15 [*brap-2(ok1492)II*], CL2166 [dvIS19 (*gst-4::gfp*)], YF67 [*brap-2(ok1492)II;* dvIS19(*gst-4::*gfp)], MT3179 [*sem-4(n1378) I*], MT5825 [*sem-4(n1971) I*], OP57 [*unc-119(ed3) III*; wgIs57 [*sem-4*::TY1::EGFP::3xFLAG(92C12) + *unc-119(+)*]], YF162 [*brap-2(ok1492)II;* dvIS19 (*gst-4::*gfp); *sem-4(n1378) I*], YF163 [dvIS19 (*gst-4::*gfp); *sem-4(n1378) I*], LD1250 [IS008 (*skn-1b/c::gfp::rol-6)*], YF164 [IS008 (*skn-1b/c::gfp::rol-6)*; *sem-4(n1378) I*], YF167 [*brap-2(ok1492)II; sem-4(n1378) I*], YF168 [*brap-2(ok1492)II; unc-119(ed3) III*; wgIs57 [*sem-4*::TY1::EGFP::3xFLAG(92C12) + *unc-119(+)*]], YF170 [IS008 (*skn-1b/c::gfp::rol-6)*; *sem-4(n1971) I*], YF171 [IS008 (*skn-1b/c::gfp::rol-6)*; *unc-119(ed3) III*; wgIs57 [*sem-4*::TY1::EGFP::3xFLAG(92C12) + *unc-119(+)*]], YF174 [*brap-2(ok1492)II; sem-4(n1971) I*], YF175 [dvIS19 (*gst-4::*gfp); *sem-4(n1971) I*], YF176 [*brap-2(ok1492)II;* dvIS19 (*gst-4::*gfp); *sem-4(n1971) I*], LD001 [IS007 (*Pskn-1::gfp::rol-6)*], YF177 [IS007 (*Pskn-1::gfp::rol-6*; *sem-4(n1971) I],* YF178[IS007 (*Pskn-1::gfp::rol-6*); *unc-119(ed3) III*; wgIs57 [*sem-4*::TY1::EGFP::3xFLAG(92C12) + *unc-119(+)*]], DR466 [*him-5 (e1490)V*], AH102 [*lip-1(zh15) IV*].

2.2 RNAi

For this experiment, *E. coli* HT115 was transformed with dsRNA (double stranded RNA) of *sem-4* and empty vector pL4440. The cells were grown overnight at 37^{o}C on LB+AMP plate, and one colony from each plate was transferred into 2mL of LB+AMP and grown overnight at 37^{o}C in a shaker. Next, freshly made RNAi plates (Appendix A) were seeded with 100uL suspension of each bacterial culture and allowed to dry overnight. Worms, *brap-2(ok1492);gst-4::gfp,* were synchronized by bleaching and allowed to grow untill L4 stage on regular NGM plates and then transferred to RNAi plates containing dsRNA of *sem-4* or empty vector pL4440 for one day. Finally, L4 stage worms were observed under confocal microscope (section 2.3) using z-stack option, where the section of the worm with the highest GFP expression was chosen for the analysis. GFP expression was quantified with ImageJ® 64 Software by tracing each worm individually. The background fluorescence was quantified as an average of three small areas in the close proximity of the worm and was subtracted from the fluorescence values of the worm. The experiment was repeated three times and a minimum of 10 worms were analyzed for each trial.

2.3 Confocal microscopy and fluorescence quantification

Expression of genes with a GFP fusion tag were visualized in *vivo* by confocal microscopy (LSM 700 Zeiss) using z-stack option. Worms were grown to L4/young adult stage, transferred onto slide with a 2% Agarose pad and immobilized with 2 mM Levamisole. Worms were then covered with coverslip and sealed with nail polish. Slides were left to dry for 2 minutes and then observed under confocal microscope with 20X, 40X or 63X objective at excitation of 488nm (Alexa 488), and z-stack pictures were taken. The images with the highest GFP expression were used for the analysis. Fluorescence was quantified by tracing each worm

manually and mean fluorescence per area was obtained using ImageJ® 64 Software, where the background fluorescence was subtracted. For each experiment, a minimum of 10 worms were analyzed. Statistical analysis (student T-test) and graphs were generated using Graphpad Prism® 6.0 Software. The following strains were analyzed using confocal microscopy: CL2166 [dvIS19 (*gst-4::gfp*)], YF67 [*brap-2(ok1492)II;* dvIS19(*gst-4::*gfp)], OP57 [*unc-119(ed3) III*; wgIs57 [*sem-4*::TY1::EGFP::3xFLAG(92C12) + *unc-119(+)*]], YF162 [*brap-2(ok1492)II;* dvIS19 (*gst-4::*gfp); *sem-4(n1378) I*], YF163 [dvIS19 (*gst-4::*gfp); *sem-4(n1378) I*], YF167 [*brap-2(ok1492)II; sem-4(n1378) I*], YF168 [*brap-2(ok1492)II; unc-119(ed3) III*; wgIs57 [*sem-4*::TY1::EGFP::3xFLAG(92C12) + *unc-119(+)*]],YF175 [dvIS19 (*gst-4::*gfp); *sem-4(n1971) I*], YF176 [*brap-2(ok1492)II;* dvIS19 (*gst-4::*gfp); *sem-4(n1971) I*], YF177 [*skn-1::gfp (*IS007); *sem-4(n1971) I],* YF178[*skn-1::gfp (*IS007); *unc-119(ed3) III*; wgIs57 [*sem-4*::TY1::EGFP::3xFLAG(92C12) + *unc-119(+)*]].

2.4 Generation of double mutants

The production of double mutant worms was performed in multiple steps. First, hermaphrodites of one strain were crossed with *him-5 (e1490)* males, in a 1:2 ratio (*i.e*. 5 hermaphrodites and 10 males were placed onto one unseeded NGM plate). Next, male progeny were picked and crossed with L2 of the second strain. The progeny of the last cross were picked onto individual plates (F1 generation) and allowed to lay eggs (F2 generation). F1 generation was tested for the presence of the required mutation by Single Worm Polymerase Chain Reaction (SW-PCR) (Section 2.5) or using confocal microscopy. In case of confocal microscopy, a minimum of 15 worms (F2 generation) were picked and tested for the presence of the mutation. All positive F2 plates were re-picked into individual plates (F3 generation), and were re-tested as described above. In few instances, genotype confirmation did not require SW-PCR or confocal

microscopy, as the phenotypic distinction was sufficient to identify double mutants (*i.e.* YF164 [IS008 (*skn-1b/c::gfp::rol-6)*; *sem-4(n1378) I*], roller with inability to lay eggs).

2.5 Single worm PCR

SW-PCR was performed in order to identify the presence of a mutation in the strain. Worms were picked individually into PCR tubes containing 4 uL of Lysis Buffer (Proteinase K (NEB), 1X ThermoPol buffer, ddH_2O) and frozen at -80^oC for a minimum of 30 minutes. Tubes were then transferred into a PCR machine (Biometra T Personal Thermocycler) in order to deactivate Proteinase K (65^oC for 1 hour, 95^oC for 15 min). Next, 20 ul of PCR mix (described below) was added into each tube and the PCR reaction was performed as described below. PCR products were mixed with 6X loading dye and run in a 1% Agarose (Sigma) gel at 100V using Gel XL Ultra V-2 gel box (Labnet Interantional Inc.). The presence of wild-type or mutant bands was detected by exposing the gel under UV light.

PCR mix for 10 reactions:

- 1ul Primer FOR
- 1ul Primer REV
- 1ul Taq DNA Polymerase
- 20ul ThermoPol Buffer
- 20ul dNTP
- 157ul ddH_2O

PCR cycle

1. 95^oC for 5 minutes
2. 95^oC for 15 seconds
3. 55^oC for 15 seconds
4. 75^oC for 60 seconds
5. Repeat 35 times – steps 2-4
6. 75^oC for 5 minutes

2.6 Oxidative stress assays and survival

This stress assay was used in order to test strain sensitivity to oxidative stress induced by Paraquat (Section 2.8), the quantity of ROS generation (Section 2.6) and differential gene expression (Section 2.10). For all experiments, Paraquat was used in various concentrations, and action of paraquat is demonstrated in Supplementary Fig.1. Paraquat (Methyl viologen dichloride hydrate) (Sigma (856177 Aldrich)) was dissolved in filtered ddH_2O to stock concentration of 1M. The stock concentration was kept at -20^oC and used as required. Strains were grown to the L4 stage before Paraquat treatment. In experiments involving ROS and gene expression quantification, worms were placed in 100 mM Paraquat for 1 hour, and then washed with M9 buffer (Appendix A) three times. For survival assays, L4 stage worms were transferred to plates containing 2 mM Paraquat and scored for survival every day. Worms were transferred to fresh plates every five days. All experiments were repeated at least three times.

2.7 ROS quantification assay

The production of ROS (reactive oxygen species) was quantified using a commercially available dye, 2,7-dichlorodihydrofluorescein-diacetate (DCFDA). The levels of ROS were measured in four strains before and after 100 mM Paraquat stress: N2, *brap-2(ok1492), sem-4(n1378),* and *sem-4(n1971)* using two methods: a hybrid multimode microplate reader and confocal microscopy. For both experiments, all strains were synchronized and grown to L4 stage, and then incubated with 0 mM or 100 mM Paraquat for 1 hour. After incubation, worms were washed with M9 buffer three times, and then used for the experiment. For the microplate reader, 200 worms/well from each strain were transferred into each well of a black 96-well plate, and mixed with 100 µL of 50 µM DCFDA (diluted in 1X PBS). The fluorescence was measured kinetically every two minutes for five hours (300 minutes in total) using the BioTek, Synergy H4

microplate reader at excitation 485 nm and emission 520 nm, at 25^{o}C (protocol adapted from (Yang et al. 2013)). All readings were performed in triplicates for each strain and treatment, and average fluorescence was used to generate the graphs. The production of ROS in the same four strains was confirmed by using confocal microscopy. The procedure was followed as described above with the following changes: after Paraquat treatment worms were placed in 1 mL of 25 μM DCFDA, and incubated for 1 hour in the dark. After incubation, worms were washed three times with M9 buffer, and then observed under the confocal microscope (protocol adapted from (Lu et al. 2014)) as described above (Section 2.2). The action of DCFDA is shown in Supplementary Fig.2.

2.8 Lifespan Survival assays

Adults from eight strains: N2*, skn-1(+), sem-4(n1378), sem-4(n1971), sem-4(+), skn-1(+);sem-4(n1378), skn-1(+);sem-4(n1971)* and *skn-1(+);sem-4(+)* were bleached in order to obtain a synchronized population of worms. Next, juveniles from all strains were allowed to grow to L4 stage and then 15 worms/plate were transferred into new plates containing fluorodeoxyuridine (FUDR), a commercially available compound that halts egg-laying to simplify worm scoring, for a total of 45 worms/strain. Worms were then counted every two days, and a worm was pronounced dead if it was unresponsive to touch using a worm pick. Results were entered into OASIS Software and were analyzed statistically by OASIS Software (Yang et al. 2011), where Kaplan-Meier estimator, Mean Lifespan and Long rank test were generated. The graphs were produced by using Graphpad Prism® 6.0. This experiment was performed independently three times. The Mean Lifespan values obtained from the three trials (OASIS Software) were analyzed for significance by using Graphpad Prism® 6.0 (Student-t test).

Similar to the Lifespan assay, the survival assay was performed using the same procedure with a

few changes. For this experiment, three strains were used: N2*, sem-4(n1378),* and *sem-4(n1971)*. Sixty L4 stage worms were transferred onto new plates containing FUDR and 2 mM Paraquat. Worms were then counted every 24 hours. A worm was pronounced dead if it was unresponsive to touch using a worm pick. Results were analyzed statistically using OASIS Software (Yang et al. 2011) and graphs produced using Graphpad Prism® 6.0. This experiment was performed independently three times. Statistical analyses were performed by OASIS and include Kaplan-Meier estimator, Mean Lifespan and Long rank test.

2.9. Subcloning

For this experiment, transcription factors SKN-1 and SEM-4, were subcloned into mammalian expression vectors. First, the *sem-4* gene EST was subcloned using Gateway cloning system (Invitrogen) into pDONR^{TM} 221 vector (BP reaction, BP Clonase II). The reaction was transformed into OneShot Omni Max 2T1^{R} cells. The cells were grown on an LB plate containing 50 ug/uL of Kanamycin (KAN), and colonies were screened with M13 FOR primer and GW SEM-4 REV primer (Appendix B). The positive colonies were grown overnight in 2 mL LB+KAN, plasmid DNA was extracted using GenElute Plasmid Miniprep Kit (Sigma). The sequence was confirmed by TCAG DNA Sequencing Facilities (Sick Kids, Toronto). The positive sample was used for LR reaction, where *sem-4* gene was subcloned into p3XFLAG-tagged vector (V1899.2). The LR reaction (LR Clonase II, Invitrogen) product was transformed into OneShot Omni Max 2T1^{R} cells. The cells were grown overnight at 37^{o}C on LB plate containing Ampicillin (AMP). Colonies were screened using GW SEM-4 FOR and GW SEM-4 REV primers (Appendix). The positive colonies were grown in LB+AMP overnight, and plasmid DNA was extracted using GenElute Plasmid Miniprep Kit (Sigma). The sample that matched >97% of sequencing was used for Nucleobond Xtra Midi plasmid DNA isolation (Clontech).

The final construct was the used for cell transfection and co-immunoprecipitation. The *skn-1* gene was subcloned into GFP vector using In-Fusion Dry-Down PCR Cloning Kit by ClonTech. The subcloning was performed by previous graduate student.

2.10. Expression and co-immunoprecipitation of proteins

For this experiment, each construct was transfected individually, co-transfected with the vector control (negative control), and co-transfected with each other (i.e. SKN-1::GFP and SEM-4::3XFlag) into 60% confluent Human Embryonic Kidney (HEK) 293T cells using 10 cm plates. The cells were allowed to grow for another 48 hours and harvested. Next, input lysates (30 uL/sample) were kept, and the rest (approximately 1mL of lysate) was used for co-immunoprecipitation assay. For this assay, lysates were incubated for 1 hour on a rocker at 4^{o}C with monoclonal mouse ANTI-FLAG M2 (Sigma) or monoclonal rabbit anti-GFP antibody (Cell Signaling) and protein A Sepharose beads (CL-48, GE Healthcare). Next, beads were washed with Wash Buffer (Appendix A) three times, resuspended in 2X SDS, boiled for 5 minutes at 100^{o}C, centrifuged for 2 minutes at 2800xg and then loaded on 8% acrylamide gel. After running the gel for 20 minutes at 85V and 45 minutes at 185V on Biorad Apparatus, proteins on the gel were transferred into PVDF membrane using Trans-Blot Semi-Dry Transfer Cell (Biorad). The membranes were blotted for 30 minutes at room temperature with 5% Skim Milk in TBST, and then probed with 1^{o} antibody overnight at 4^{o}C on a rocker, using mouse anti-Flag (1:5000) for p3XFlag-SEM-4 and rabbit anti-GFP (1:5000) for peGFP-SKN-1. Next, the membranes were washed three times, 30 minutes each with 1X TBST buffer, and probed with 2^{o} antibody: goat-anti-mouse HRP for p3XFLAG-SEM-4 (1:20000) and goat-anti-rabbit HRP for pGFP-SKN-1 (1:20000) for 45 minutes at room temperature, rocking. The membranes were washed three times, 20 minutes each, with 1X TBST at room temperature on the rocker. After the washes,

membranes were incubated for 1 min with Pierce™ ECL Western Blotting Substrate (Thermoscientific) and exposed to the CL-XPosure™ film (Thermoscientific) in the dark room.

The same rationale as described above was used for interactions with MDT-15, with a few changes: *sem-4* gene was subcloned into an expression vector that would produce GST-tagged protein. We then co-transfected the cells with MDT-15::HA, and co-immunoprecipitated with GST beads or anti-HA antibody.

2.11 RNA isolation and RT-qPCR

For the purpose of quantification of mRNA levels of specific genes in various strains of *C.elegans*, RNA was isolated from whole worms. First, mix staged worms were grown on Nematode Growth Media (NGM) plates until confluent. Next, worms were washed three times with M9 buffer and used for RNA isolation immediately or frozen at -80^{o}C. RNA isolation was performed using TRI reagent (Sigma), where worms were vortexed for 15 minutes at 4^{o}C, mixed with chloroform and centrifuged for 15 minutes at 12000 x g at 4^{o}C. The top clear layer was transferred into a new 1.5mL tube, and mixed with chloroform again and centrifuged. The top layer from this second tube was transferred into a new tube and mixed with 2-Propanol in 1:1 ratio and centrifuged for 10 minutes at 12000 x g. The RNA pellet was washed twice with 70% Ethyl Alcohol (diluted with DEPC water (RNase, DNase free water)), and diluted in 10 ul of DEPC water. In order to remove DNA from the sample, the RNA sample was treated with DNase enzyme (Invitrogen, AM1906) for 25 minutes at 37^{o}C, and the DNase reaction was stopped by adding DNase deactivation enzyme and centrifuged. Next, the top clear layer was transferred into a new Eppendorf tube and the concentration of RNA was determined using NanoDrop 2000 (Thermo Scientific). For each sample, 0.5 μg of RNA was used for RNA to cDNA reaction with Applied Biosystem RNA to cDNA kit, where 20 uL reaction was set up

according to manufacturer's protocol in triplicates. Levels of mRNA were measured using SYBR Advantage qPCR Premix (Clontech) on Qiagen Rotor-Gene Q, and compared to levels in N2 worms (wildtype control). The internal control gene that was used for analysis was *act-1*. The relative ratio was quantified using $\Delta\Delta C_T$ method, where relative expression of the target gene was quantified according to the formula:

2^(-((Strain target C_T - N2 target C_T) - (Strain ACT-1 C_T - N2 ACT-1 C_T)))

2.12 *sem-4* expression in *brap-2(ok1492)*

In order to test the affect of BRAP-2 on localization of SEM-4, double mutants of OP57 [*unc-119(ed3) III*; wgIs57 [*sem-4*::TY1::EGFP::3xFLAG(92C12) + *unc-119(+)*]] and YF(*brap-2(ok1492))* were generated. Presence of the *brap-2(ok1492)* allele was tested using SW-PCR, and expression of SEM-4::GFP was confirmed under confocal microscope (LSM 700 Zeiss) using z-stack option. Localization and expression of SEM-4::GFP in OP57;YF15 worms was visualized with confocal microscope and then compared to the expression and localization of SEM-4::GFP in OP57 worms. The experiment was repeated three times, and a minimum of 10 worms were visualized for each trial.

2.13 Primer design

All primers for RT-qPCR experiments were generated using Primer3, a free online tool (http://simgene.com/Primer3). The primers for genotyping were generated manually based on the required region.

2.14 Statistical analysis

Statistical analysis for RT-qPCR values, Image J fluorescence results, and the mean of the Mean Lifespan were performed using a Student-t test from Graphpad Prism ® 6.0 Software. Each statistical analysis consisted of at least three biological replicates, and n number is identified in figure legends. C_T values for RT-qPCR results were derived from technical triplicates for each biological replicate.

Lifespan and survival plot statistics (Kaplan-Meier estimator, Mean Lifespan and Long rank test) were generated by OASIS software. Both assays were performed three times, with 45-60 worms per trial and strain.

3. Results

The main purpose of this study is to determine the role of SEM-4 in regulating the oxidative stress pathway in *C. elegans*. SEM-4 is an eight zinc-finger containing transcription factor, and is expressed in neurons, muscle cells, coelomocytes, vulval precursor cells, hypodermal cells, and tail blast cells (Toker et al. 2003). *C. elegans* with *sem-4* mutations, or overexpression of SEM-4 are viable and readily available, which makes it possible to test for the effect of SEM-4 in BRAP-2/SKN-1/ROS pathway.

3.1 SEM-4 affects transcriptional expression of *gst-4* in *brap-2(ok1492)* mutant worms

An initial RNAi screen (Section 1.5, Figure 9) identified 20 candidate transcription factors by qualitative analysis, and thus we were interested in quantifying *Pgst-4* expression in *brap-2;Pgst-4::gfp* and *Pgst-4::gfp* worms with RNAi knockdown of our chosen candidate gene, *sem-4*. We observed a significant decrease (38.4%, $p<0.0001$) in GFP levels only in worms with a *brap-2* mutant background (Figure 10).

In order to verify the RNAi results, we generated double mutant worms of *sem-4(-)* and *brap-2;Pgst-4::gfp,* and *sem-4(-);Pgst-4::gfp*. Quantification of *gst-4'*s promoter efficiency in these strains revealed an 28.7% (*sem-4(n1378)*) and 31.3% (*sem-4(n1971)*) decrease in GFP levels in the absence of *sem-4* in *brap-2* strain, and no change was observed in wild-type strain (Figure 11). In addition, RT-qPCR results showed that *gst-4* mRNA levels are significantly decreased by 70% and 40% in *brap-2* and N2, respectively, upon introduction of the mutation in *sem-4* gene (Figure 12A,B).

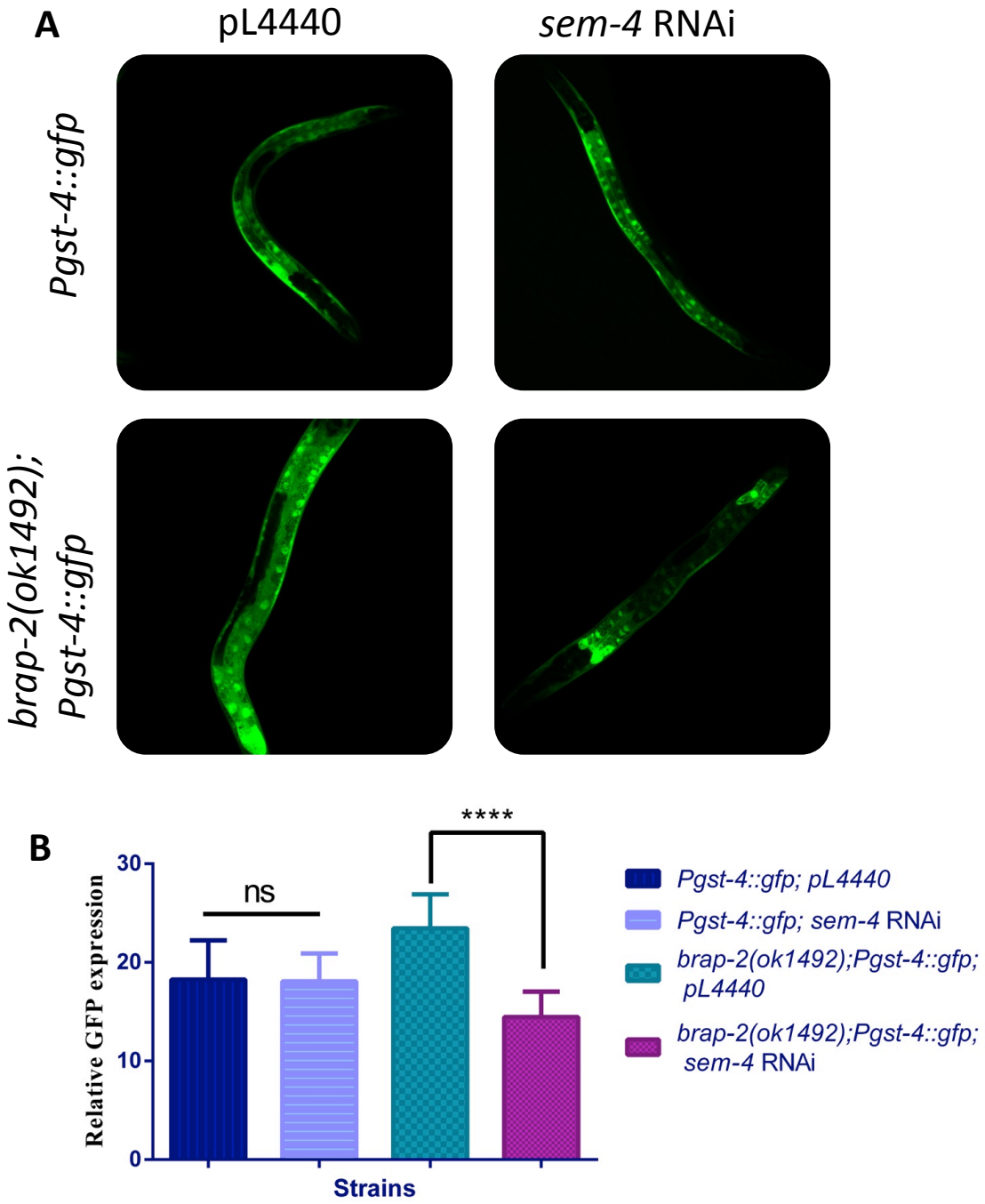

Figure 10. SEM-4 affects expression of *gst-4* in *brap-2(ok1492)* mutant worms. *brap-2(ok1492)* mutant worms and wild type worms were fed *sem-4* RNAi and empty vector, pL4440. **A**. *brap-2* mutants show decrease in *gst-4* expression when fed with *sem-4* RNAi in comparison to worms fed with empty vector. There is no significant difference in expression of *gst-4* in wild type worms fed by *sem-4* RNAi or empty vector . **B.** Non significant (p=0.9066) results obtained in wild type worms fed with empty vector (n=24) or *sem-4* RNAi (n=26), while *brap-2* showed significant difference ($p<0.0001$) between empty vector (n=11) and *sem-4* RNAi (n=10). *gst-4* expression was quantified using ImajeJ ® Software. Statistical analysis (student t-test) and graph were generated using Graphpad Prism ® 6.0 Software.

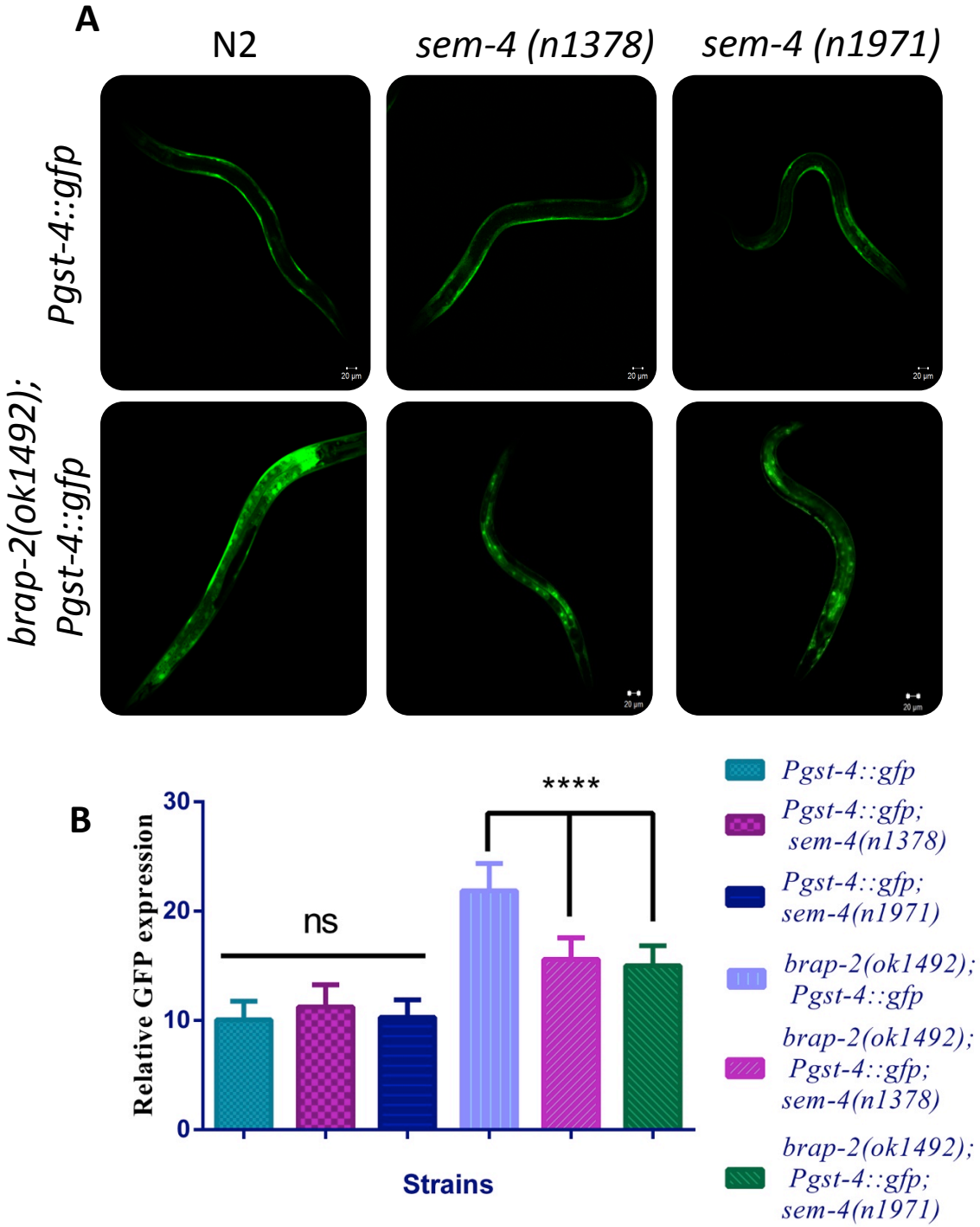

Figure 11. Mutation in *sem-4* significantly decreases expression of *gst-4* in *brap-2* worms. Double mutants of *sem-4* and *brap-2*, as well as *sem-4(-);Pgst-4::gfp* worms were generated. Fluoresce of all strains was observed under confocal microscope. **A.** Visual representation of *gst-4* expression in double mutants. Mutation in *sem-4* results in significant decrease of GFP in *brap-2* worms, but no affect is observed in wild type worms. **B**. Non significant ($p=0.1378$, $p=0.6792$) results obtained in wild type (n=12) worms with *sem-4(n1378)* (n=12) and *sem-4(n1971)* (n=21) mutations respectively, while *brap-2* worms showed significant difference ($p<0.0001$) between wild-type (n=10) and *sem-4(n1378)* (n=28) and *sem-4(n1971)* (n=15) mutants. *gst-4* expression was quantified using ImajeJ ® Software. Statistical analysis (student t-test) and graph were generated using Graphpad Prism ® 6.0 Software.

3.2. SEM-4 is a transcriptional regulator of *gst-4* during oxidative stress in *brap-2* worms.

In order to evaluate significance of SEM-4 during oxidative stress, we carried out the following experiment. We quantified the expression of *gst-4* in *sem-4(-), brap-2,* and *brap-2;sem-4(-)* worms in the presence of oxidative stress in the form of paraquat treatment. Levels of *gst-4* mRNA increased after 100 mM paraquat treatment in all strains, with the greatest increase in *brap-2* strain, followed by *brap-2;sem-4(n1378)* and *brap-2;sem-4(n1971)* (Figure 12B). However, the increase detected in *sem-4(n1378)* and *sem-4(n1971)* worms is similar to that of N2 (Figure 12A). Thus, SEM-4 is required to increase expression of *gst-4* in *brap-2* worms during oxidative stress.

In addition, there was significant difference in *Pgst-4::gfp* expression following paraquat treatment in *sem-4* single mutants when compared to the wild-type (Figure 13). For this experiment, all strains were grown to L3 stage and transferred to 2mM paraquat plates for 24 hours. Confocal images were taken after 24 hours of exposure to paraquat, and worms grown to L4 stage. Results of the experiment demonstrated reduction of *gst-4* expression in hypodermal cells in *sem-4* mutants in comparison to N2 worms. It was also noticed that exposure to different concentrations of paraquat and time of exposure affect *gst-4* expression in *sem-4* mutant, where pro-longed exposure demonstrated requirement of SEM-4 in wild-type worms during oxidative stress. Overall, these results confirm that *sem-4* is a transcriptional regulator of *gst-4* in the BRAP-2/SKN-1/ROS detoxification pathway.

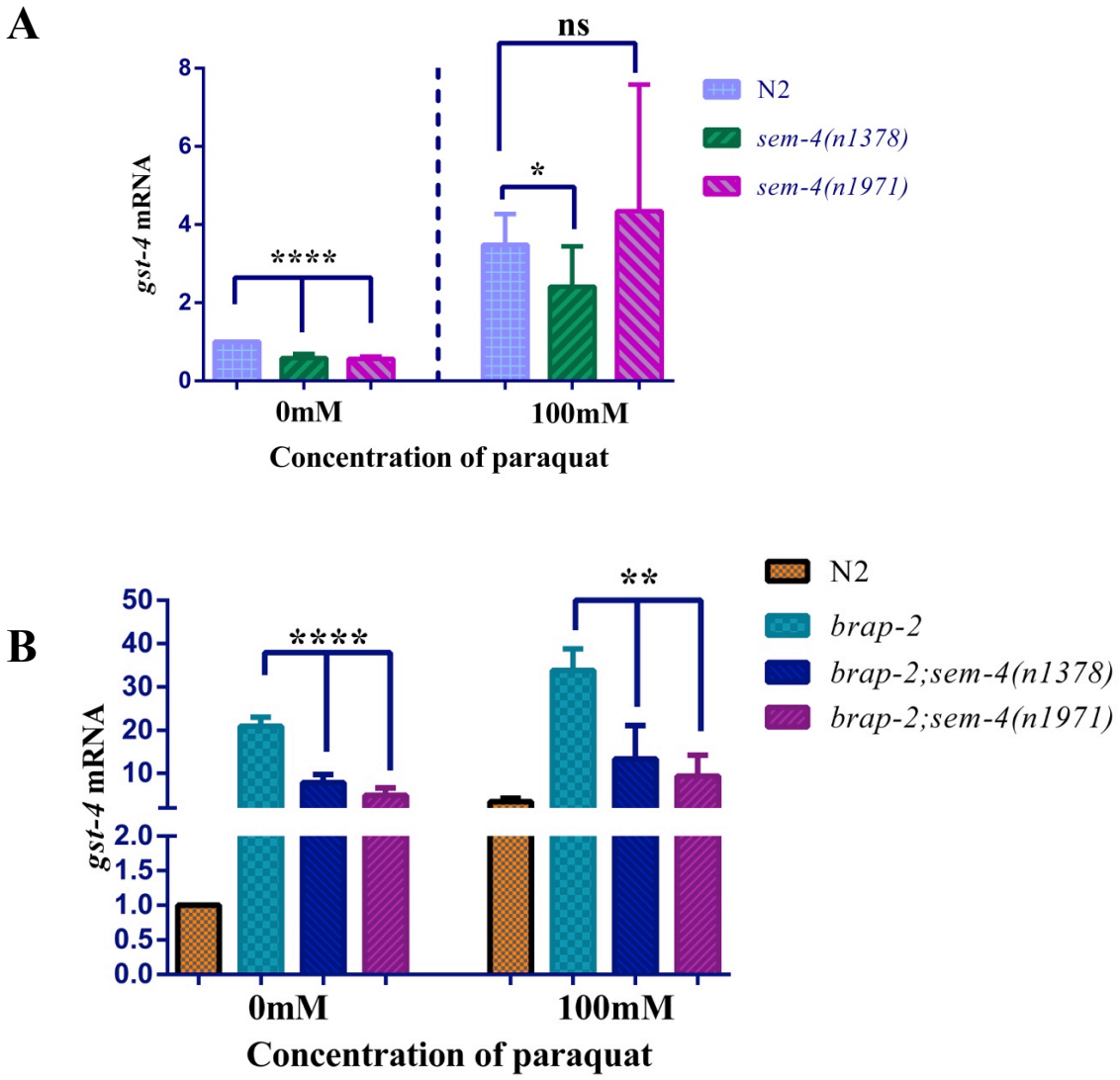

Figure 12. *brap-2* requires SEM-4 for enhanced *gst-4* expression before and after oxidative stress. Single *sem-4* mutants and *sem-4;brap-2* double mutants were exposed to 0mM and 100mM paraquat for one hour. RNA of all strains was used to measure expression of *gst-4* mRNA with qRT-PCR. All expressions were normalized to expression of reference gene, *act-1*. **A**. Mutation in *sem-4* (*sem-4(n1378)* (n=6); *sem-4(n1971)* (n=4))significantly($p<0.0001$) lowers *gst-4* expression in N2 worms (n=8) in the absence of oxidative stress. There was no significant difference ($p=0.4742$) in mRNA levels between *sem-4(n1971)*(n=4) mutant and wild type worms, and slightly significant difference ($p=0.0403$) between *sem-4(n1378)* (n=7) and N2 worms after exposure to paraquat. **B.** *brap-2* worms with added mutation in *sem-4* reported significant decrease ($p<0.0001$) in *gst-4* mRNA levels before ((*brap-2*;*sem-4(n1378),* n=5; *brap-2*;*sem-4(n1971),* n=4, $p<0.0001$) and after (*brap-2*;*sem-4(n1378),* n=4, $p=0.0041$; *brap-2*;*sem-4(n1971),* n=3, $p=0.0012$) paraquat treatment. mRNA levels are quantified by quantitative RT-PCR. Statistical analysis (student t-test) and graph were generated using Graphpad Prism ® 6.0 Software

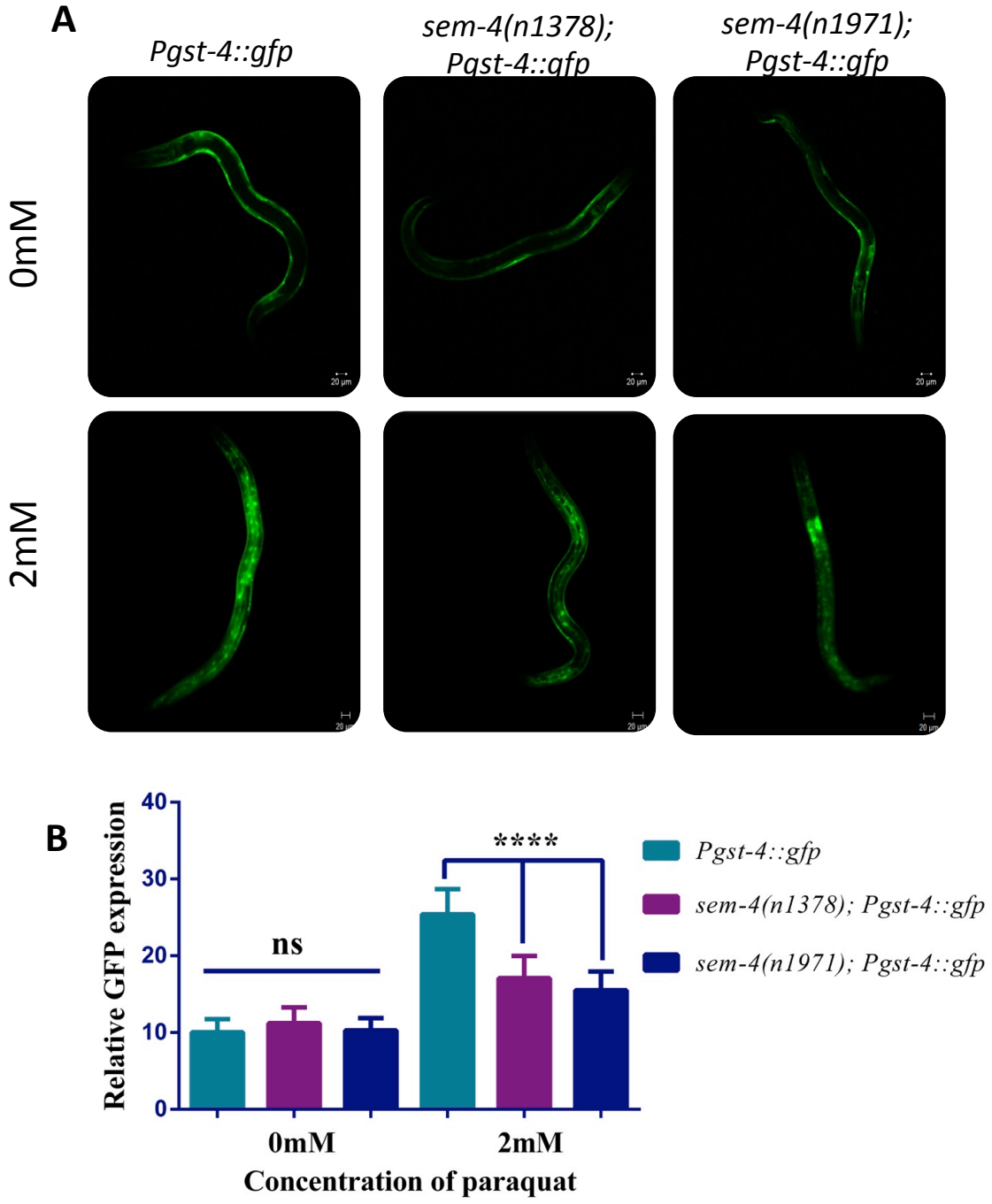

Figure 13. SEM-4 regulates transcription of *gst-4* in the hypodermal cells during oxidative stress. Treatment of worms with 2mM paraquat for 24 hours resulted in significant increase of GFP in all strains**. A.** Visual representation of *gst-4* expression in treated and untreated worms. The increase was visible in all tissues in wild type worms, but *sem-4(-)* mutant worms showed increase only in intestinal nuclei. **B.** Level of GFP was elevated by 2.53 fold in wild type worms, while *sem-4(-)* mutants showed only 1.5 fold increase. There is a significant difference ($p<0.0001$) in GFP fluorescence levels between wild type (n=20) and *sem-4(-)* mutant strains (n=31, n=26) after paraquat stress. *gst-4* expression was quantified using ImajeJ ® Software. Statistical analysis (student t-test) and graph were generated using Graphpad Prism ® 6.0 Software

3.3. SEM-4 does not physically interact with SKN-1 or MDT-15 to activate expression of *gst-4*

Since ELT-3, the first candidate gene from the *gst-4* suppression screen, was shown to physically interact with SKN-1 (Hu Q et al. Manuscript in preparation) and required to promote *gst-4* expression, we decided to test for the ability of SEM-4 to interact with SKN-1. We sub-cloned the SEM-4 transcription factor into a mammalian expression vector that would produce FLAG-tagged protein. We co-transfected this construct with SKN-1::GFP into HEK 293T cells, and co-immunoprecipitated with anti-FLAG or anti-GFP antibody. However, we were not able to detect a physical interaction between SKN-1 and SEM-4.

In addition, it was recently reported that SKN-1 physically interacts with MDT-15, one of the subunits of a mediator complex, where MDT-15 binds to SKN-1 and forms transcription factor complex to regulate expression of stress response genes (Goh et al. 2014). Thus, we wished to determine whether SEM-4 forms a complex with MDT-15, and therefore interacts with SKN-1 through MDT-15. For this experiment, we used the same rationale as described above with a few changes: we sub-cloned *sem-4* into an expression vector that would produce GST-tagged protein. We then co-transfected the cells with MDT-15::HA, and co-immunoprecipitated with GST beads or anti-HA antibody. From this assay, we were not able to demonstrate an interaction between SEM-4 and MDT-15.

Furthermore, according to recently published data on modENCODE® (the research project of 11 subprojects to identify functional elements in *C.elegans* and *D.melanogaster* genomes) (Celniker et al. 2009) by the "Snyder" group, SEM-4 does not bind to the promoter region of *gst-4* ((727bp (Leiers et al. 2003)). Thus, SEM-4 regulates expression of *gst-4* by different mechanism then activating the promoter of *gst-4*.

3.4 SEM-4 regulates the expression of *skn-1*

Since it was established that SEM-4 does not bind to the promoter of *gst-4,* and does not physically interact with SKN-1 and MDT-15, we decided to check whether expression of *skn-1* is affected in *sem-4* mutant worms. It was recently reported by "Snyder" group that SEM-4 binds to the promoter region and first intron of *skn-1a* and *skn-1c* (Figure 14A). As I have described previously (Section 1.2.4.1), SKN-1C isoform is mostly associated with oxidative stress response. Thus, we have decided to quantify mRNA levels of *skn-1c* using RT-qPCR in *sem-4* mutants. Expression of *skn-1c* decreased by 40-50% in *sem-4* mutant worms (Figure 14B). In addition, a *sem-4* overexpressing strain (*sem-4(+))* displayed a 30% increase in *skn-1c* (Figure 14B). We also determined that *skn-1c* mRNA levels increased 2-fold in *brap-2* mutants, which subsequently dropped when a *sem-4* mutation is introduced. Indeed, *brap-2;sem-4(n1378)* reported wild-type expression of *skn-1c,* while *brap-2;sem-4(n1971)* strain showed a 2.83 fold decrease in *skn-1c* mRNA levels compared to *brap-2* worms. However, *brap-2;sem-4(+)* strain reported no-significant difference in expression of *skn-1c* when compared to *brap-2* worms (Figure 14B).

Nuclear localization of SKN-1C in the intestine after paraquat stress further demonstrates the role of SEM-4 in expression of *skn-1c*. For this experiment, *sem-4(n1971);skn-1::gfp* and *sem-4(+);skn-1::gfp* double mutant strains were generated, grown to L4 stage and transferred to 2 mM Paraquat plates for 24 hours. Nuclear localization of SKN-1 was observed using confocal microscopy, and it was noted that no nuclear SKN-1 was detected in intestinal cells in *sem-4(n1971);skn-1::gfp* worms, while intestinal nuclei contained SKN-1 in *skn-1::gfp* strain, as well as in *sem-4(+);skn-1::gfp* worms (Figure 15). Overall, these results demonstrate that SEM-4 regulates the transcriptional expression of SKN-1C. In addition, SEM-4 might affect nuclear

localization of SKN-1C following oxidative stress, but it can be justified to overall presence of SKN-1C in *sem-4(n1971)* mutants.

3.5 SEM-4 affects the expression of several known SKN-1's target genes

Along with GST-4, SKN-1 is a transcription factor for other Phase II detoxification enzymes. Therefore, our lab was interested in determining changes in the expression levels of other SKN-1 targets. We therefore examined the expression of *gst-7, gst-10,* and *gcs-1* in *sem4(-)* and *brap-2(ok1492);sem4(-)* mutant strains (Figure 16). mRNA levels of *gst-7* and *gcs-1* are significantly decreased in *brap-2(ok1492)* worms that possess a mutation in the *sem-4* gene, but no significant change is observed in the expression of *gst-10*. These results suggest that SEM-4 regulates the expression of several, but not all SKN-1 transcriptional targets.

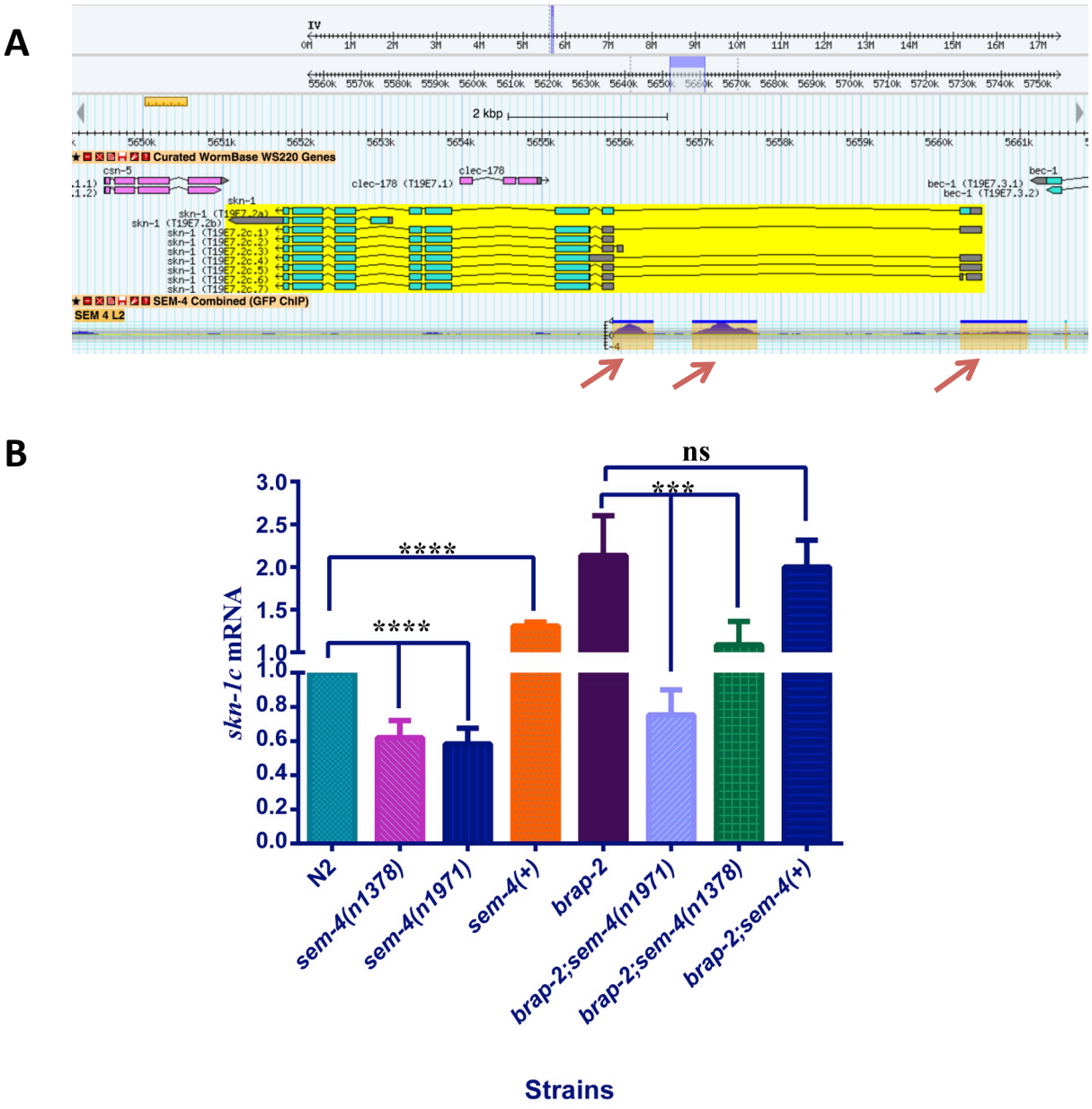

Figure 14. SEM-4 regulates the expression of *skn-1c*. A. SEM-4 binds to promoter region and first intron region of *skn-1*. Red arrows point to SEM-4 binding regions. Figure adapted from modEncode® website. http://gbrowse.modencode.org/fgb2/gbrowse/worm/. **B.** mRNA levels of *skn-1c* are significantly affected by SEM-4. Overexpression of *sem-4* lead to increase by 30% ($p<0.0001$, n=3), while *sem-4(-)* mutant strains reported decrease in *skn-1c* mRNA levels by 40% ($p<0.0001$, n=5) in *sem-4(n1378)* and by 50% ($p<0.0001$, n=3) in *sem-4(n1971)*. SEM-4 regulated expression of *skn-1c* in *brap-2* strain as well. Significantly lower level of *skn-1c* mRNA is reported in *sem-4(n1971);brap-2* (65% decrease, p=0.0001, n=5) and *sem-4(n1378);brap-2* (54% decrease, p=0.0008, n=6) double mutants in comparison to *brap-2* worms (n=6). There is no significant difference in *sem-4(+);*brap-2 strain (p=0.6667, n=3) in comparison to *brap-2* worms. mRNA levels are quantified by quantitative RT-PCR with *act-1* as a reference gene. Statistical analysis (student t-test) and graph were generated using Graphpad Prism ® 6.0 Software

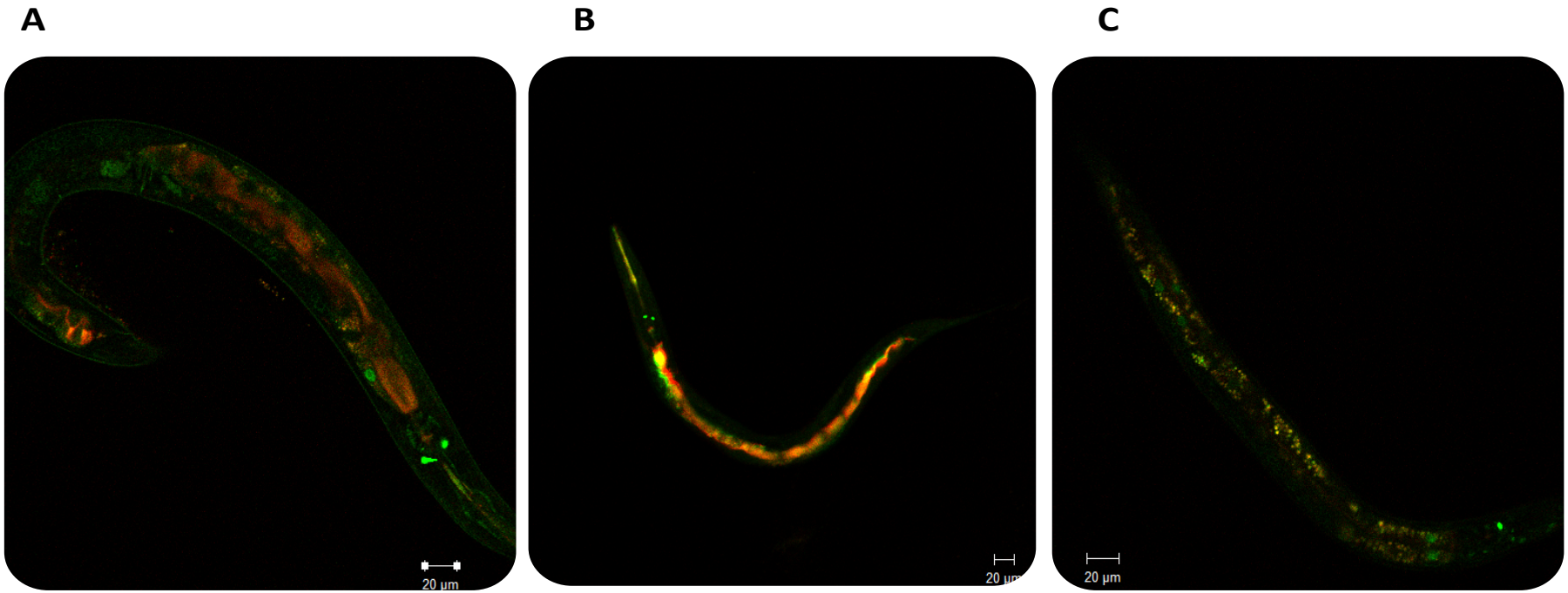

Figure 15. Intestinal nuclear localization of SKN-1C after paraquat stress is dependent on SEM-4. Worms were grown to L3 stage and transferred to 2mM paraquat plates for 24 hours (worms grew to L4 stage). Images were obtained with confocal microscopy and checked for SKN-1C nuclear localization. All worms are shown under two filters: Alexa 488 (detects GFP) and Texas Red (detects autofluorescence in the worm); superimposion of two filters demonstrates expression of SKN-1B/C and SEM-4 (True fluorescence). **A** *skn-1::gfp* showed regular expression of *skn-1b* in ASI neurons, and nuclear localization of SKN-1C. **B.** Absence of SEM-4 completely abolished ability of SKN-1C to translocate to intestinal nuclei, but no change in SKN-1B is observed (*sem-4(n1971);skn-1::gfp*). **C.** Overexpression of SEM-4 in *skn-1::gfp* worms didn't affect SKN-1C nuclear localization, and expression of SKN-1B stayed constant(*sem-4(+);skn-1::gfp).* Images were obtained with confocal microscopy, 20X Objective, Zeiss 700.

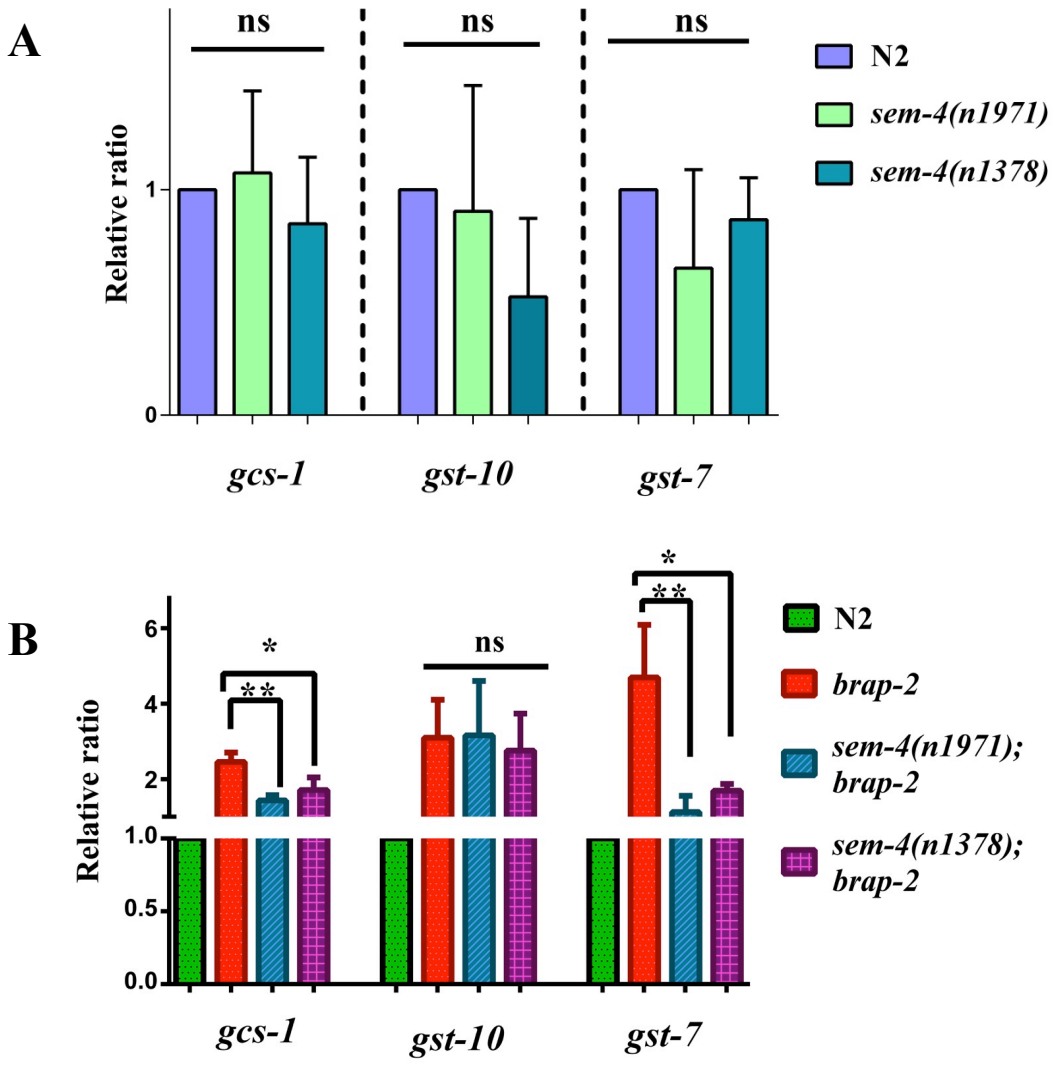

Figure 16. SEM-4 affects the expression of several known SKN-1 target genes in *brap-2* worms. mRNA levels of three SKN-1 targets (*gcs-1, gst-7* and *gst-10)* were measured and quantified in six strains (single *sem-4* mutants and *brap-2;sem*-4 double mutants) with qRT-PCR. **A**. Single *sem-4* mutation does not affect mRNA levels of *gcs-1, gst-10* and *gst-7* in comparison to N2 strain (n=3 for each targets/strains). **B**. Two SKN-1 targets are downregulated in *brap-2;sem-4(-)* double mutant strains. Significant decrease in mRNA levels of *gcs-1* is observed in *brap-2;sem-4(n1971)* (p=0.0035, 42%) strain and in *brap-2;sem-4(n1378)* (p=0.0357, 30%) in comparison to *brap-2* worms. The same trend is observed in mRNA levels of *gst-7* in *brap-2;sem-4(n1971)* (p=0.0057, 76%) and *brap-2;sem-4(n1378)* (p=0.0114, 64%) strain in comparison to *brap-2* worms. There is no effect of SEM-4 on expression of *gst-10* (p=0.953, p=0.695). mRNA levels are quantified by quantitative RT-PCR with *act-1* as a reference gene. Statistical analysis (student t-test) and graph were generated using Graphpad Prism ® 6.0 Software

3.6. SEM-4 is required for the detoxification of ROS

Besides testing the transcriptional levels of antioxidant enzymes in *sem-4* worms, we used a functional assay to determine the ability of SEM-4 to increase GST-4 levels and reduce ROS *in vivo*. Therefore, we quantified ROS levels using 2,7-dichlorodihydrofluorescein-diacetate (DCFDA) dye in three strains: N2, *sem-4(n1378),* and *sem-4(n1971),* before and after applying 100 mM paraquat stress. For this experiment, all strains were synchronized and grown to L4 stage, and then incubated with 0 mM or 100 mM Paraquat for 1 hour. Following this assay, a significant increase in ROS production was observed in both *sem-4* strains in comparison to N2 (Figure 17). It was expected that *sem-4* mutant strains would produce more ROS (Figure 17).

Thus, in order to confirm and visualize ROS production results described above, we decided to observe production of ROS in the same three strains using confocal microscopy. It is important to note all *sem-4(n1971)* worms were dead by day two after the treatment. These observations suggest that *sem-4* plays important roles in the ROS detoxification pathway. Visualization using confocal microscopy confirmed ROS production results, with the highest ROS production being detected in *sem-4(n1971)*, and followed by *sem-4(n1378)* mutants (Figure 18). The lowest ROS levels were recorded in N2 worms. The experiment was performed with at least 15 worms per strain.

Therefore, the loss of *sem-4* elevates ROS production following oxidative stress induction, demonstrating its importance in regulating the detoxification of ROS.

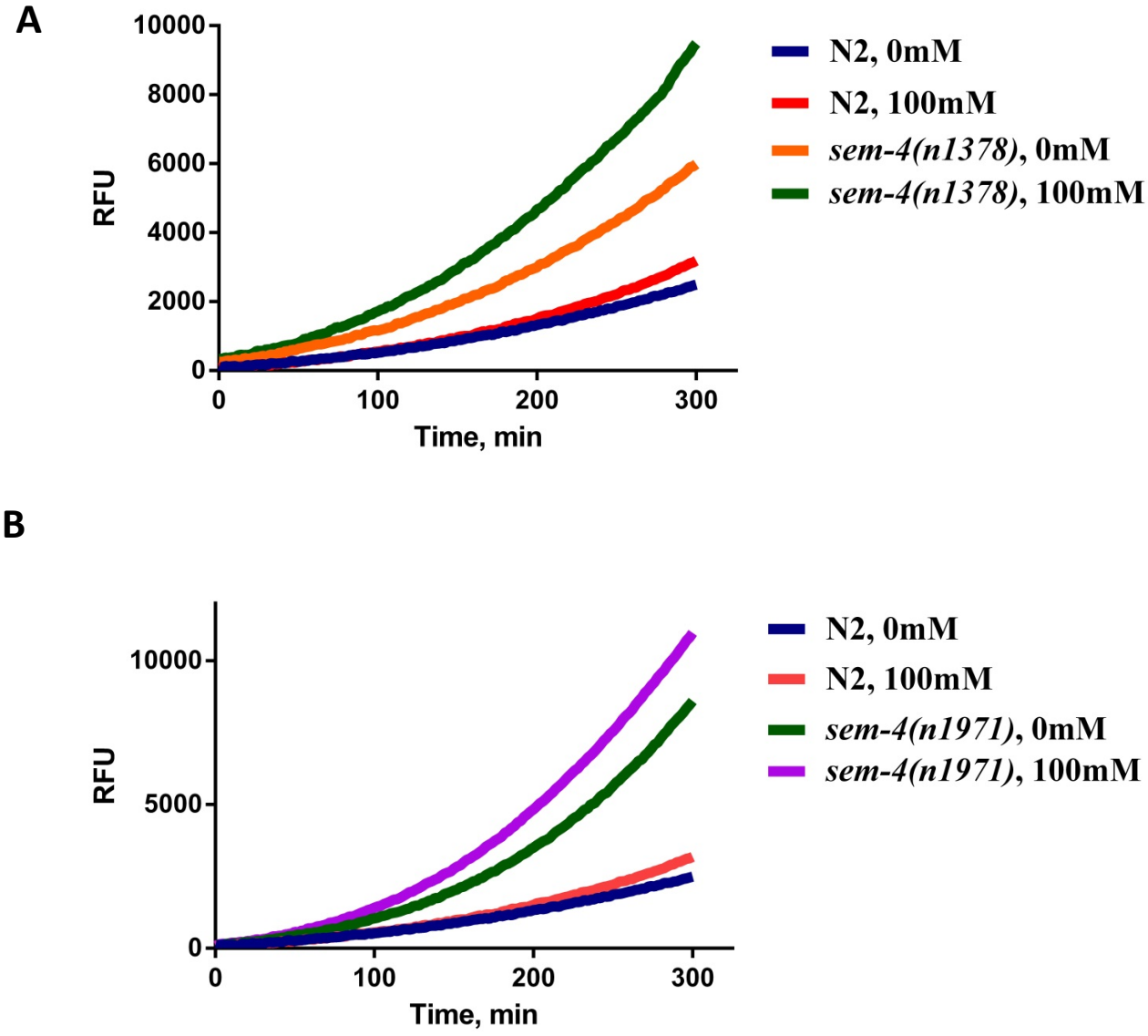

Figure 17. **SEM-4 is required to reduce ROS production *in vivo*.** Wild type and *sem-4* mutant strains were treated with 0mM or 100mM paraquat for one hour and then mixed with 50µM DCFDA dye in 96-well plates, and plates were read for 300 minutes by microplate reader. ROS production was recorded as relative fluorescence unit (RFU). **A –** Comparison of ROS production in *sem-4(n1378)* and wild type strains. There is 3 fold difference in ROS production between treated *sem-4* mutant and N2 worms (N2 = 3185.5 RFU, *sem-4(n1378)* = 9483.5 RFU). **B –** relative fluorescence produced by untreated (0mM) and treated (100mM) N2 and *sem-4(n1971)* worms. *sem-4(n1971)* show increase after paraquat treatment at 300 minutes (N2 = 3185.5, *sem-4(n1971)* = 10978.33). Each line in Figure A and B represents average RFU of 600 worms (200 worms/well, 3 wells per strain and treatment).

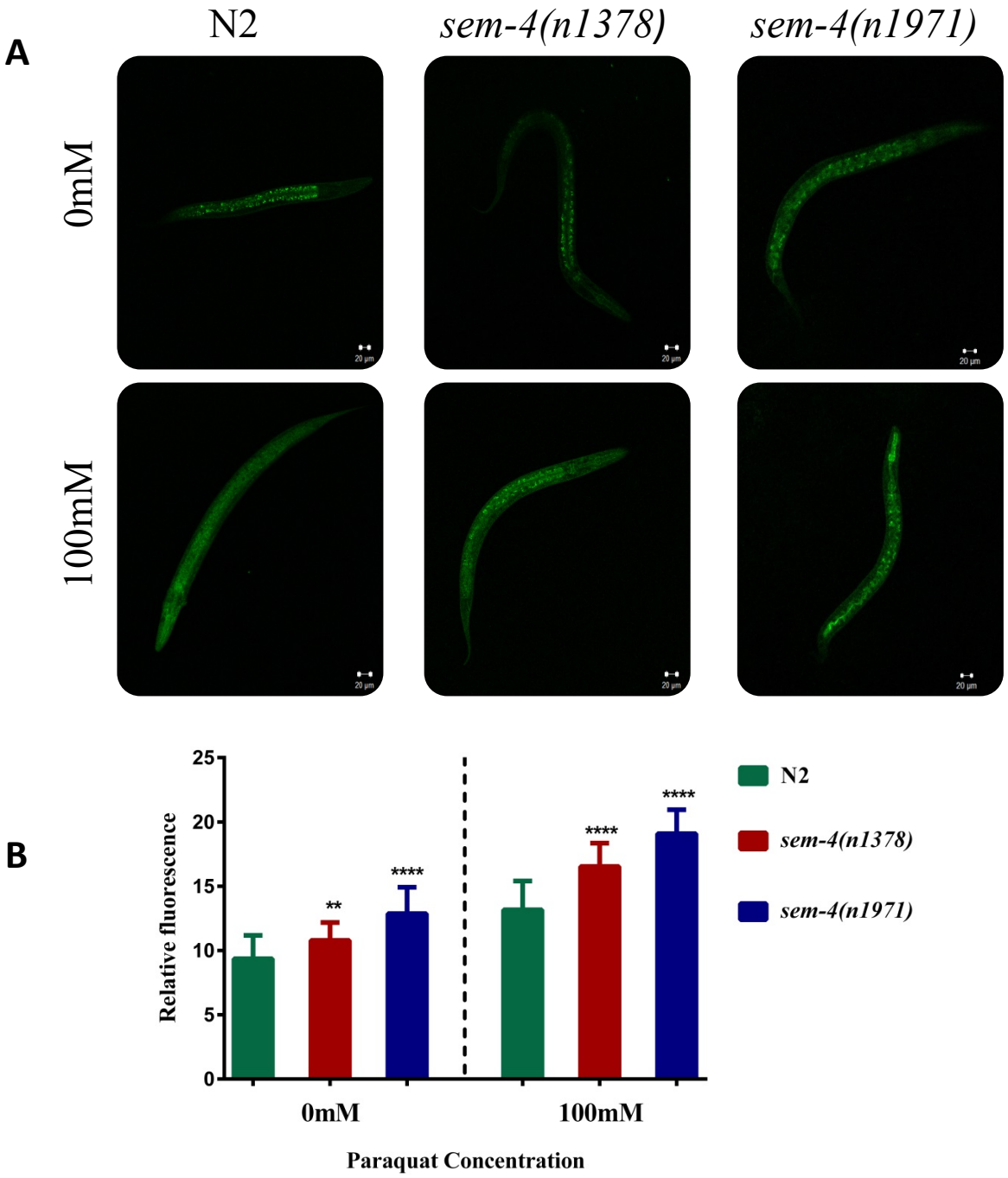

Figure 18. **Intercellular *in vivo* ROS production is dependent on presence of SEM-4**. Wild type and *sem-4* mutant strains were treated with 0mM or 100mM paraquat for one hour and then stained with 25µM DCFDA dye for one hour. All strains were observed under confocal microscope and checked for production of ROS. **A**. Visual representation of untreated and treated worms producing ROS, represented in green fluorescence. **B.** Treated and untreated *sem-4* mutant worms demonstrate significantly higher levels of ROS in comparison to wild type. Untreated mean fluorescence values: : N2 - 9.35 ± 0.47, n=15; *sem-4(n1378)* – 10.78 ±0.28, n=24; *sem-4(n1971)* – 12.87 ±0.51, n=16. Treated mean fluorescence values: N2 - 13.17 ± 0.53, n=18; *sem-4(n1378)* – 16.54 ±0.40, n=20; *sem-4(n1971)* – 19.09 ±0.37, n=25. Statistical analysis (student t-test) and graph were generated using Graphpad Prism ® 6.0 Software.

3.7 SEM-4 is required for lifespan extension

Previous studies have reported a link between the overexpression of detoxification enzymes and longevity. Thus we investigated whether worms overexpressing *sem-4* and worms with *sem-4* mutations have an effect on this previously reported increased lifespan of *skn*-1 overexpressing (*skn-1(+))* worms (Tullet et al. 2008). Following a lifespan analysis, we confirmed the previously reported increased lifespan in *skn-1(+)* worms compared to N2 worms (27 and 19 days respectively). Next, we determinded that the lifespan of wild-type and *skn-1* overexpressing (*skn-1(+))* worms is significantly decreased with an N-terminal mutation in *sem-4 [sem-4(n1971)],* while a C-terminal mutation of *sem-4 [sem-4(n1378)]* does not affect worm longevity (Figure 19A,D). The mean results (analyzed by Student's t-test) have demonstrated that out of the single mutants, only the *sem-4(n1971)* strain had a significantly shortened lifespan in comparison to N2 (4.14 days or 21.8%) (Figure 19B,C), while *skn-1(+)* had prolonged lifespan by 8.1 days (42.5%) as previously reported. In addition, both *sem-4(-);skn-1(+)* double mutants have significantly lowered lifespan compared to that of the *skn-1(+)* strain by 12.1 days (44.6%) (*sem-4(n1971))* and 7.0 days (25.9%) (*sem-4(n1378))*. Lastly, *sem-4* overexpressing worms (*sem-4(+))* significantly prolonged lifespan in *skn-1(+)* worms, by 6.0 days (21.9%) (Figure 19C,E). Overall, the examination of lifespan has demonstrated that *sem-4* is required for lifespan extension in the wild-type, as well as in *skn-1* overexpressing worms.

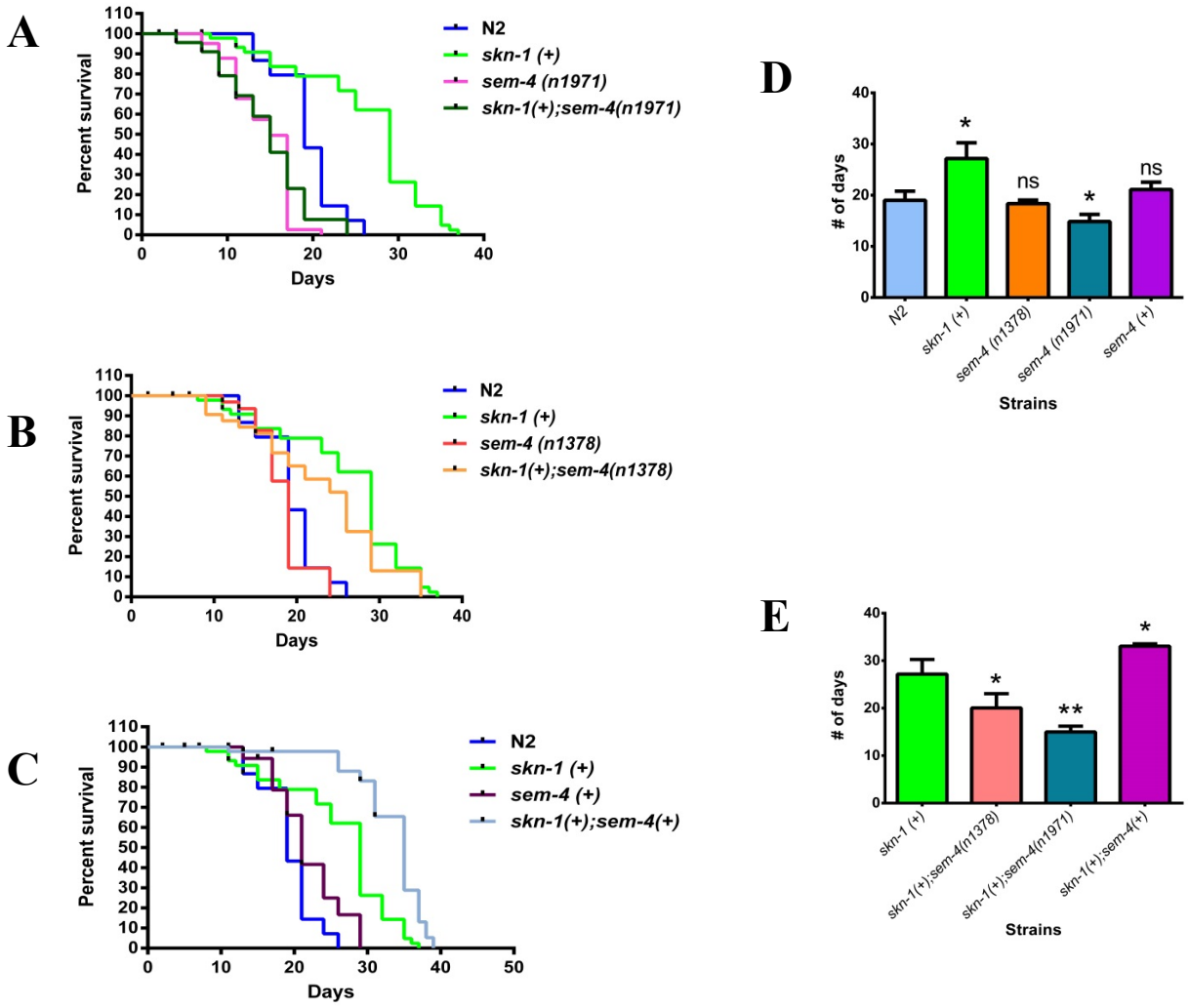

Figure 19. SEM-4 is required for lifespan extension of *C.elegans.* Lifespan was observed on eight strains. All strains were synchronized and transferred to FUDR plates at L4 stage. Plates were observed every two days and results recorded. **A.** Lifespan of wild-type and *skn-1* overexpressing worms is slightly affected by C-terminal mutation in *sem-4 (sem-4(n1378)).* **B** Lifespan of wild-type and *skn-1* overexpressing worms is significantly decreased by N-terminal mutation in *sem-4 (sem-4(n1971)).* **C**. Lifespan of wild-type and *skn-1* overexpressing worms is significantly increased by overexpression of *sem-4 (sem-4(+)).* **D**. Mean of lifespan of single mutants is compared to N2 strain. Only *skn-1(+)* (p=0.017) and *sem-4(n1971) (*p=0.034) are significantly different from N2. **E.** Comparison of mean lifespans of worms with *skn-1(+).* All *sem-4 (-)* mutant strains showed significant difference in lifespan: *sem-4(n1971)* decreased lifespan of *skn-1(+)* by 45% of 12.18 days (p=0.003), and *sem-4(n1378)* decreased lifespan of *skn-1(+)* by 26% of 7.11 days (p=0.046) . Overexpression of *sem-4 (+)* increased lifespan of *skn-1(+)* worms by 22% or 5.88 days (p=0.031). Data was analyzed using OASIS software. Statistical analysis (student t-test) and graph were generated using Graphpad Prism ® 6.0 Software

3.8 Increased lifespan is dependent on detoxification genes

With this significant increase in lifespan seen in *sem-4(+);skn-1(+)* worms, we decided to test for expression levels of *skn-1, gst-4, gst-7* and *gst-10*. For this, we isolated mRNA from N2, *skn-1(+), sem-4(+),* and *sem-4(+);skn-1(+)* strains and quantified the mRNA levels of the above listed genes by quantitative RT-PCR. The results displayed a significant, 2.5-fold increase in *gst-4* mRNA levels and a moderate increase in *gst-7* and *gst-10* mRNA levels was observed in *sem-4(+);skn-1(+)* compared to wild-type worms (Figure 20A). In addition, we tested mRNA levels of the same SKN-1 targets, *gst-4, gst-7* and *gst-10,* in *skn-1(+);sem-4(-)* strains (Figure 20B). We have observed significant decrease in all targets, and the most drastic decrease was shown by *gst-4,* where mRNA levels were reduced by 84% in comparison to *skn-1(+)* strain. This suggests that SEM-4 is necessary for the expression of Phase II detoxification enzymes, and thus a vital transcription factor in oxidative stress pathway.

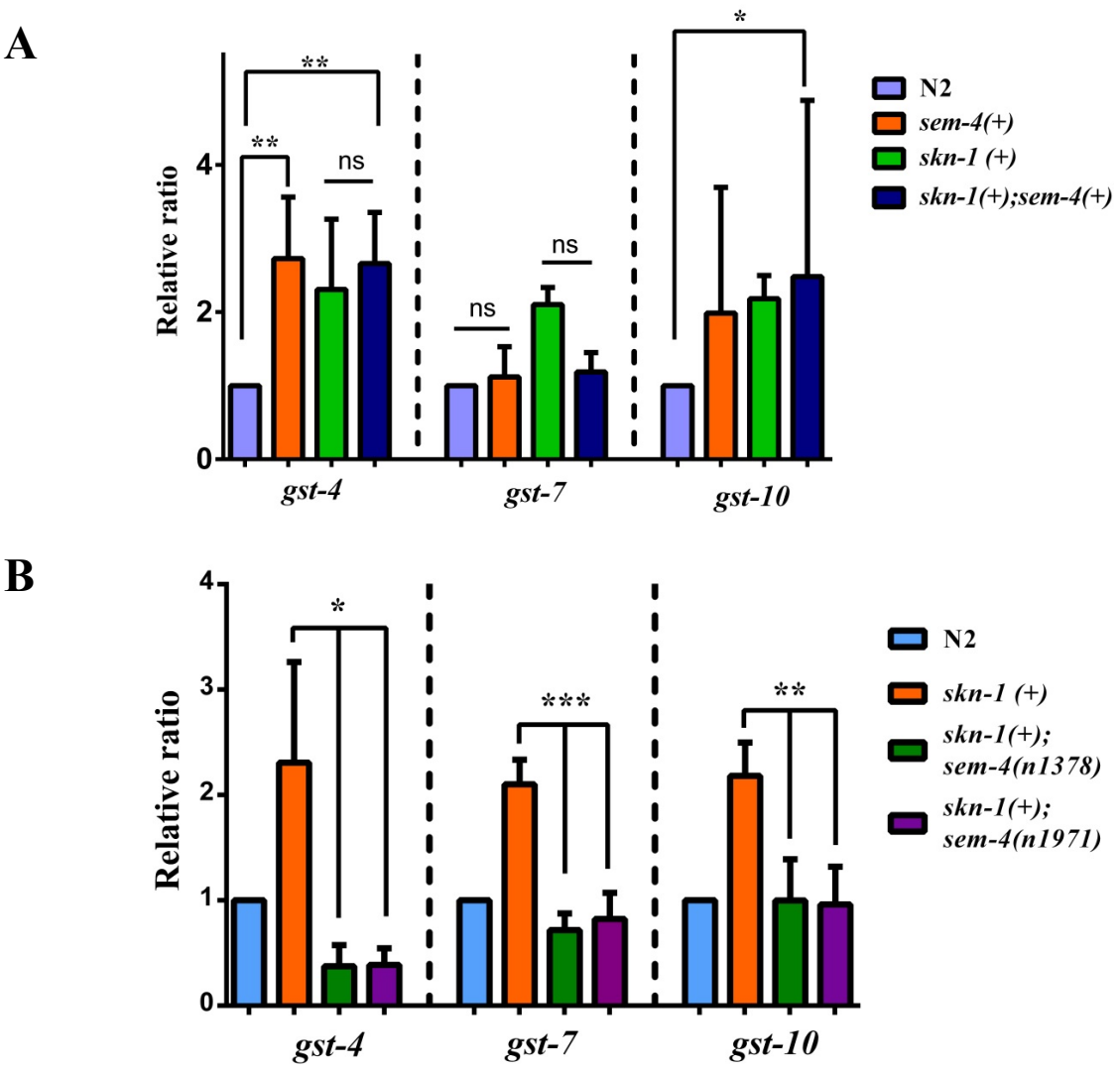

Figure 20. Increased lifespan is dependent on detoxification genes. mRNA levels of three SKN-1 targets (*gst-4, gst-7* and *gst-10)* were measured and quantified in six strains (single *sem-4(+), sem-4(-)*, *skn-1(+);sem-4(+)* and *skn-1(+);sem-4(-)* double mutants) with qRT-PCR; and two SKN-1 targets, *gst-4* and *gst-7,* were measured in *sem-4(+)* and *brap-2;sem-4(+)*strains. **A.** mRNA levels of SKN-1 targets are increased in *sem-4* overexpressing worms. Expression of SKN-1 targets is similar in *sem-4(+);skn-1(+)* worms in comparison to *skn-1(+)* strain. **B.** mRNA levels of SKN-1 targets were decreased in *sem-4(-);skn-1(+)* in comparison to *skn-1(+)* worms. All targets show the same transcriptional deactivation in *sem-4(-);skn-1(+)* strains. The most drastic decrease is observed in expression of *gst-4* in *sem-4(-);skn-1(+)* strain in comparison to *skn-1(+)* worms (84%, p=0.0198). mRNA levels are quantified by quantitative RT-PCR with *act-1* as a reference gene. Statistical analysis (student t-test) and graph were generated using Graphpad Prism ® 6.0 Software

3.9 Survival following oxidative stress is dependent on SEM-4

We decided to test the importance of *sem-4* on the survival of worms following oxidative stress induction using 2 mM paraquat. For this experiment, *sem-4(n1971), sem-4(n1378),* and N2 worms were allowed to grow to L4 stage and then transferred to 2 mM paraquat + 0.05mg/mL FUDR plates. Worms were checked every 24 hours, and the experiment lasted on average for 524.6 hours (Figure 21A). It was found that *sem-4(n1971)* worms die first with median survival of 78.47 hours. On the other hand, median survival of N2 is 363.87 hours, and median survival of *sem-4(n1378)* is 238.72 hours (Figure 21B). These results demonstrate that the loss of functional SEM-4 is detrimental for worm survival when exposed to paraquat, and the null mutation affects survival more severely than the C-terminal mutation. In addition, inability of *sem-4* worms to survive in oxidative stress conditions corresponds to the detection of very high levels of ROS *in vivo* (described in Section 3.6).

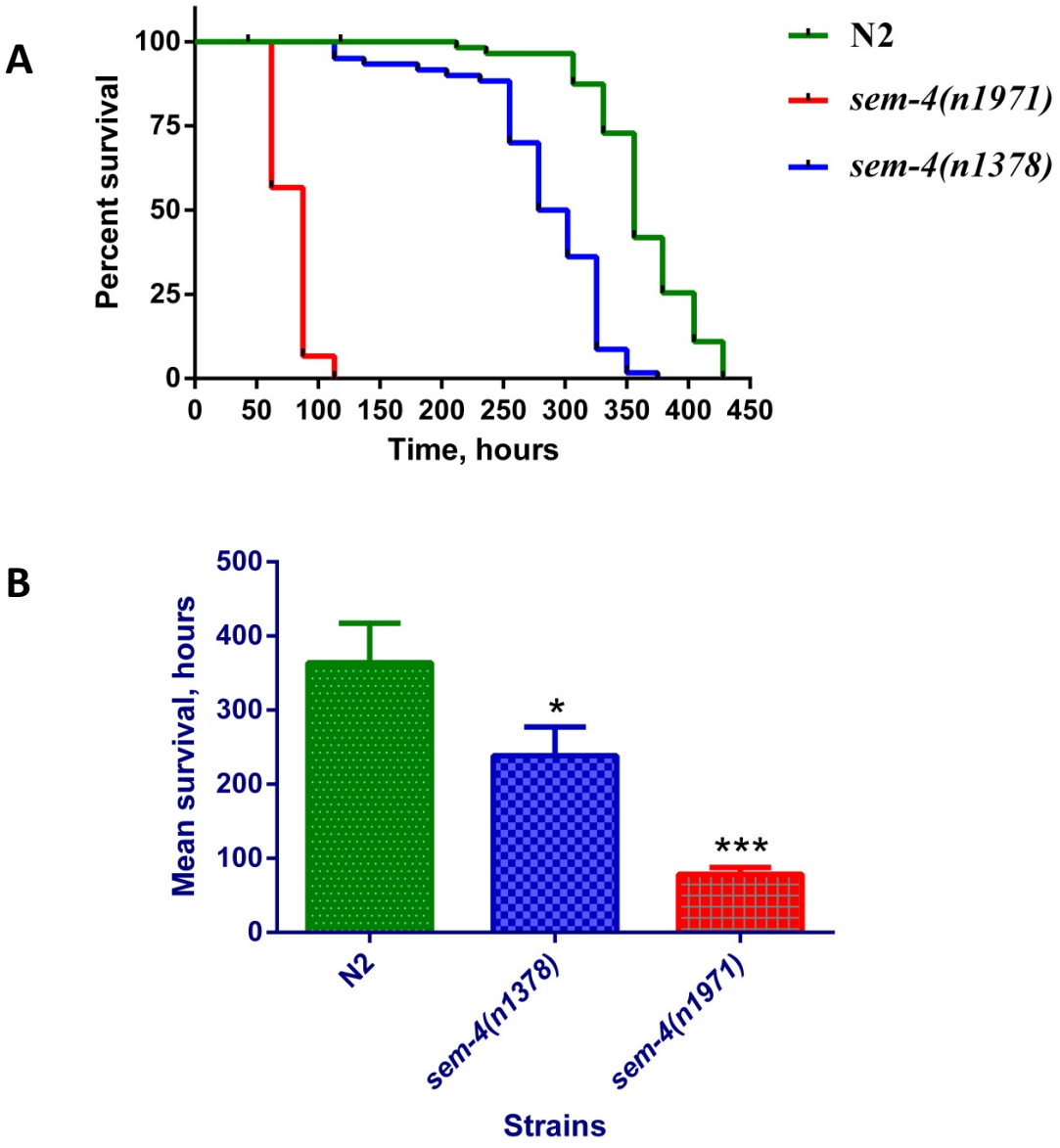

Figure 21. Survival following oxidative stress is dependent on SEM-4. A. Survival of tree strains tested on 2mM paraquat plates showed necessity of SEM-4 for *C.elegans.* The shortest lifespan is observed in *sem-4(n1971),* mean lifespan is 78.82 hours. The longest survival is observed in wild type worms, mean lifespan is 362.5 hours, and *sem-4(n1378)* worms survived for 282.94 hours. **B.** Mean results for three trials. Survival of *sem-4(n1971)* is decreased by 78% (p=0.0008) in comparison to N2 and survival of *sem-4(n1378)* is decreased by 34% (p=0.0303). Data was analyzed using OASIS software. Statistical analysis (student t-test) and graph were generated using Graphpad Prism ® 6.0 Software

3.10 Localization of SEM-4 in wildtype and *brap-2(ok1492)* worms

Previous studies have shown that *sem-4* is expressed in neurons, coelomocytes, hypodermis, vulval precursor cells, and tail blast cells (Figure 22) while expression of *sem-4* in the intestine was not reported. Since SKN-1 intestinal nuclear localization is enhanced in a *brap-2* mutant background (Hu et al. Manuscript in preparation), we asked whether BRAP-2 affects the intestinal nuclear localization of SEM-4. For this purpose, we generated double mutants of *sem-4(+)::gfp* and *brap-2* worms, and observed SEM-4 localization using confocal microscopy (Figure 22). We were able to detect expression of *sem-4* in the intestinal nuclei and hyp7 nuclei (Figure 22), and there was no difference in expression and nuclear localization of SEM-4 in *brap-2* mutant worms (Figure 22). This data suggests that BRAP-2 does not regulate SEM-4 localization in *C.elegans.*

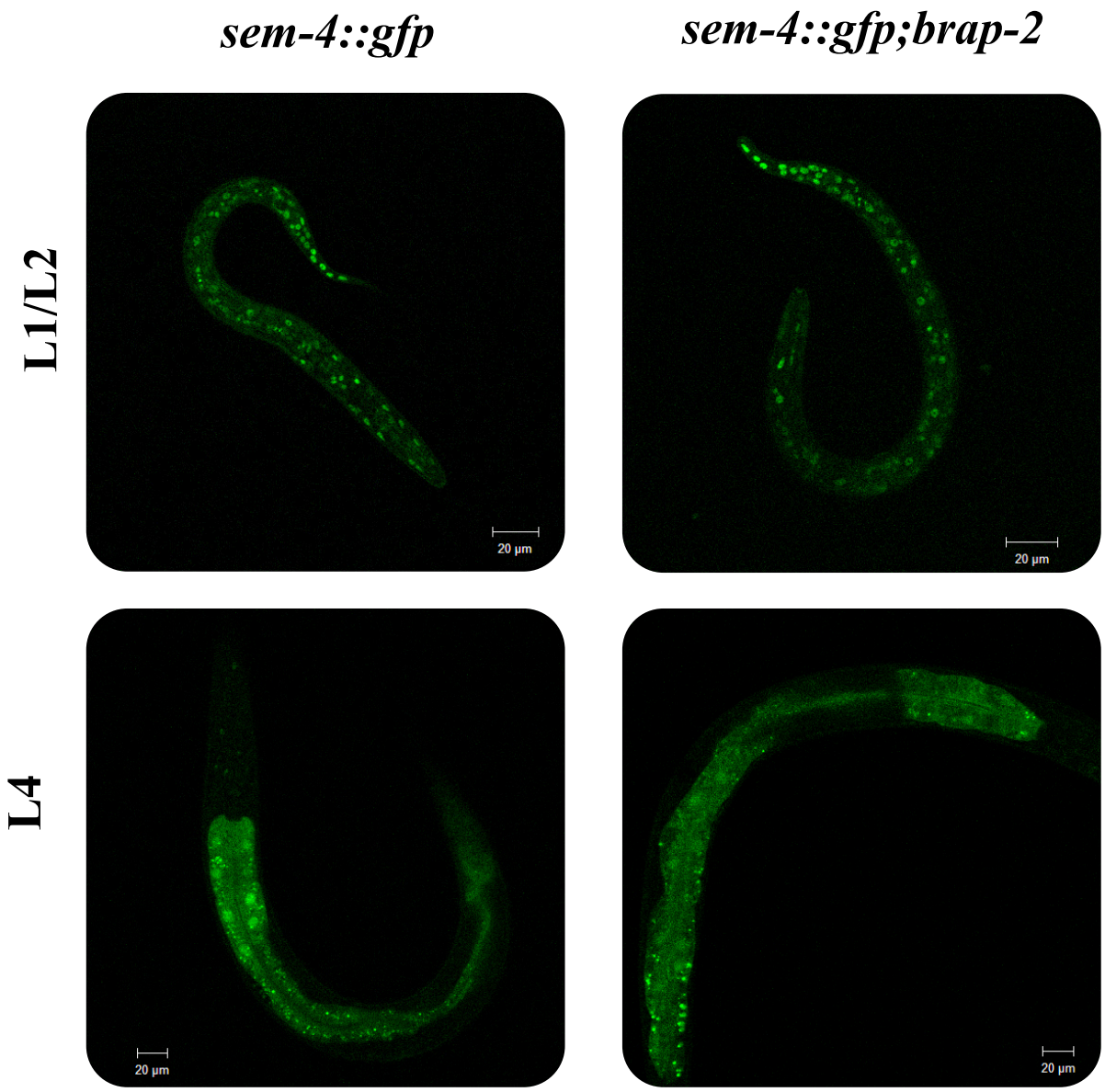

Figure 22. Localization and expression of *sem-4* is independent of *brap-2* mutation. SEM-4 is shown to express in hypodermal, neuronal, rectal nuclei and intestinal nuclei. Vulval expression is not visible on the images. Wild-type *sem-4* overexpressing and *sem-4::gfp;brap-2* worms are shown to express *sem-4* in hypodermal, neuronal, rectal nuclei in L1/L2 stages. Expression of *sem-4* in intestinal nuclei is visible in *sem-4::gfp* and *sem-4::gfp; brap-2* mutant worms at L4 stage. *brap-2* mutation did not alter expression and localization of *sem-4*. Images were taken with 200X and 400X magnifications.

3.11. SEM-4 regulates expression of *daf-16*

Since we have determined that SEM-4 regulates expression of *skn-1c,* we decided to check whether another transcription factor, DAF-16, is affected by SEM-4. For that purpose, we quantified *daf-16* mRNA in six strains: N2, *sem-4* mutants, *brap-2,* and *brap-2;sem-4* double mutants. Obtained results showed that mRNA levels of *daf-16* increased by 2-fold in *brap-2* worms. However, we were not able to detect significantly increased levels of *sod-3* expression in *brap-2* worms by RT-qPCR and confocal microscopy in our previous work (Hu et al. Manuscript in preparation). Most importantly, RT-qPCR analysis displayed that transcription of *daf-16* drops by 25% in *sem-4* mutants compared to N2 worms. In addition, the double mutant strains *brap-2;sem-4(n1378)* and *brap-2;sem-4(n1971)* show significantly lower expression of *daf-16* in comparison to that of *brap-2* single mutants, by 2-fold, and 2.5-fold, respectively (Figure 23B). Indeed, it was reported by the Snyder group that SEM-4 binds to both promoter and intronic regions of *daf-16*, and results were posted on the ChIP database on modENCODE® (Figure 23A). This evidence provides additional support that SEM-4 plays a significant role in the oxidative stress response, by regulating the expression of two vital transcription factors in this pathway, SKN-1 and possibly DAF-16. Future work focusing on how SEM-4 regulates *daf-16* expression is necessary in order to further elucidate the role of SEM-4 in oxidative stress pathway.

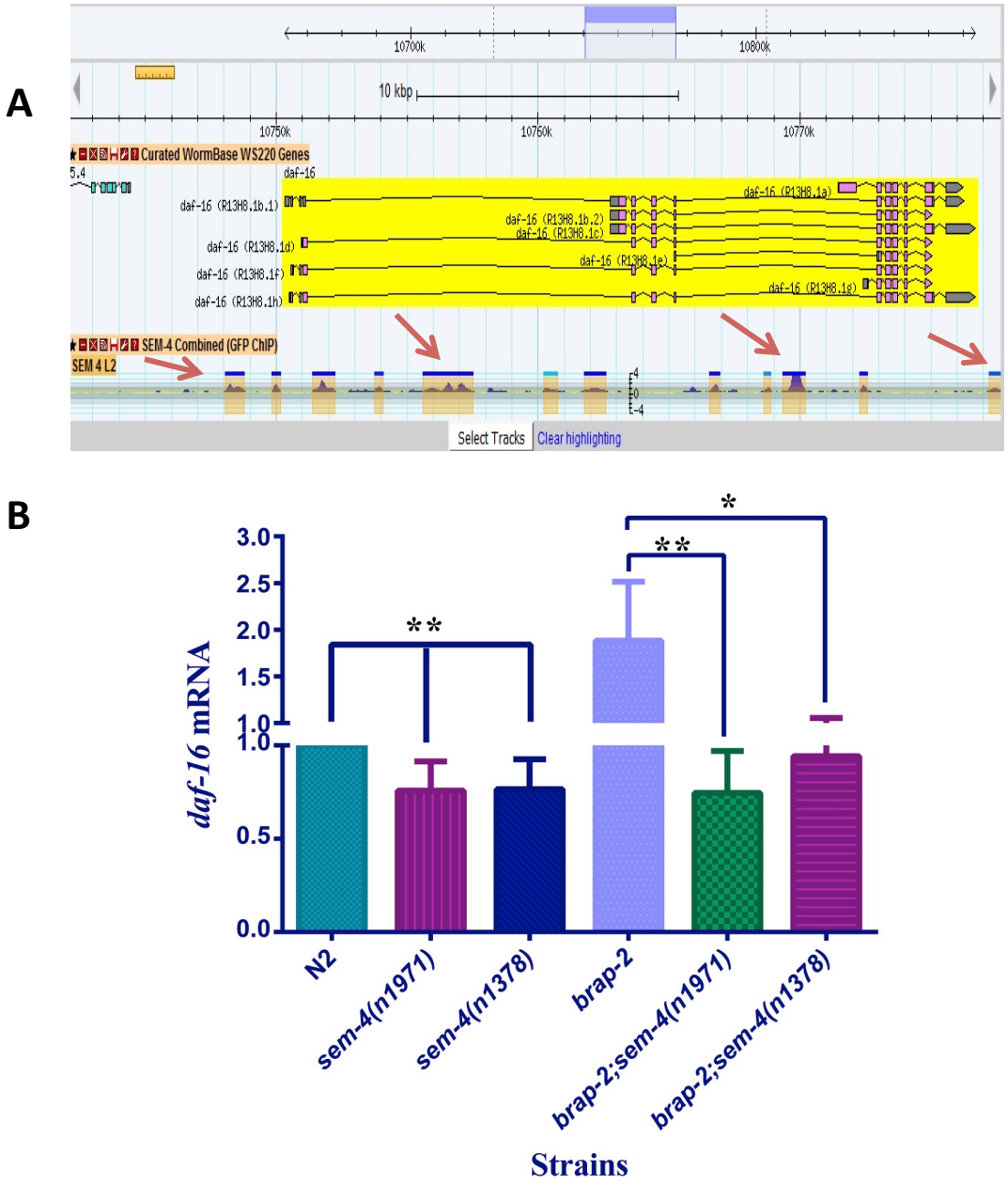

Figure 23. SEM-4 might be transcriptional activator of *daf-16*. A. SEM-4 binds to promoter region, intron regions and 3'UTR region of *daf-16*. Red arrows point to regions of SEM-4 binding. Figure adapted from modEncode ® website. http://gbrowse.modencode.org/fgb2/gbrowse/worm/. **B.** mRNA levels of *daf-16* are significantly affected by SEM-4. Mutation in *sem-4* results in 25% decrease in *daf-16* mRNA in both strains (*sem-4(n1971),* p=0.0044, n=4; *sem-4(n1378),* p=0.0056, n=5)**.** Increased expression in *brap-2* (p=0.006, n=6) is decreased by 2.5 fold in *sem-4(n1971);brap-2* strain (p=0.009, n=4) and by 2 fold in *brap-2;sem-4(n1378)* strain (p=0.02, n=4). mRNA levels are quantified by quantitative RT-PCR with *act-1* as a reference gene. Statistical analysis (student t-test) and graph were generated using Graphpad Prism ® 6.0 Software

4. Discussion

Our research has shown SEM-4 as a necessary transcription factor during oxidative stress. In particular, our identification of SEM-4 as a transcriptional regulator for *skn-1c* allowed us to hypothesize the pathway for regulation of expression of *gst-4* by SEM-4 in wild-type and *brap-2* mutant worms (Figure 25). Lower expression of two other SKN-1 targets, *gcs-1* and *gst-7,* in *brap-2;sem-4* mutant animals can also be explained by lower mRNA levels of *skn-1c* in these mutants.

Previous research has identified SEM-4 as a crucial developmental protein in the worm, and its expression was reported to be indispensable for proper development of the vulva, some motor neurons, touch receptor neurons and coelomocytes (Basson and Horvitz 1996; Grant et al. 2000). In addition to previously reported tissues, we have found expression of SEM-4 in intestinal nuclei and hyp7 (main body syncytium) nuclei (Figure 22). Since most of the ROS detoxification in the worm takes place in the intestine (Murphy and Hu 2013) and transcription factors affecting stress response are expected to be present in intestinal nuclei, the localization of SEM-4 in intestinal nuclei allowed us to draw connections to the novel role of SEM-4 in the oxidative stress response. Additionally, expression of SEM-4 in hyp7 supports the importance of SEM-4 for detoxification process during oxidative stress.

The initial RNAi screen (Figure 9) determined that transcription of detoxification enzyme, *gst-4*, is lowered in the absence of SEM-4 in *brap-2* mutants. We have found that mRNA levels of *gst-4* are significantly lower, not only in *brap-2;sem-4* worms, but in *sem-4* single mutants as well. Further research showed that short exposure to paraquat is sufficient to see a significant difference in expression of *gst-4* in *brap-2;sem-4* double mutants in comparison to *brap-2* animals. On the other hand, single *sem-4* mutants require longer exposure to paraquat in order to demonstrate a significant difference in expression of *gst-4* in comparison to wild-type

worms. The expression of *gst-4* was mostly halted in hypodermal cells, which can be explained by a higher expression of *sem-4* in these cells; the expression of *gst-4* in intestinal nuclei in *sem-4* mutants was similar to the wild-type animals. Next, we reported a significant increase of *gst-4* mRNA in *sem-4* overexpressing worms in comparison to the wild-type. Overall, we concluded that SEM-4 is required for expression of *gst-4*.

After determining that SEM-4 affects expression of *gst-4,* we next looked into its mechanism of regulation. Since we could not detect a physical interaction of SEM-4 with SKN-1 or MDT-15, and there is no reported binding of SEM-4 on the *gst-4* promoter region in the database ModENCODE®, we have eliminated a possibility of SEM-4 directly regulating expression of *gst-4*. Therefore, we looked into SEM-4 regulating expression of *skn-1,* where SEM-4 binds to the promoter and intron regions of *skn-1* (reported by ModENCODE®). First, we have noticed a drastic decrease in mRNA levels of *skn-1c* (SKN-1C isoform is associated with the stress response pathway) in *sem-4* mutants, and a significant increase in *sem-4* overexpressing worms. The same decrease in *skn-1c* expression was valid for *brap-2* mutant animals by introduction of *sem-4* mutation in comparison to *brap-2* worms. The results suggest that expression of *skn-1c* is regulated by SEM-4 independently from BRAP-2. As we have described earlier, inhibition of BRAP-2 activates RAS/ERK-1,2 pathway, and therefore regulates expression and nuclear localization of SKN-1. We believe that SEM-4 physically binds to the promoter of *skn-1c* and activates its expression. Furthermore, we detected that intestinal nuclear localization of SKN-1C after paraquat stress was halted in *sem-4* null mutants. We were uncertain whether SEM-4 regulates SKN-1C nuclear localization on top of activating transcription of *skn-1c*, or whether low levels of SKN-1C in *sem-4(n1971)* worms do not allow detection of intestinal nuclear SKN-1C. Since we could not detect a physical interaction between SKN-1 and SEM-4, and we cannot conclude that SEM-4 aids in nuclear localization of SKN-1C,

we speculate that the observed results correspond with low levels of SKN-1C in *sem-4(n1971)* animals. In brief, we came to the conclusion that expression of *gst-4* is regulated by SEM-4 thorough *skn-1*.

Furthermore, SEM-4 is necessary for increased lifespan of *skn-1* overexpressing and wild-type worms. The lifespan assay results agreed with previously reported longevity of *skn-1* overexpressing worms in comparison to wild-type animals (Tullet et al. 2008). Since SEM-4 is required to activate expression of *skn-1,* we hypothesized that increased lifespan of *skn-1* overexpressing worms was halted by *sem-4* mutation in the worms. Indeed, we showed that null *sem-4* mutation significantly shortened lifespan of nematodes independently of overexpression of *skn-1*. Next, lifespan of long-lived mutants was prolonged by addition of *sem-4* transgene, and *skn-1(+);sem-4(+)* worms reported significantly longer lifespan in comparison to *skn-1(+)* worms. Expression levels of detoxification enzymes in those worms can explain the lifespan results. As a of matter of fact, mRNA levels of SKN-1 targets: *gst-4, gst-7* and *gst-10,* reported significant increases in *skn-1(+);sem-4(+)* animals in comparison to wild-type, and a significant drop in expression of the enzymes was detected in *skn-1(+);sem-4(-)* worms in comparison to *skn-1(+)* and wild-type animals. Overall, we showed that SEM-4 is necessary for the lifespan of wild-type and *skn-1(+) C. elegans,* and lifespan is dependent on expression levels of SKN-1C targets.

Our functional assay showed the necessity of SEM-4 to activate the detoxification response during oxidative stress. Since we have noticed that *sem-4* mutants produce significantly higher levels of ROS in comparison to wild-type worms before and after oxidative stress, we strongly believe that insufficient amount of detoxification enzymes are produced in *sem-4* mutants to cope with an overproduction of ROS. Indeed, we have reported above that the expression of *gst-4* is halted in *sem-4* mutants before and after oxidative stress. Even though we

did not test expression levels of other detoxification enzymes after the paraquat stress in *sem-4* mutant worms, we believe that they might be also affected by absence of SEM-4. Despite the fact that we were not able to test ROS production in *sem-4* overexpressing worms (see *Limitations of the study)*, higher mRNA levels of *skn-1c* and *gst-4* in *sem-4* overexpressing worms in comparison to wild-type animals allows us to speculate that ROS levels in *sem-4(+)* worms are significantly lower than in wild-type worms. Therefore, we can conclude that SEM-4 is crucial for balancing ROS levels in *C. elegans* by activating expression *gst-4* through *skn-1c.*

Even though many papers report that some long-lived mutants physiologically have higher levels of ROS, and that the levels of ROS is not a demonstrator for lifespan expectations (Lapointe and Hekimi 2010; Yang and Hekimi 2010; Schaar et al. 2015), our survival assay of *sem-4* mutant worms showed the direct link between GST-4 production and mean lifespan during oxidative stress. As it was described earlier, we have observed a drastic decrease in survival of wild-type worms with *sem-4(n1971)* mutation on paraquat plates. Furthermore, C-terminal *sem-4* mutants also demonstrated reduced survival in comparison to the wild-type worms, but the effect was not as dramatic as with a *sem-4* N-terminal mutation. Since both *sem-4* mutants affected the survival of *C. elegans* during constant oxidative stress conditions, we can conclude that SEM-4 is an essential gene for the oxidative stress response pathway. Since there is a more drastic reduction in the lifespan and survival of *sem-4(n1971)* in comparison to *sem-4(n1378)* worms, and lower mRNA levels of *skn-1c* and *gst-4* in *sem-4(n1971)* were detected in comparison to *sem-4(n1378),* we came to the conclusion that the *sem-4(n1971)* mutation showed a stronger effect during oxidative stress.

Considering this novel function of SEM-4, we believe that it might be involved in more than one pathway for the oxidative stress response. Indeed, we speculate the importance of SEM-4 in transcriptional activation of more than one transcription factor for detoxification enzymes.

We have noticed that besides binding to *skn-1* promoter region, SEM-4 is reported by ModENCODE® (Celniker et al. 2009) to bind to both promoter and intron regions of *daf-16.* As a matter of fact, mRNA levels of *daf-16* in *sem-4* mutants showed significant reduction in comparison to wild-type and *brap-2* worms. Therefore, we believe that SEM-4 is a master regulator of two transcription factors in the oxidative stress pathway, SKN-1 and possibly DAF-16. Overall, we found a novel role for SEM-4, and propose the model for the oxidative stress response pathway that is regulated by SEM-4 (Figure 25).

Limitations of the study

Throughout the course of our research we have encountered a few study limitations.

First, we were unable to check ROS levels in *sem-4* overexpressing worms. As it was mentioned before we have used DCFDA dye to quantify ROS levels in the worms, and DCFDA produces fluorescence after reacting with ROS molecules (Supplementary Figure 2). Our *sem-4(+)* strain is SEM-4::GFP, and therefore expresses GFP protein. Since, fluorescence produced by DCFDA after reacting with ROS molecules is detected by the same wavelength as detection of GFP we were unable to test ROS production in GFP worms using DCFDA dye.

Second, expression of SEM-4 in intestinal nuclei is very weak and was achieved by higher excitation in comparison to detection of SEM-4 in hypodermal cells.

Lastly, we had to perform lifespan on FUdR (Fluorodeoxyuridine) containing plates. Due to the fact that *sem-4* mutant animals are egg-laying defective, and their lifespan determined by the time of eggs hatching in the vulva, it is impossible to track lifespan of *sem-4* mutants on regular NGM plates. Therefore, we had to perform lifespan assays on plates containing this DNA synthesis inhibitor. However, it is possible that lifespan was slightly altered by presence of FUdR, but since all strains were grown under the same conditions, we are confident in our obtained results.

5. Future work

Together, these results indicate a newly identified role of SEM-4 in regulating expression of phase II detoxification enzymes and preventing the harmful effects caused by overproduction of ROS. These findings allow us to consider additional experiments to support our results.

First, we are interested in testing the potential for *in vivo* binding of SEM-4 to *skn-1c* promoter. For this experiment, we are planning to use ChIP assay on *sem-4(+)::gfp* and *sem-4(+)::gfp;brap-2(ok1492)* strains. Since *sem-4(+)::gfp* strain transcribes SEM-4::GFP, we can use anti-GFP antibody to pull-down DNA sequences bound to SEM-4. We predict to see higher affinity between SEM-4 and *Pskn-1c* in *sem-4(+);brap-2(ok1492)* worms in comparison to *sem-4(+)* worms.

Second, we would like to determine which of the zinc fingers domains of SEM-4 is required to activate transcription of *skn-1c*. For that experiment, we could clone zinc fingers of SEM-4 and use luciferase assay to check for transcriptional activity of the promoter for *skn-1c*. We predict that the first five zinc fingers will show stronger binding in contrast to last three.

Besides testing mRNA levels for each gene separately by RT-qPCR in *sem-4* mutants, we believe it is useful to obtain an mRNA microarray profile for *sem-4(n1971)* worms (*sem-4* null mutants). The results of an mRNA microarray could provide an overview of up-regulated and down-regulated genes by *sem-4* mutation, and that will allow us to make more specific hypotheses regarding relevant pathways. After the mRNA microarray, all the genes of interest will be verified by RT-qPCR.

In addition, our lab tested for an interaction between SEM-4 and BRAP-2. For this experiment, we subcloned SEM-4 into mammalian expression vectors that would produce FLAG-tagged protein. We co-transfected that construct with mGST-BRAP-2 into HEK293T cells, and co-immunoprecipitated with GST beads; then we performed Western Blot assay to

detect the expression of SEM-4 and BRAP-2 (in the same way as described in section 2.9 and 2.10). As a result, we were able to detect expression of both, SEM-4 and BRAP-2 (Figure 24); and also detect physical interaction between SEM-4 and BRAP-2 (Figure 24). Unfortunately, we were unsuccessful in our attempts to obtain the same results with the use of anti-Flag antibody to pulldown BRAP-2 with SEM-4 to confirm the interaction. The possible interaction of SEM-4 with BRAP-2 might be associated with the role of BRAP-2 in the RAS pathway, where SEM-4 disrupts BRAP-2-KSR-2 complex and allows activation of RAS pathway. On the other hand, SEM-4 might be interacting with the 14-3-3 homolog and BRAP-2 at the same time, and contribute to the stability of 14-3-3-KSR-BRAP-2 complex. Therefore, we would need to repeat that interaction with additional negative and positive controls and further investigate the role of SEM-4 in RAS pathway nuclear localization of target proteins.

Next, we would like to confirm a previously reported interaction between SEM-4 and FTT-2. The complex of DAF-16 and FTT-2/PAR-5 blocks DAF-16 from entering the nucleus (Berdichevsky et al. 2006). Dissociation from FTT-2 allows DAF-16 to enter the nucleus and activate its targets. We are interested in determining whether interaction of SEM-4 with FTT-2 disrupts the DAF-16-FTT-2 complex. Besides that, we would like to quantify mRNA levels of DAF-16 targets, and examine whether short survival and high ROS levels correspond with phase I detoxification enzymes in addition to phase II detoxification enzymes.

Further development of the study would include testing affect of SEM-4 on another transcription factor involved in ROS detoxification pathway, *hif-1* (Hypoxia Inducible Factor 1). According to ModENCODE® (Celniker et al. 2009) database by "Snyder" group, SEM-4 binds to promoter, intron and 3'UTR regions of *hif-1*, and that data makes it possible to speculate that SEM-4 might be a regulator of all three transcription factors involved in oxidative stress response.

As mentioned above, detection of ROS levels in GFP containing strains (*sem-4(+), skn-1(+),* and *sem-4(+);skn-1(+)*) was not feasible due to the nature of the experiment. Therefore, we would like to quantify ROS levels in all strains, including GFP strains, using another dye, such as MitoSox (absorption at 510nm and emission at 580nm) (Yang and Hekimi 2010). This dye has been used on live worms, as well as on isolated mitochondria.

Further study is required to test whether the same results are observed in *sem-4* mutant worms with treatment using different oxidative reagents. There are multiple studies that use Arsenite, hydrogen peroxide, and tert-Butyl in combination with paraquat to test production of detoxification enzymes and ROS. All the reagents can be used for short and long exposure on live worms with gradient concentration.

The expansion of this study would be to look into mammalian orthologs of SEM-4. As it was described earlier, there are four known mammalian genes: SALL1/2/3/4 that share homology with SEM-4. None of these gene products was associated with oxidative stress previously. It is curious whether SALL proteins regulate expression of Nrf2 (mammalian ortholog of SKN-1), and thus regulates expression of detoxification enzymes in mammals. For that purpose, it is probably best to start with RNAi for SALL1/2/3/4 in mammalian cell lines, and perform mRNA microarray to determine up-regulated and down-regulated genes. If the experiments on mammalian cells show the same trend as in *C. elegans,* the studies can then be furthered applied to studies on mice. Moreover, I believe that SEM-4, a protein involved in development and proper function of neurons in *C.elegans*, should be screened in neurodegenerative disease studies. Since mammalian ortholog of SEM-4, SALL2, is associated with ovarian cancer, studies in *C.elegans* should also look into expression and functionality of SEM-4 in different cancers in order to further investigate role of SEM-4 in age-related diseases.

6. Conclusion

Even though there are still many unknown pathways and proteins that regulate oxidative stress response, I have discovered the new player, SEM-4, in the ROS detoxification pathway. Furthermore, I have demonstrated that SEM-4 is not only a regulator of detoxification enzyme, *gst-4*, but also a master regulator responsible for activation of SKN-1, a transcription factor for phase II detoxification enzymes. Moreover, I speculate that SEM-4 affects transcription of *daf-16* as well, and therefore allows proper oxidative stress response in the worm. Indeed, no previous research has concentrated on transcriptional regulation of *skn-1* and *daf-16,* which makes my study novel in the field. I have supported my finding by demonstrating expression of SEM-4 in intestinal nuclei of *C.elegans* and most of the ROS detoxification takes place in the intestine of the animal. Besides previously reported transcription factors affecting lifespan, SKN-1 and DAF-16, I have found that increased lifespan is dependent on SEM-4, and SEM-4 was never associated with the longevity in previous studies. In addition, we discovered that SEM-4 is crucial for balancing ROS levels by regulating expression of *skn-1c* in *C. elegans,* and survival during oxidative stress is dependent on SEM-4. I also hypothesized that SEM-4 might be part of the RAS pathway due to possible interaction with BRAP-2, and SEM-4 was never described to be a player in the RAS pathway. Overall, SEM-4 and its orthologs were never associated with oxidative stress response pathway and longevity, and I have found a novel role for SEM-4. The research I have started with looking into the role of SEM-4 in oxidative stress pathway should be taken further in order to identify more players in ROS detoxification pathway, and to determine possible ways to protect us, humans, from detrimental outcomes after exposure to ROS. To conclude my study I propose a model for SEM-4 regulation of the oxidative stress response pathway (Figure 25).

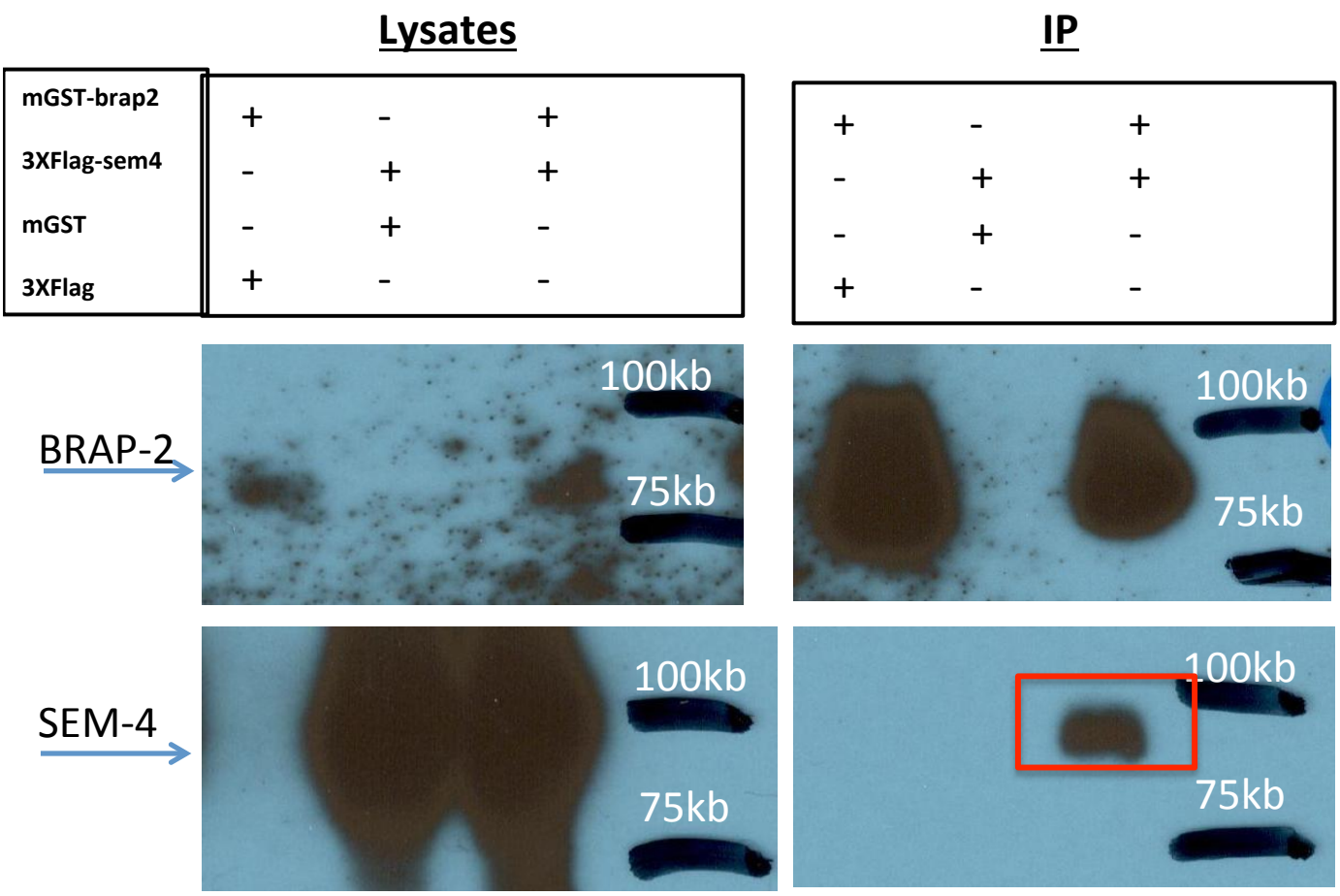

Figure 24. *In vitro* interaction of SEM-4 and BRAP-2. Western Blot analysis of BRAP-2 and SEM-4 interaction in HEK293T cells. Cells were co-transfected with 3xFlag-SEM-4 and mGST-BRAP-2, and incubated for 72 hours in tissue culture incubator. Lysates were pulled down with GST beads. Results show expression of both proteins, BRAP-2 and SEM-4; and physical interaction between BRAP-2 and SEM-4.

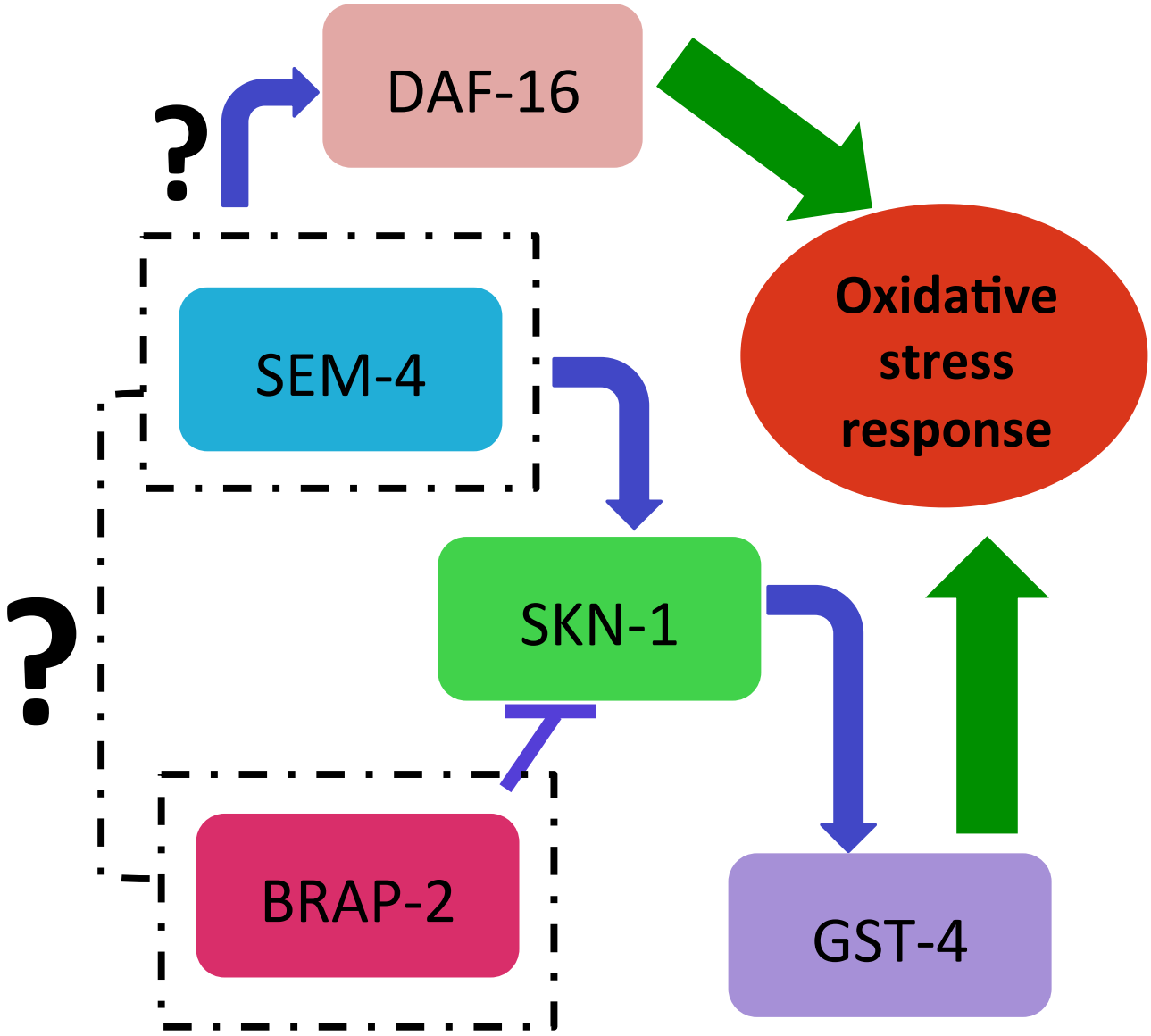

Figure 25. Proposed model of action of SEM-4 to promote oxidative stress response. SEM-4 is responsible for transcriptional activation of SKN-1 and that leads to the oxidative stress response. The effect of SEM-4 on DAF-16 and BRAP-2 requires further research.

7. Bibliography:

Alper S, McElwee MK, Apfeld J, Lackford B, Freedman JH, Schwartz DA. 2010. The Caenorhabditis elegans germ line regulates distinct signaling pathways to control lifespan and innate immunity. *The Journal of biological chemistry* **285**(3): 1822-1828.

An JH, Blackwell TK. 2003. SKN-1 links C. elegans mesendodermal specification to a conserved oxidative stress response. *Genes & development* **17**(15): 1882-1893.

An JH, Vranas K, Lucke M, Inoue H, Hisamoto N, Matsumoto K, Blackwell TK. 2005. Regulation of the Caenorhabditis elegans oxidative stress defense protein SKN-1 by glycogen synthase kinase-3. *Proceedings of the National Academy of Sciences of the United States of America* **102**(45): 16275-16280.

Arantes-Oliveira N, Berman JR, Kenyon C. 2003. Healthy animals with extreme longevity. *Science* **302**(5645): 611.

Asada M, Ohmi K, Delia D, Enosawa S, Suzuki S, Yuo A, Suzuki H, Mizutani S. 2004. Brap2 functions as a cytoplasmic retention protein for p21 during monocyte differentiation. *Molecular and cellular biology* **24**(18): 8236-8243.

Basson M, Horvitz HR. 1996. The Caenorhabditis elegans gene sem-4 controls neuronal and mesodermal cell development and encodes a zinc finger protein. *Genes & development* **10**(15): 1953-1965.

Berdichevsky A, Viswanathan M, Horvitz HR, Guarente L. 2006. C. elegans SIR-2.1 interacts with 14-3-3 proteins to activate DAF-16 and extend life span. *Cell* **125**(6): 1165-1177.

Bishop NA, Guarente L. 2007. Two neurons mediate diet-restriction-induced longevity in C. elegans. *Nature* **447**(7144): 545-549.

Blackwell TK, Steinbaugh MJ, Hourihan JM, Ewald CY, Isik M. 2015. SKN-1/Nrf, stress responses, and aging in Caenorhabditis elegans. *Free radical biology & medicine*.

Bowerman B, Eaton BA, Priess JR. 1992. skn-1, a maternally expressed gene required to specify the fate of ventral blastomeres in the early C. elegans embryo. *Cell* **68**(6): 1061-1075.

Brenner S. 1974. The genetics of Caenorhabditis elegans. *Genetics* **77**(1): 71-94.

Calkins MJ, Johnson DA, Townsend JA, Vargas MR, Dowell JA, Williamson TP, Kraft AD, Lee JM, Li J, Johnson JA. 2009. The Nrf2/ARE pathway as a potential therapeutic target in neurodegenerative disease. *Antioxidants & redox signaling* **11**(3): 497-508.

Cargill SL, Carey JR, Muller HG, Anderson G. 2003. Age of ovary determines remaining life expectancy in old ovariectomized mice. *Aging cell* **2**(3): 185-190.

Celniker SE, Dillon LA, Gerstein MB, Gunsalus KC, Henikoff S, Karpen GH, Kellis M, Lai EC, Lieb JD, MacAlpine DM et al. 2009. Unlocking the secrets of the genome. *Nature* **459**(7249): 927-930.

Chen JS, Hu HY, Zhang S, He M, Hu RM. 2009. Brap2 facilitates HsCdc14A Lys-63 linked ubiquitin modification. *Biotechnology letters* **31**(5): 615-621.

Christensen K, Johnson TE, Vaupel JW. 2006. The quest for genetic determinants of human longevity: challenges and insights. *Nature reviews Genetics* **7**(6): 436-448.

Clancy DJ, Gems D, Harshman LG, Oldham S, Stocker H, Hafen E, Leevers SJ, Partridge L. 2001. Extension of life-span by loss of CHICO, a Drosophila insulin receptor substrate protein. *Science* **292**(5514): 104-106.

Clejan L, Cederbaum AI. 1989. Synergistic interactions between NADPH-cytochrome P-450 reductase, paraquat, and iron in the generation of active oxygen radicals. *Biochemical pharmacology* **38**(11): 1779-1786.

Coletta A, Pinney JW, Solis DY, Marsh J, Pettifer SR, Attwood TK. 2010. Low-complexity regions within protein sequences have position-dependent roles. *BMC systems biology* **4**: 43.

Davies RG, Wagstaff KM, McLaughlin EA, Loveland KL, Jans DA. 2013. The BRCA1-binding protein BRAP2 can act as a cytoplasmic retention factor for nuclear and nuclear envelope-localizing testicular proteins. *Biochimica et biophysica acta* **1833**(12): 3436-3444.

Dibble CC, Manning BD. 2013. Signal integration by mTORC1 coordinates nutrient input with biosynthetic output. *Nature cell biology* **15**(6): 555-564.

Ezziane Z. 2012. Analysis of the Hox epigenetic code. *World journal of clinical oncology* **3**(4): 48-56.

Fabrizio P, Pozza F, Pletcher SD, Gendron CM, Longo VD. 2001. Regulation of longevity and stress resistance by Sch9 in yeast. *Science* **292**(5515): 288-290.

Fatima S, Wagstaff KM, Loveland KL, Jans DA. 2015. Interactome of the negative regulator of nuclear import BRCA1-binding protein 2. *Scientific reports* **5**: 9459.

Finkel T, Holbrook NJ. 2000. Oxidants, oxidative stress and the biology of ageing. *Nature* **408**(6809): 239-247.

Flachsbart F, Caliebe A, Kleindorp R, Blanche H, von Eller-Eberstein H, Nikolaus S, Schreiber S, Nebel A. 2009. Association of FOXO3A variation with human longevity confirmed in German centenarians. *Proceedings of the National Academy of Sciences of the United States of America* **106**(8): 2700-2705.

Friedman DB, Johnson TE. 1988. A mutation in the age-1 gene in Caenorhabditis elegans lengthens life and reduces hermaphrodite fertility. *Genetics* **118**(1): 75-86.

Fu X, Tang Y, Dickinson BC, Chang CJ, Chang Z. 2015. An oxidative fluctuation hypothesis of aging generated by imaging H(2)O(2) levels in live Caenorhabditis elegans with altered lifespans. *Biochemical and biophysical research communications* **458**(4): 896-900.

Fulcher AJ, Roth DM, Fatima S, Alvisi G, Jans DA. 2010. The BRCA-1 binding protein BRAP2 is a novel, negative regulator of nuclear import of viral proteins, dependent on phosphorylation flanking the nuclear localization signal. *FASEB journal : official publication of the Federation of American Societies for Experimental Biology* **24**(5): 1454-1466.

Glover-Cutter KM, Lin S, Blackwell TK. 2013. Integration of the unfolded protein and oxidative stress responses through SKN-1/Nrf. *PLoS genetics* **9**(9): e1003701.

Goh GY, Martelli KL, Parhar KS, Kwong AW, Wong MA, Mah A, Hou NS, Taubert S. 2014. The conserved Mediator subunit MDT-15 is required for oxidative stress responses in Caenorhabditis elegans. *Aging cell* **13**(1): 70-79.

Grant K, Hanna-Rose W, Han M. 2000. sem-4 promotes vulval cell-fate determination in Caenorhabditis elegans through regulation of lin-39 Hox. *Developmental biology* **224**(2): 496-506.

Haigis MC, Yankner BA. 2010. The aging stress response. *Molecular cell* **40**(2): 333-344.

Harman D. 1956. Aging: a theory based on free radical and radiation chemistry. *Journal of gerontology* **11**(3): 298-300.

-. 1972. The biologic clock: the mitochondria? *Journal of the American Geriatrics Society* **20**(4): 145-147.

Harrison DE, Strong R, Sharp ZD, Nelson JF, Astle CM, Flurkey K, Nadon NL, Wilkinson JE, Frenkel K, Carter CS et al. 2009. Rapamycin fed late in life extends lifespan in genetically heterogeneous mice. *Nature* **460**(7253): 392-395.

Holzenberger M, Dupont J, Ducos B, Leneuve P, Geloen A, Even PC, Cervera P, Le Bouc Y. 2003. IGF-1 receptor regulates lifespan and resistance to oxidative stress in mice. *Nature* **421**(6919): 182-187.

Honda S, Ishii N, Suzuki K, Matsuo M. 1993. Oxygen-dependent perturbation of life span and aging rate in the nematode. *Journal of gerontology* **48**(2): B57-61.

Honda Y, Honda S. 1999. The daf-2 gene network for longevity regulates oxidative stress resistance and Mn-superoxide dismutase gene expression in Caenorhabditis elegans. *FASEB journal : official publication of the Federation of American Societies for Experimental Biology* **13**(11): 1385-1393.

Hsu AL, Murphy CT, Kenyon C. 2003. Regulation of aging and age-related disease by DAF-16 and heat-shock factor. *Science* **300**(5622): 1142-1145.

Hu Q, D'Amora D, MacNeil L, Walhout M, Kubiseski TJ. C. elegans BRAP-2 regulates SKN-1/ELT-3 in response to oxidative stress through the ERK/MAPK partway. Manuscript in preparation.

Huang Y, Li W, Su ZY, Kong AT. 2015. The complexity of the Nrf2 pathway: beyond the antioxidant response. *The Journal of nutritional biochemistry*.

Inoue H, Hisamoto N, An JH, Oliveira RP, Nishida E, Blackwell TK, Matsumoto K. 2005. The C. elegans p38 MAPK pathway regulates nuclear localization of the transcription factor SKN-1 in oxidative stress response. *Genes & development* **19**(19): 2278-2283.

Itoh K, Chiba T, Takahashi S, Ishii T, Igarashi K, Katoh Y, Oyake T, Hayashi N, Satoh K, Hatayama I et al. 1997. An Nrf2/small Maf heterodimer mediates the induction of phase II detoxifying enzyme genes through antioxidant response elements. *Biochemical and biophysical research communications* **236**(2): 313-322.

Itoh K, Wakabayashi N, Katoh Y, Ishii T, Igarashi K, Engel JD, Yamamoto M. 1999. Keap1 represses nuclear activation of antioxidant responsive elements by Nrf2 through binding to the amino-terminal Neh2 domain. *Genes & development* **13**(1): 76-86.

Jia K, Chen D, Riddle DL. 2004. The TOR pathway interacts with the insulin signaling pathway to regulate C. elegans larval development, metabolism and life span. *Development* **131**(16): 3897-3906.

Johnson SC, Rabinovitch PS, Kaeberlein M. 2013. mTOR is a key modulator of ageing and age-related disease. *Nature* **493**(7432): 338-345.

Kaeberlein M, Powers RW, 3rd, Steffen KK, Westman EA, Hu D, Dang N, Kerr EO, Kirkland KT, Fields S, Kennedy BK. 2005. Regulation of yeast replicative life span by TOR and Sch9 in response to nutrients. *Science* **310**(5751): 1193-1196.

Kagias K, Ahier A, Fischer N, Jarriault S. 2012. Members of the NODE (Nanog and Oct4-associated deacetylase) complex and SOX-2 promote the initiation of a natural cellular reprogramming event in vivo. *Proceedings of the National Academy of Sciences of the United States of America* **109**(17): 6596-6601.

Kapahi P, Zid BM, Harper T, Koslover D, Sapin V, Benzer S. 2004. Regulation of lifespan in Drosophila by modulation of genes in the TOR signaling pathway. *Current biology : CB* **14**(10): 885-890.

Kenyon C. 2005. The plasticity of aging: insights from long-lived mutants. *Cell* **120**(4): 449-460.

Kenyon C, Chang J, Gensch E, Rudner A, Tabtiang R. 1993. A C. elegans mutant that lives twice as long as wild type. *Nature* **366**(6454): 461-464.

King ER, Wong KK. 2012. Insulin-like growth factor: current concepts and new developments in cancer therapy. *Recent patents on anti-cancer drug discovery* **7**(1): 14-30.

Kobayashi A, Kang MI, Okawa H, Ohtsuji M, Zenke Y, Chiba T, Igarashi K, Yamamoto M. 2004. Oxidative stress sensor Keap1 functions as an adaptor for Cul3-based E3 ligase to regulate proteasomal degradation of Nrf2. *Molecular and cellular biology* **24**(16): 7130-7139.

Kohlhase J, Chitayat D, Kotzot D, Ceylaner S, Froster UG, Fuchs S, Montgomery T, Rosler B. 2005. SALL4 mutations in Okihiro syndrome (Duane-radial ray syndrome), acro-renal-ocular syndrome, and related disorders. *Human mutation* **26**(3): 176-183.

Kolch W. 2005. Coordinating ERK/MAPK signalling through scaffolds and inhibitors. *Nature reviews Molecular cell biology* **6**(11): 827-837.

Koon JC, Kubiseski TJ. 2010. Developmental arrest of Caenorhabditis elegans BRAP-2 mutant exposed to oxidative stress is dependent on BRC-1. *The Journal of biological chemistry* **285**(18): 13437-13443.

Kuhnlein RP, Bronner G, Taubert H, Schuh R. 1997. Regulation of Drosophila spalt gene expression. *Mechanisms of development* **66**(1-2): 107-118.

Lai CH, Chou CY, Ch'ang LY, Liu CS, Lin W. 2000. Identification of novel human genes evolutionarily conserved in Caenorhabditis elegans by comparative proteomics. *Genome research* **10**(5): 703-713.

Laplante M, Sabatini DM. 2012. mTOR signaling in growth control and disease. *Cell* **149**(2): 274-293.

Lapointe J, Hekimi S. 2010. When a theory of aging ages badly. *Cellular and molecular life sciences : CMLS* **67**(1): 1-8.

Leiers B, Kampkotter A, Grevelding CG, Link CD, Johnson TE, Henkle-Duhrsen K. 2003. A stress-responsive glutathione S-transferase confers resistance to oxidative stress in Caenorhabditis elegans. *Free radical biology & medicine* **34**(11): 1405-1415.

Leung CK, Wang Y, Deonarine A, Tang L, Prasse S, Choe KP. 2015. Retraction for Leung et al., A Negative-Feedback Loop between the Detoxification/Antioxidant Response Factor SKN-1 and Its Repressor WDR-23 Matches Organism Needs with Environmental Conditions. *Molecular and cellular biology* **35**(18): 3254.

Li S, Ku CY, Farmer AA, Cong YS, Chen CF, Lee WH. 1998. Identification of a novel cytoplasmic protein that specifically binds to nuclear localization signal motifs. *The Journal of biological chemistry* **273**(11): 6183-6189.

Lin K, Dorman JB, Rodan A, Kenyon C. 1997. daf-16: An HNF-3/forkhead family member that can function to double the life-span of Caenorhabditis elegans. *Science* **278**(5341): 1319-1322.

Lu T, Aron L, Zullo J, Pan Y, Kim H, Chen Y, Yang TH, Kim HM, Drake D, Liu XS et al. 2014. REST and stress resistance in ageing and Alzheimer's disease. *Nature* **507**(7493): 448-454.

Martindale JL, Holbrook NJ. 2002. Cellular response to oxidative stress: signaling for suicide and survival. *Journal of cellular physiology* **192**(1): 1-15.

Matheny SA, Chen C, Kortum RL, Razidlo GL, Lewis RE, White MA. 2004. Ras regulates assembly of mitogenic signalling complexes through the effector protein IMP. *Nature* **427**(6971): 256-260.

McCubrey JA, Steelman LS, Chappell WH, Abrams SL, Wong EW, Chang F, Lehmann B, Terrian DM, Milella M, Tafuri A et al. 2007. Roles of the Raf/MEK/ERK pathway in cell growth, malignant transformation and drug resistance. *Biochimica et biophysica acta* **1773**(8): 1263-1284.

Mertenskotter A, Keshet A, Gerke P, Paul RJ. 2013. The p38 MAPK PMK-1 shows heat-induced nuclear translocation, supports chaperone expression, and affects the heat tolerance of Caenorhabditis elegans. *Cell stress & chaperones* **18**(3): 293-306.

Moi P, Chan K, Asunis I, Cao A, Kan YW. 1994. Isolation of NF-E2-related factor 2 (Nrf2), a NF-E2-like basic leucine zipper transcriptional activator that binds to the tandem NF-E2/AP1 repeat of the beta-globin locus control region. *Proceedings of the National Academy of Sciences of the United States of America* **91**(21): 9926-9930.

Morris JZ, Tissenbaum HA, Ruvkun G. 1996. A phosphatidylinositol-3-OH kinase family member regulating longevity and diapause in Caenorhabditis elegans. *Nature* **382**(6591): 536-539.

Morrison DK. 2001. KSR: a MAPK scaffold of the Ras pathway? *Journal of cell science* **114**(Pt 9): 1609-1612.

Mukhopadhyay A, Tissenbaum HA. 2007. Reproduction and longevity: secrets revealed by C. elegans. *Trends in cell biology* **17**(2): 65-71.

Murakami S, Motohashi H. 2015. Roles of Nrf2 in cell proliferation and differentiation. *Free radical biology & medicine* **88**(Pt B): 168-178.

Murphy CT, Hu PJ. 2013. Insulin/insulin-like growth factor signaling in C. elegans. *WormBook : the online review of C elegans biology*: 1-43.

Netzer C, Bohlander SK, Hinzke M, Chen Y, Kohlhase J. 2006. Defining the heterochromatin localization and repression domains of SALL1. *Biochimica et biophysica acta* **1762**(3): 386-391.

O'Neill C, Kiely AP, Coakley MF, Manning S, Long-Smith CM. 2012. Insulin and IGF-1 signalling: longevity, protein homoeostasis and Alzheimer's disease. *Biochemical Society transactions* **40**(4): 721-727.

Oh SW, Mukhopadhyay A, Dixit BL, Raha T, Green MR, Tissenbaum HA. 2006. Identification of direct DAF-16 targets controlling longevity, metabolism and diapause by chromatin immunoprecipitation. *Nature genetics* **38**(2): 251-257.

Ohmachi M, Rocheleau CE, Church D, Lambie E, Schedl T, Sundaram MV. 2002. C. elegans ksr-1 and ksr-2 have both unique and redundant functions and are required for MPK-1 ERK phosphorylation. *Current biology : CB* **12**(5): 427-433.

Okuyama T, Inoue H, Ookuma S, Satoh T, Kano K, Honjoh S, Hisamoto N, Matsumoto K, Nishida E. 2010. The ERK-MAPK pathway regulates longevity through SKN-1 and insulin-like signaling in Caenorhabditis elegans. *The Journal of biological chemistry* **285**(39): 30274-30281.

Oliveira RP, Porter Abate J, Dilks K, Landis J, Ashraf J, Murphy CT, Blackwell TK. 2009. Condition-adapted stress and longevity gene regulation by Caenorhabditis elegans SKN-1/Nrf. *Aging cell* **8**(5): 524-541.

Papaconstantinou J. 2009. Insulin/IGF-1 and ROS signaling pathway cross-talk in aging and longevity determination. *Molecular and cellular endocrinology* **299**(1): 89-100.

Pawlikowska L, Hu D, Huntsman S, Sung A, Chu C, Chen J, Joyner AH, Schork NJ, Hsueh WC, Reiner AP et al. 2009. Association of common genetic variation in the insulin/IGF1 signaling pathway with human longevity. *Aging cell* **8**(4): 460-472.

Riddle DL, Swanson MM, Albert PS. 1981. Interacting genes in nematode dauer larva formation. *Nature* **290**(5808): 668-671.

Robida-Stubbs S, Glover-Cutter K, Lamming DW, Mizunuma M, Narasimhan SD, Neumann-Haefelin E, Sabatini DM, Blackwell TK. 2012. TOR signaling and rapamycin influence longevity by regulating SKN-1/Nrf and DAF-16/FoxO. *Cell metabolism* **15**(5): 713-724.

Rodriguez M, Snoek LB, De Bono M, Kammenga JE. 2013. Worms under stress: C. elegans stress response and its relevance to complex human disease and aging. *Trends in genetics : TIG* **29**(6): 367-374.

Runchel C, Matsuzawa A, Ichijo H. 2011. Mitogen-activated protein kinases in mammalian oxidative stress responses. *Antioxidants & redox signaling* **15**(1): 205-218.

Sakaguchi A, Matsumoto K, Hisamoto N. 2004. Roles of MAP kinase cascades in Caenorhabditis elegans. *Journal of biochemistry* **136**(1): 7-11.

Schaar CE, Dues DJ, Spielbauer KK, Machiela E, Cooper JF, Senchuk M, Hekimi S, Van Raamsdonk JM. 2015. Mitochondrial and cytoplasmic ROS have opposing effects on lifespan. *PLoS genetics* **11**(2): e1004972.

Schieber M, Chandel NS. 2014. TOR signaling couples oxygen sensing to lifespan in C. elegans. *Cell reports* **9**(1): 9-15.

Shaye DD, Greenwald I. 2011. OrthoList: a compendium of C. elegans genes with human orthologs. *PloS one* **6**(5): e20085.

Shikauchi Y, Saiura A, Kubo T, Niwa Y, Yamamoto J, Murase Y, Yoshikawa H. 2009. SALL3 interacts with DNMT3A and shows the ability to inhibit CpG island methylation in hepatocellular carcinoma. *Molecular and cellular biology* **29**(7): 1944-1958.

Simonis N, Rual JF, Carvunis AR, Tasan M, Lemmens I, Hirozane-Kishikawa T, Hao T, Sahalie JM, Venkatesan K, Gebreab F et al. 2009. Empirically controlled mapping of the Caenorhabditis elegans protein-protein interactome network. *Nature methods* **6**(1): 47-54.

Son Y, Kim S, Chung HT, Pae HO. 2013. Reactive oxygen species in the activation of MAP kinases. *Methods in enzymology* **528**: 27-48.

Suh Y, Atzmon G, Cho MO, Hwang D, Liu B, Leahy DJ, Barzilai N, Cohen P. 2008. Functionally significant insulin-like growth factor I receptor mutations in centenarians. *Proceedings of the National Academy of Sciences of the United States of America* **105**(9): 3438-3442.

Syntichaki P, Tavernarakis N. 2004. Genetic models of mechanotransduction: the nematode Caenorhabditis elegans. *Physiological reviews* **84**(4): 1097-1153.

Takashima O, Tsuruta F, Kigoshi Y, Nakamura S, Kim J, Katoh MC, Fukuda T, Irie K, Chiba T. 2013. Brap2 regulates temporal control of NF-kappaB localization mediated by inflammatory response. *PloS one* **8**(3): e58911.

Tebay LE, Robertson H, Durant ST, Vitale SR, Penning TM, Dinkova-Kostova AT, Hayes JD. 2015. Mechanisms of activation of the transcription factor Nrf2 by redox stressors, nutrient cues, and energy status and the pathways through which it attenuates degenerative disease. *Free radical biology & medicine* **88**(Pt B): 108-146.

Toker AS, Teng Y, Ferreira HB, Emmons SW, Chalfie M. 2003. The Caenorhabditis elegans spalt-like gene sem-4 restricts touch cell fate by repressing the selector Hox gene egl-5 and the effector gene mec-3. *Development* **130**(16): 3831-3840.

Tormos AM, Talens-Visconti R, Nebreda AR, Sastre J. 2013. p38 MAPK: a dual role in hepatocyte proliferation through reactive oxygen species. *Free radical research* **47**(11): 905-916.

Torres M, Forman HJ. 2003. Redox signaling and the MAP kinase pathways. *BioFactors* **17**(1-4): 287-296.

Tullet JM, Hertweck M, An JH, Baker J, Hwang JY, Liu S, Oliveira RP, Baumeister R, Blackwell TK. 2008. Direct inhibition of the longevity-promoting factor SKN-1 by insulin-like signaling in C. elegans. *Cell* **132**(6): 1025-1038.

Van Raamsdonk JM, Hekimi S. 2010. Reactive Oxygen Species and Aging in Caenorhabditis elegans: Causal or Casual Relationship? *Antioxidants & redox signaling* **13**(12): 1911-1953.

Vellai T, Takacs-Vellai K, Zhang Y, Kovacs AL, Orosz L, Muller F. 2003. Genetics: influence of TOR kinase on lifespan in C. elegans. *Nature* **426**(6967): 620.

Weinberg F, Chandel NS. 2009. Reactive oxygen species-dependent signaling regulates cancer. *Cellular and molecular life sciences : CMLS* **66**(23): 3663-3673.

Willcox BJ, Donlon TA, He Q, Chen R, Grove JS, Yano K, Masaki KH, Willcox DC, Rodriguez B, Curb JD. 2008. FOXO3A genotype is strongly associated with human longevity. *Proceedings of the National Academy of Sciences of the United States of America* **105**(37): 13987-13992.

Yang HC, Chen TL, Wu YH, Cheng KP, Lin YH, Cheng ML, Ho HY, Lo SJ, Chiu DT. 2013. Glucose 6-phosphate dehydrogenase deficiency enhances germ cell apoptosis and causes defective embryogenesis in Caenorhabditis elegans. *Cell death & disease* **4**: e616.

Yang JS, Nam HJ, Seo M, Han SK, Choi Y, Nam HG, Lee SJ, Kim S. 2011. OASIS: online application for the survival analysis of lifespan assays performed in aging research. *PloS one* **6**(8): e23525.

Yang W, Hekimi S. 2010. A mitochondrial superoxide signal triggers increased longevity in Caenorhabditis elegans. *PLoS biology* **8**(12): e1000556.

Yoon SO, Yun CH, Chung AS. 2002. Dose effect of oxidative stress on signal transduction in aging. *Mechanisms of ageing and development* **123**(12): 1597-1604.

Appendix A - Media and Reagents

1. Nematode Growth Plates (NGM)

Recipe for 1L:

- 2.5g Peptone (powder)
- 3.0g NaCl (powder)
- 17.0 g Agar (powder)
- top up to 1L with ddH_2O

Procedure:

- Mix well and autoclave with appropriate setting for 50 minut
- Let media cool down to 55-60^oC
- Add the following components to pre-cooled media:
  - 1mL of 5mg/ml Cholesterol
  - 1mL of 1M $MgSO_4$
  - 1mL of 1M $CaCl_2$
  - 25mL of 1M KPO_4
- Mix all components using stirrer and stir bar
- Aliquot media into the plates (3cm, 6cm or 10cm plates)
- Let media to solidify
- Seed plates with appropriate volume of OP50

2. RNAi plates

- Prepare NGM as described above with addition of following components after autoclaved and pre-cooled media:
  - 1mL of 100mg/mL Ampicillin
  - 2.5 mL of 5mg/mL Tetracycline
  - 0.4 mL of 1M IPTG
- Mix all components using stirrer and stir bar
- Aliquot media into the 3cm plates
- Let media to solidify
- Seed plates with appropriate volume of HTT115

3. M9 Buffer

Recipe for 1L:

- 5.8g of $Na_2HPO_4 \cdot 7H_2O$ (powder)
- 3.0g of KH_2PO_4 (powder)
- 5.0g of NaCl (powder)
- 0.25g of $MgSO_4 \cdot 7H_2O$ (powder)
- - top up to 1L with ddH_2O

Procedure:

- Mix well by stirring
- Aliquot 125mL, 250mL or 500mL into bottles
- Autoclave using liquid cycle for 50 minutes

4. Luria Broth (LB)

Recipe for 1L:

- 10.0g NaCl
- 10.0g Tryptone
- 5.0g Yeast Extract
- top up to 1L with ddH_2O

Procedure:

- Mix well by stirring
- Aliquot 500mL into bottles
- Autoclave using liquid cycle for 50 minutes

5. Luria Broth Agar (LB Agar)

- Add 15.0g of Agar to LB before autoclaving
- Aliquot media into 10cm plates
- Let media to solidify

Appendix B – List of Primers

Primer name	Primer sequence	Primer Description
brap-2 olok14925	5'-GTCAGCACCGAAAATGTGTCAG	5' SW-PCR primer for *brap-2(ok1492)* mutant
brap-2 ok14923B	5'-CAGACAACGTCGAATGATCTC	3' SW-PCR primer for *brap-2(ok1492)* mutant
brap-2 ok14925	5'-GAGTGTATTCGAGTTTGATTCCC	5' SW-PCR primer for non *brap-2(ok1492)* worm
brap-2 ok1492N23	5'-TTTGTTCTGCCTAGGAATAAGTG	3' SW-PCR primer for non *brap-2(ok1492)* worm
ACT-1 qPCR For	5'-GTCGGTATGGGACAGAAGGA	5' qPCR primer to quantify *act-1*
ACT-1 qPCR Rev	5'-GCTTCAGTGAGGAGGACTGG	3' qPCR primer to quantify *act-1*
SKN-1C qPCR For	5'-TACTCACCGAGCATCCACCA	5' qPCR primer to quantify *skn-1c*
SKN-1C qPCR Rev	5'-TGATCAGCAGGAGCCACTTG	3' qPCR primer to quantify *skn-1c*
DAF-16 qPCR For	5'-TGGAATTCAATCGTGTGGAA	5' qPCR primer to quantify *daf-16*
DAF-16 qPCR Rev	5'-ATGAATATGCTGCCCTCCAG	3' qPCR primer to quantify *daf-16*
GST-4 qPCR For	5'-TGCTCAATGTGCCTTACGAG	5' qPCR primer to quantify *gst-4*
GST-4 qPCR Rev	5'-AGTTTTTCCAGCGAGTCCAA	3' qPCR primer to quantify *gst-4*
GST-10 qPCR For	5'-ATTCGAAGACATTCGGTTCG	5' qPCR primer to quantify *gst-10*
GST-10 qPCR Rev	5'-AACATGTCGAGGAAGGTTGC	3' qPCR primer to quantify *gst-10*
GST-7 qPCR For	5'-AATTCGTGGAGCTGGAGAGA	5' qPCR primer to quantify *gst-7*
GST-7 qPCR Rev	5'-CAGCAACCGAGTTGACTTGA	3' qPCR primer to quantify *gst-7*
GCS-1qPCR For	5'-CCAATCGATTCCTTTGGAGA	5' qPCR primer to quantify *gcs-1*
GCS-1 qPCR Rev	5'-GCTACTTCCGGGAATGTGAA	3' qPCR primer to quantify *gcs-1*
GWSEM4FOR	5-GGGGACAAGTTTGTACAAAAAAGCAGGCTTCATGAATGAGCTGCTCGCCGAG	Gateway 5' primer for screen of *sem-4* gene
GWSEM4REV	5-GGGGACCACTTTGTACAAGAAAGCTGGGTACTAAGAGGGTGGTGGGGTTGC	Gateway 3' primer for screen of *sem-4* gene

Appendix C – Supplementary Figures

A

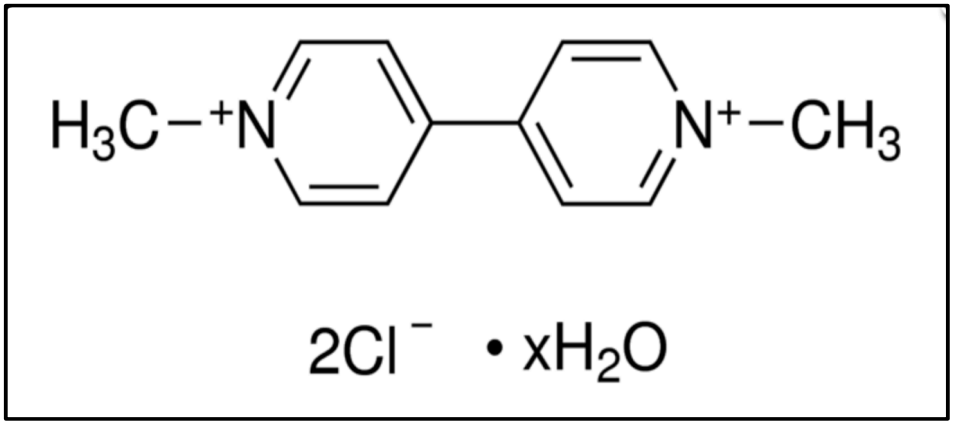

B

$$NADPH + O_2 \longrightarrow NADP^+ + O_2^- \quad (1)$$

$$NADPH + paraquat \longrightarrow NADP + paraquat\ radical \quad (2)$$

$$Paraquat\ radical + O_2 \longrightarrow paraquat + O_2^- \quad (3)$$

$$O_2^- + O_2^- \xrightarrow{2H^+} H_2O_2 + O_2 \quad (4)$$

$$Paraquat\ radical + H_2O_2 \longrightarrow \cdot OH + OH^- + paraquat \quad (5)$$

Supplementary Figure 1. Paraquat and its mechanism of action. A. Chemical structure of paraquat (methyl viologen dichloride). **B.** Mechanism of action of paraquat during reaction with NADPH (Nicotinamide Adenine Dinucleotide Phosphatase). Adapted from Clejan and Cederbaum, 1989.

Appendix C – Supplementary Figures

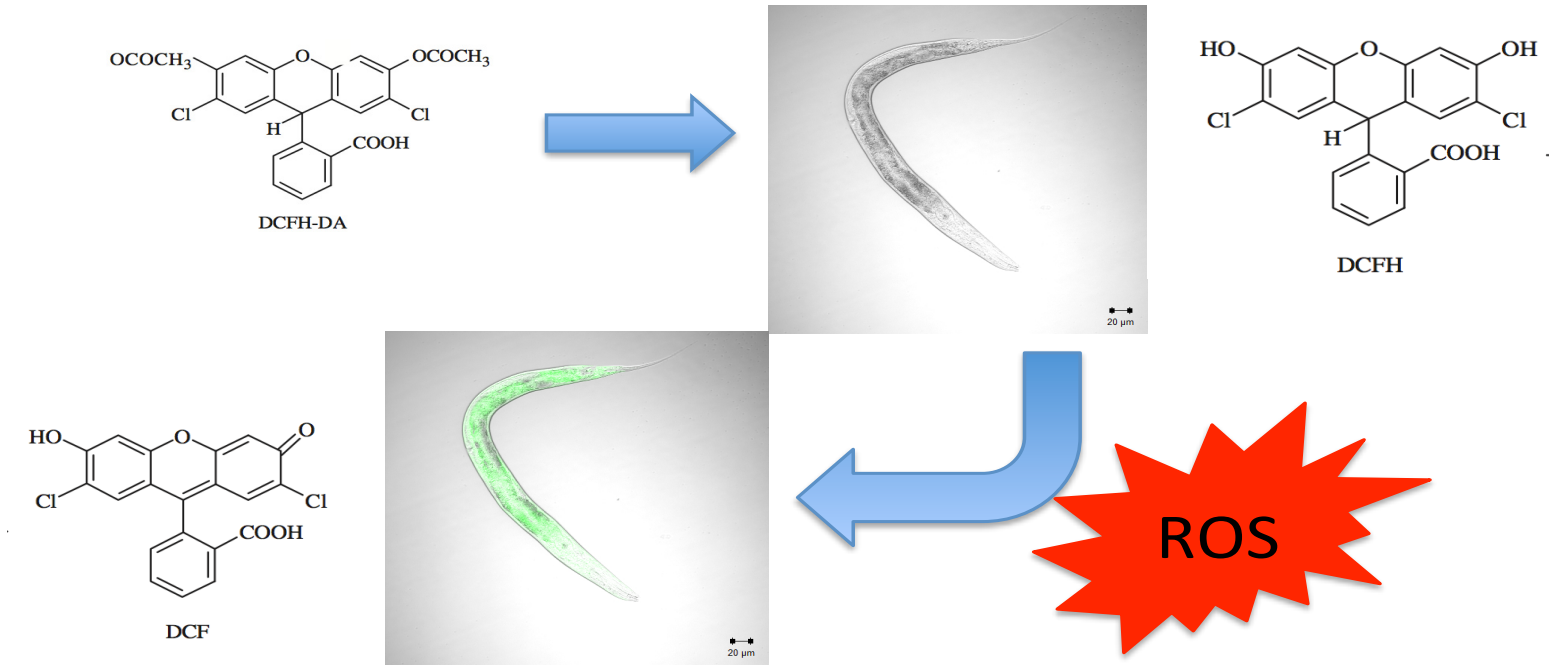

Supplementary Figure 2. Schematic representation of mechanism of action of DCFDA. 2',7'-diacetate dicloroflurescein loses two acetate groups upon enterance to living cell. Interaction with ROS molecules leads to oxidation of the molecule into 2',7'-dicloroflurescein (DCF), which is highly fluorescent.